FINAL REPORT ON

LOW-COST RADAR SENSORS FOR PERSONNEL DETECTION AND TRACKING IN URBAN AREAS

Office of Naval Research
Research Grant N00014-05-1-0722

For the period May 1, 2005 through December 31, 2006

Submitted by

Professor Hao Ling

Department of Electrical and Computer Engineering
The University of Texas at Austin
Austin, TX 78712-1084

January 31, 2007

ELECTRICAL AND COMPUTER ENGINEERING
THE UNIVERSITY OF TEXAS AT AUSTIN

Engineering Science Building • Austin, Texas 78712
(512) 471-6179 • FAX (512) 471-5532

February 13, 2007

Defense Technical Information Center
8725 John J. Kingman Road
STE 0944
Ft. Belvoir, VA 22060-6218

Dear Sir:

Enclosed please find a copy of our final report for ONR Research Grant N00014-05-1-0722 entitled "Low-Cost Radar Sensors for Personnel Detection and Tracking in Urban Areas" covering the period May 1, 2005 to December 31, 2006.

Mr. Ronald Joslin is the ONR grant monitor.

Sincerely,

Hao Ling
Professor

Enclosure

REPORT DOCUMENTATION PAGE

Form Approved
OMB No. 0704-0188

1. AGENCY USE ONLY *(Leave blank)*	2. REPORT DATE	3. REPORT TYPE AND DATES COVERED
	Jan. 31, 2007	Final Report 1 May 05 - 31 Dec. 06

4. TITLE AND SUBTITLE

Final Report on Low-Cost Radar Sensors for Personnel Detection and Tracking in Urban Areas

5. FUNDING NUMBERS

Research Grant
ONR
N00014-05-1-0722

6. AUTHOR(S)

Hao Ling

7. PERFORMING ORGANIZATION NAMES(S) AND ADDRESS(ES)

The University of Texas at Austin
Department of Electrical and Computer Engineering
Austin, TX 78712-1084

8. PERFORMING ORGANIZATION REPORT NUMBER

No. 4

9. SPONSORING / MONITORING AGENCY NAMES(S) AND ADDRESS(ES)

Office of Naval Research
Ballston Centre Tower One
800 North Quincy Street
Arlington, VA 22217-5660

Program Officer
Ronald Joslin

10. SPONSORING / MONITORING AGENCY REPORT NUMBER

11. SUPPLEMENTARY NOTES

a. DISTRIBUTION / AVAILABILITY STATEMENT

Approval for Public Release
Distribution Unlimited

12. DISTRIBUTION CODE

13. ABSTRACT *(Maximum 200 words)*

This report summarizes the scientific progress on the reserach grant "Low-Cost Radar Sensors for Personnel Detection and Tracking in Urban Areas" during the period 1 May 2005 - 31 December 2006. Research on the design and implementation of low-complexity radar sensors capable of detection and tracking of humans in high-clutter enviornments is presented.

14. SUBJECT TERMS

Radar, Doppler, Direction of Arrival, Human Tracking

15. NUMBER OF PAGES

94

16. PRICE CODE

17. SECURITY CLASSIFICATION OF REPORT	18. SECURITY CLASSIFICATION OF THIS PAGE	19. SECURITY CLASSIFICATION OF ABSTRACT	20. LIMITATION OF ABSTRACT
Unclassified	Unclassified	Unclassified	

FINAL REPORT ON

LOW-COST RADAR SENSORS FOR PERSONNEL DETECTION AND TRACKING IN URBAN AREAS

Office of Naval Research
Research Grant N00014-05-1-0722

For the period May 1, 2005 through December 31, 2006

Submitted by

Professor Hao Ling

Department of Electrical and Computer Engineering
The University of Texas at Austin
Austin, TX 78712-1084

January 31, 2007

LOW-COST RADAR SENSORS FOR PERSONNEL DETECTION AND TRACKING IN URBAN AREAS

Project Starting Date: May 1, 2005

Reporting Period: May 1, 2005 – December 31, 2006

Principal Investigator: Professor Hao Ling
(512) 471-1710
ling@ece.utexas.edu

Graduate Students: A. Lin, S. Sundar Ram, P. Tabrizi, Y. Kim

Undergraduate Students: J. Soric, N. Whitelonis

A. SCIENTIFIC OBJECTIVES:

This research program sets out to design, build and demonstrate low-cost radar sensors to detect and track human targets in high-clutter environments. As warfare has shifted from combat on open battlefields to fighting in urban areas and covert facilities, there is an increased need to detect concealed persons. Personnel detection is key to maintaining situational awareness, whether it is on a battlefield, in a city, or surrounding a building. The detection of hidden personnel in a cluttered environment, however, is a daunting task. For active radar sensing, the combination of high-clutter environments and weak radar returns from the human body precludes the use of conventional radar techniques for reliable personnel detection.

The objectives of our research program are to devise low-cost radar sensor concepts for personnel detection based on commercial wireless products, to collect an extensive database using the developed sensors and to exploit the data for personnel detection, tracking and identification. Our basic proposed concept entails the use of both Doppler and direction-of-arrival (DDOA) information to track multiple movers. The uniqueness features of our concept are: (i) the use of Doppler features from human movements to suppress stationary clutter such as buildings and walls, (ii) the use of very few receiver elements (i.e., *two*) to obtain DOA tracking of *multiple* human targets, and (iii) the use of mass-market wireless products for very low-cost sensor development.

B. SUMMARY OF RESULTS AND SIGNIFICANT ACCOMPLISHMENTS:

This program was carried out in three phases. In Phase 1, we demonstrated our DDOA concept of a low-cost, two-element radar sensor for tracking multiple persons in a high-clutter environment. In Phase 2, we extended the concept to achieve multi-dimensional tracking of multiple human targets through very low-order frequency and spatial diversities. In Phase 3, the limitations of the system were investigated and ways to improve the performance of the system were explored. Our research accomplishments in human detection and tracking include:

Phase 1: Design and demonstration of a two-element DDOA radar.

1.1. Designed, built and calibrated the radar.

1.2. Set up experiments and carried out data collection of human movements under various situations including number of humans, type of movements, different environments and radar polarizations.

1.3. Developed signal processing algorithms to process and analyze the collected data.

1.4. Demonstrated the tracking of up to three humans up to a range of 10m in indoor line-of-sight environment and through a 15" exterior brick wall.

Phase 2: Extension of the DDOA radar to achieve multi-dimensional tracking.

2.1. Incorporated a third receiver element to the radar to achieve the capability of simultaneous elevation and azimuth bearing tracking.

2.2. Extended the idea of human tracking to achieve the frontal imaging of a human subject.

2.3. Developed ranging capability to our sensor system by designing and realizing a two-frequency radar.

2.4. Developed three-dimensional tracking capability by combining the two-tone ranging capability with the three-element, elevation-azimuth tracking radar.

Phase 3: Assessment of system limitations and exploration of new concepts.

3.1. Collected in-situ transmission data of different wall types and carried out finite-difference time-domain electromagnetic simulation to understand wall penetration phenomenology.

3.2. Evaluated the effect of dynamic clutters with rotational or vibration motions on the DDOA radar sensor.

3.3. Developed a Monte Carlo simulation to establish confidence bounds on the performance of the radar in tracking multiple movers.

3.4. Explored the concepts of a multi-element array and a network of Doppler sensors to improve the performance of the 2-element DDOA radar.

The detailed descriptions of our accomplishments are discussed below.

B.1. Design and demonstration of a two-element DDOA radar. We designed and constructed a radar testbed by combining the Doppler discrimination offered by human movements with the DOA information that can be collected using an antenna array to provide the necessary information for human movement tracking. Note that conventional DOA detection requires the use of multiple receiver elements, where the number of elements must be greater than the number of targets. This leads to high cost as well as a physically bulky system below 5 GHz. Here we took advantage of the Doppler information from multiple moving humans to achieve Doppler-DOA (DDOA) tracking with only a ***two***-element array. The approach is to use the short-time Fourier processing to separate the target via their contrasting Doppler returns. Then by extracting the phase difference between the received signals at the two elements, we can determine the DOA of each mover individually. More explicitly, if we assume the time signals received at the two antenna elements to be $f_1(t)$ and $f_2(t)$, then after the Doppler processing the signals become $F_1(f_D)$ and $F_2(f_D)$, respectively. If the targets of interest generate different Doppler frequencies f_{Di} due the difference in their velocities with respect to the radar transceiver, then the DOA of target i with respect to the array boresight is given by:

$$\theta_i = \sin^{-1}\left[\frac{\angle F_1(f_{Di}) - \angle F_2(f_{Di})]}{(2\pi d/\lambda_c)}\right] \qquad (1)$$

where d is the spacing between the elements and λ_c is the RF wavelength.

To implement this concept, we designed and built a two-element receiver to extract the DDOA information simultaneously (Fig. 1). The system was designed based on two integrated receiver boards from Analog Devices. It has very low cost (under $100 for each board) and small form factor, since the boards came from mass-market products for

the wireless networking market. The system operates at 2.4 GHz. Two microstrip patch antennas were used as the front-end and a National Instruments DAQ system was used for data acquisition. Some results collected from this radar are shown in Figs. 2 and 3. Fig. 2 shows the Doppler vs. DOA plot of an acoustic subwoofer driven at 40 Hz and placed at 40 degrees with respect to the radar boresight. It shows the correct bearing angle and Doppler information at ±40Hz (the two-sided Doppler response is due to the FM modulation created by the subwoofer vibration). Fig. 3 shows the snapshot data from a person walking away from the radar. As we can see from the data, the human target includes various limb microDopplers and is not as localized as the subwoofer response. Nevertheless, reliable DDOA information can be acquired. Further, a continuous real-time tracking of the person in an indoor environment can be achieved. Fig. 4 shows how the same concept is applicable to multiple targets, as three speakers with different Doppler returns are used as test targets. The Doppler separation among the target allows the DOA of the speakers to be obtained using the two-element array. Figs. 5 and 6 show respectively the result of two and three walking human subjects recorded using the radar. The measured DOA vs. time plot shows very distinct trajectories corresponding to the azimuth bearings of the subjects as they walked during the data acquisition. Extensive testing was also conducted for different through-wall scenarios. Fig. 7 shows the data collected through a 15" exterior brick wall. A large database was collected for different parameter spaces including number of humans, types of movements, wall types and radar polarization (VV, HH).

We also quantified the maximum range of the radar by estimating all the system parameters in the radar range equation. We estimated the maximum operating range of our radar for human detection in open space to be 46 m (with a transmit power of 11dBm and a signal-to-noise ratio of 10dB at 2.4GHz). This free-space range estimate agrees fairly well with our outdoor line-of-sight measurements on human subjects. For wall attenuations of 16 dB (gypsum/wooden wall) and 20 dB (brick wall), the estimated maximum operating ranges become 34 m and 27 m, respectively. However, the impact of the wall on the DOA accuracy was significantly more complicated and unpredictable. Further follow-up studies were subsequently conducted to ascertain the wall phenomenology and are discussed later in Sec. B.3.

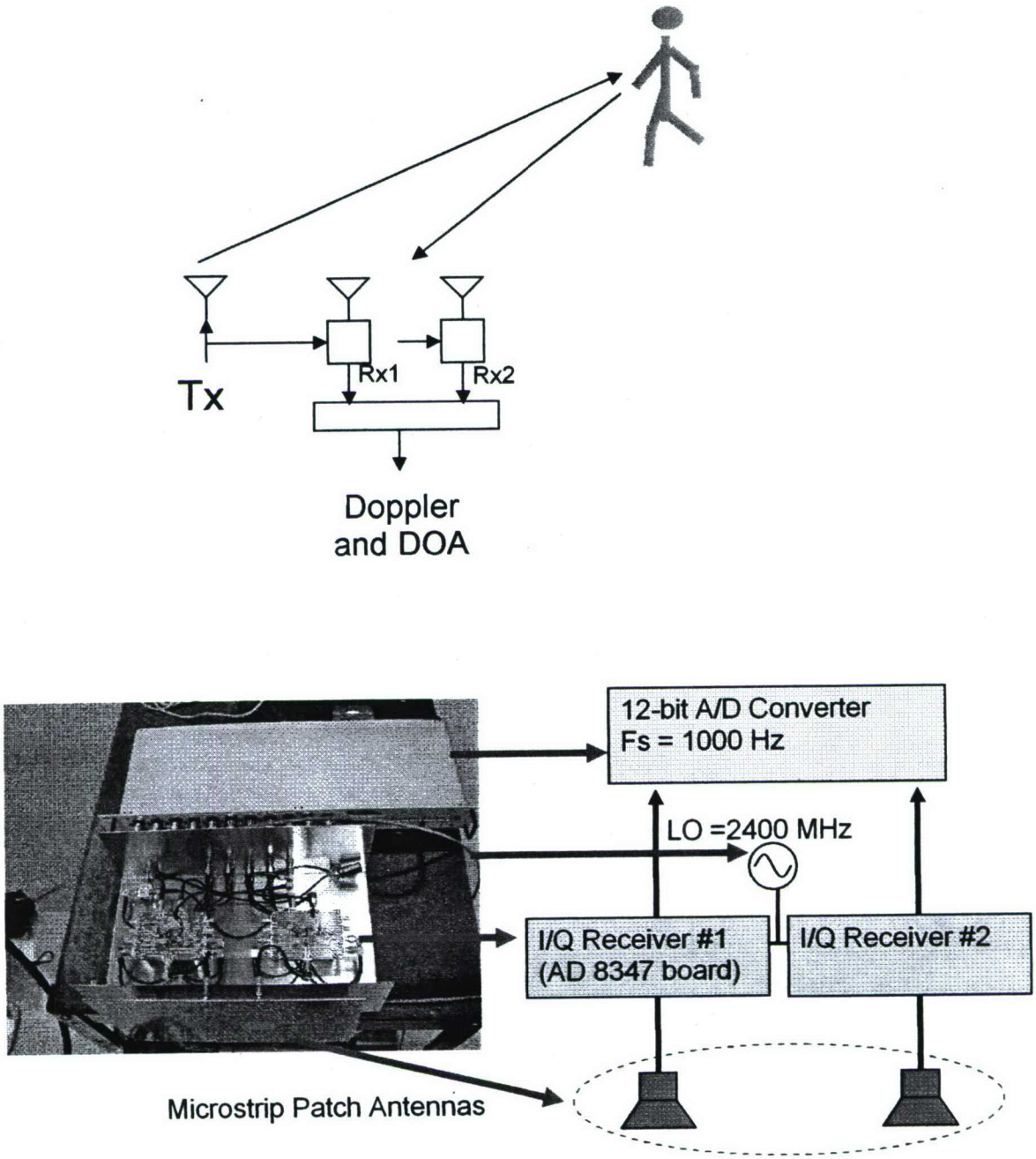

Fig. 1. A two-element radar sensor for measuring both Doppler and direction of arrival (DDOA). The sensor uses two Analog Devices integrated receiver boards, which cost less than $100 each. Data collection was carried out at 2.4 GHz.

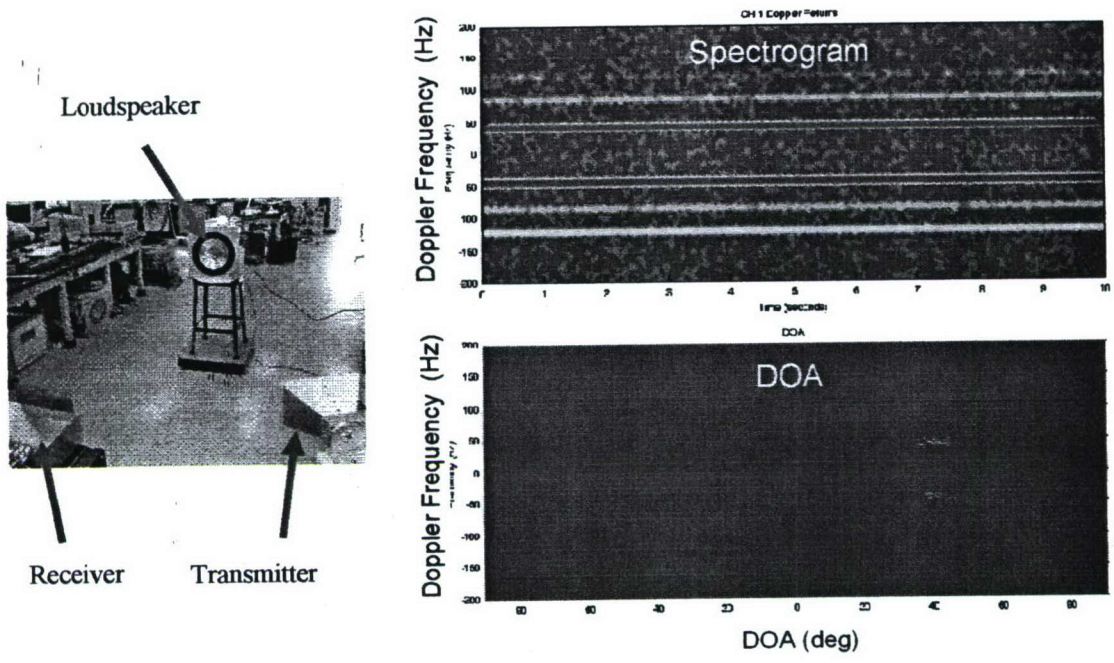

Fig. 2. Doppler and DOA of mechanical vibrations (subwoofer).

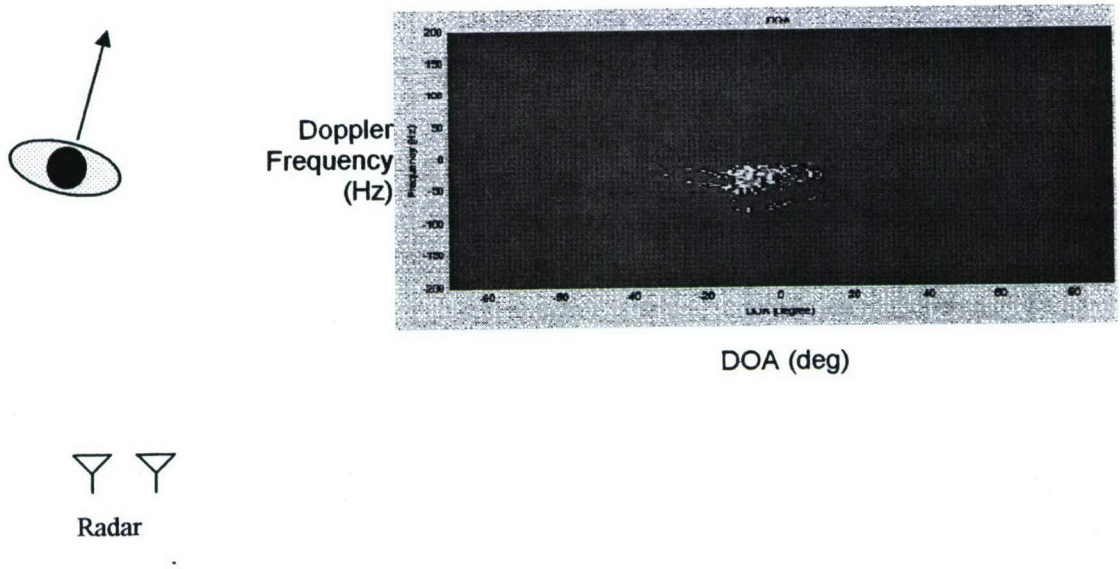

Fig. 3. Doppler and DOA of a moving person.

(a)

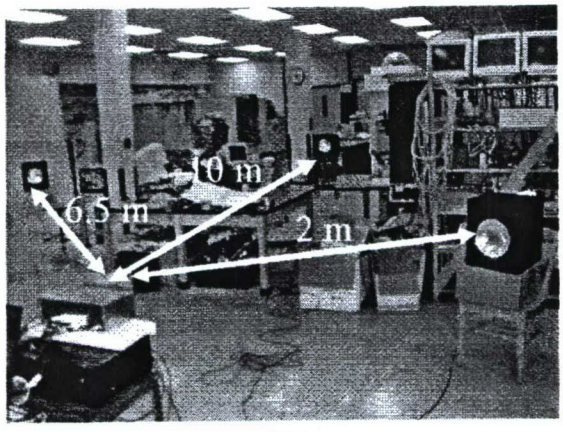

(b)

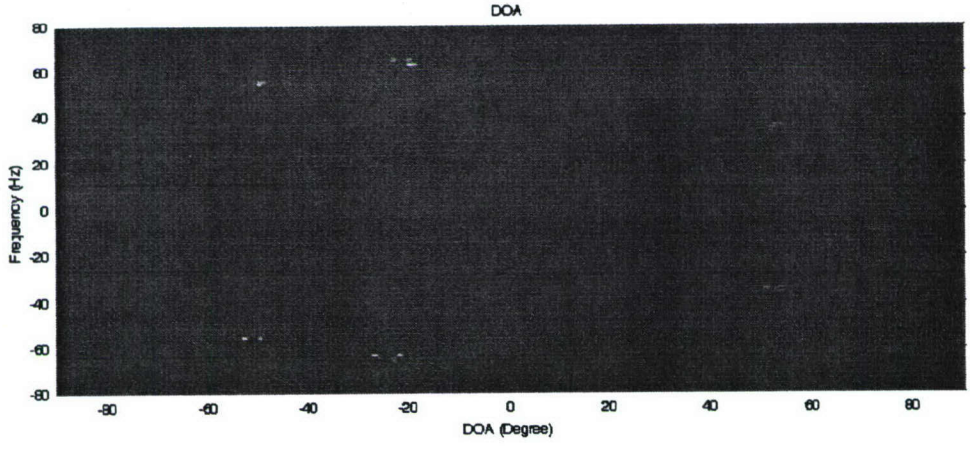

Fig. 4. Three loudspeakers measurement: (a) Setup and (b) Measured Doppler and DOA.

(a)

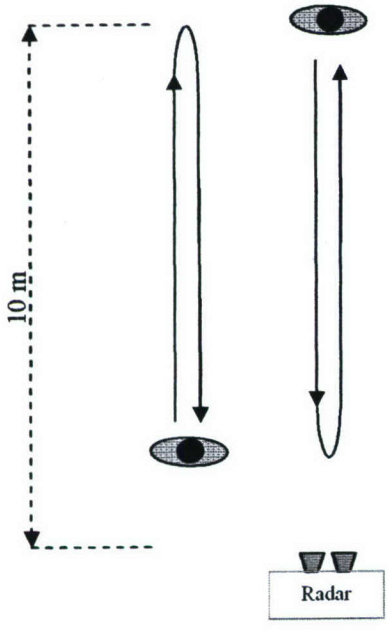

(b)

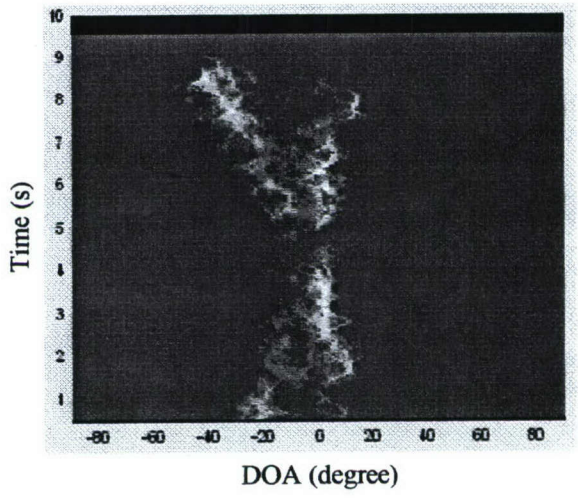

Fig. 5. Measurement of two humans walking in opposite direction: (a) Setup and (b) DOA vs. time

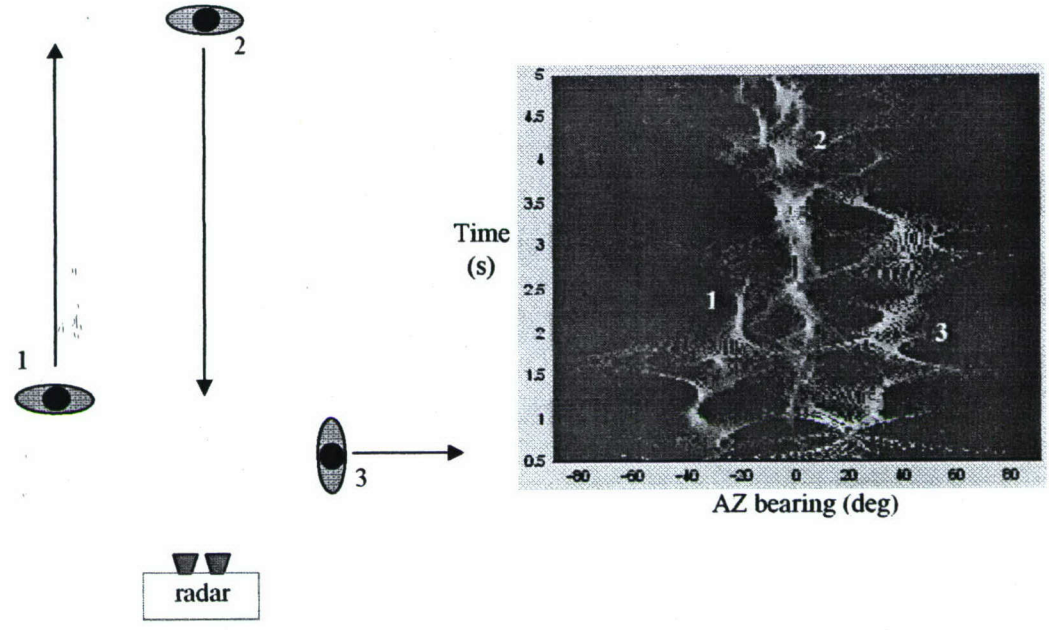

Fig. 6. Measurement of three human subjects walking in a room: (a) Setup and (b) DOA vs. time.

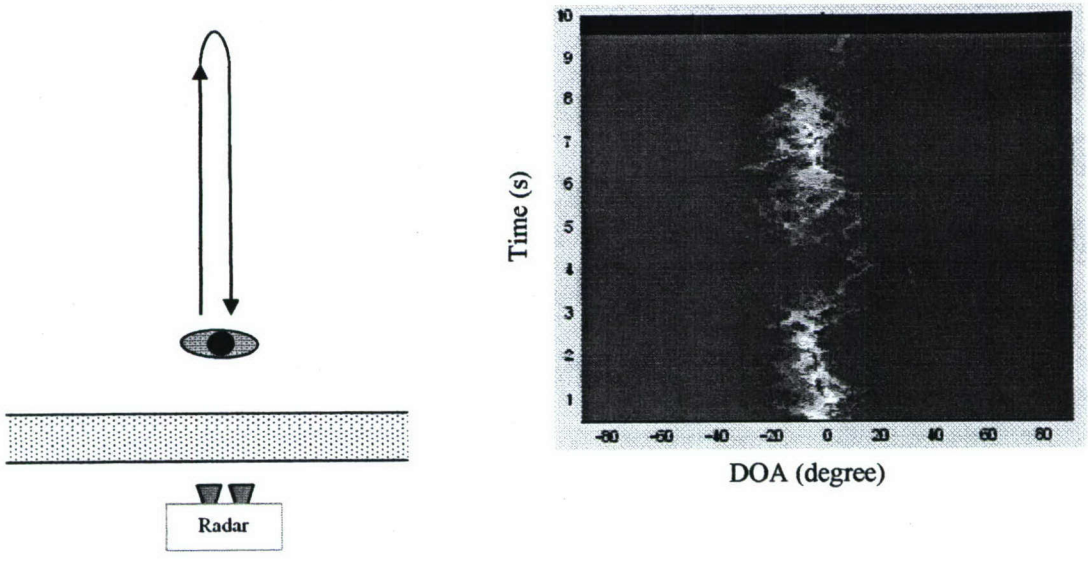

Fig. 7. Through-wall measurement of a walking human through a 15" exterior brick wall: (a) Setup and (b) DOA vs. time.

The main factor that limits the performance of this radar for multiple mover tracking is the occurrences of similar Doppler from different targets. We developed a Monte Carlo simulation to establish confidence bounds on the system performance of the radar in tracking multiple movers. In the simulation, the movers were assumed to be ideal point scatterers with random velocities and random positions in a 10m by 10m room. Fig. 8 shows the probability of successful DOA determination versus the number of movers. As expected, the percentage of successful cases decreases as the number of movers is increased. This is expected since a larger number of movers result in more occurrences of close Doppler spacing (similar radial velocities). Thus the DOA accuracy of the two-element system is strongly influenced by the number of movers. Nevertheless, a success rate of 70% can be maintained for four targets or fewer under this condition

The results of this portion of the research were reported in [J3, C1, C2].

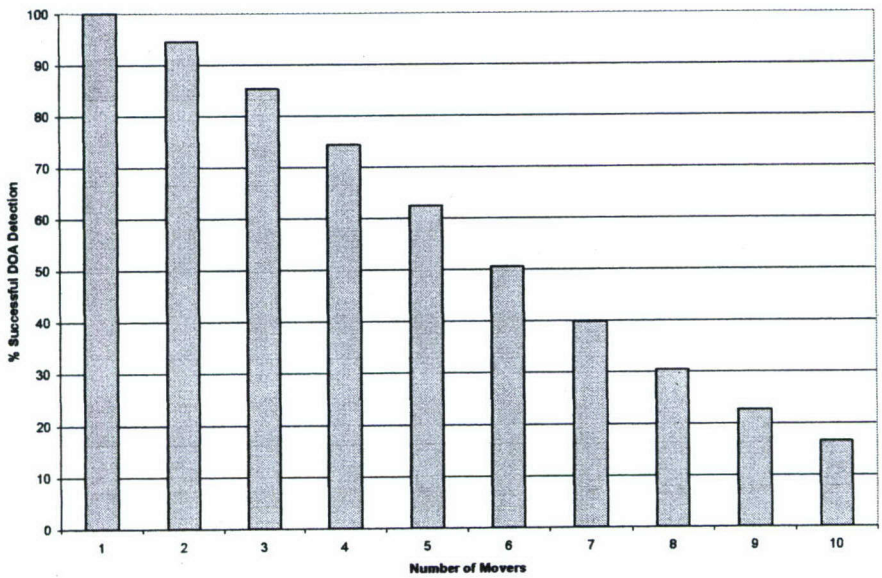

Fig. 8. Probability of successful DOA determination (to a 5° accuracy) versus the number of movers for the point scatterer model.

B.2. Extension of the DDOA radar to achieve multi-dimensional tracking. The basic concept of the two-element DDOA array can be extended to achieve multi-dimensional tracking of multiple moving targets with only a moderate increase in complexity. First, we incorporated one additional receiver element in the vertical direction of the radar to achieve the capability of simultaneous elevation and azimuth bearing tracking (see Fig. 9). The additional receiver Rx3 and the existing receiver Rx1 form a new pair of elements to provide the DOA in the elevation plane. The Doppler and DOA processing is repeated for the Rx1 and Rx3 signals, similar to the Rx1 and Rx2 signals. Finally, by correlating the DOA results in azimuth and elevation based on their associated Doppler, it is possible to achieve two-dimensional bearing sensing of multiple movers, provided that the movers have different Doppler frequencies.

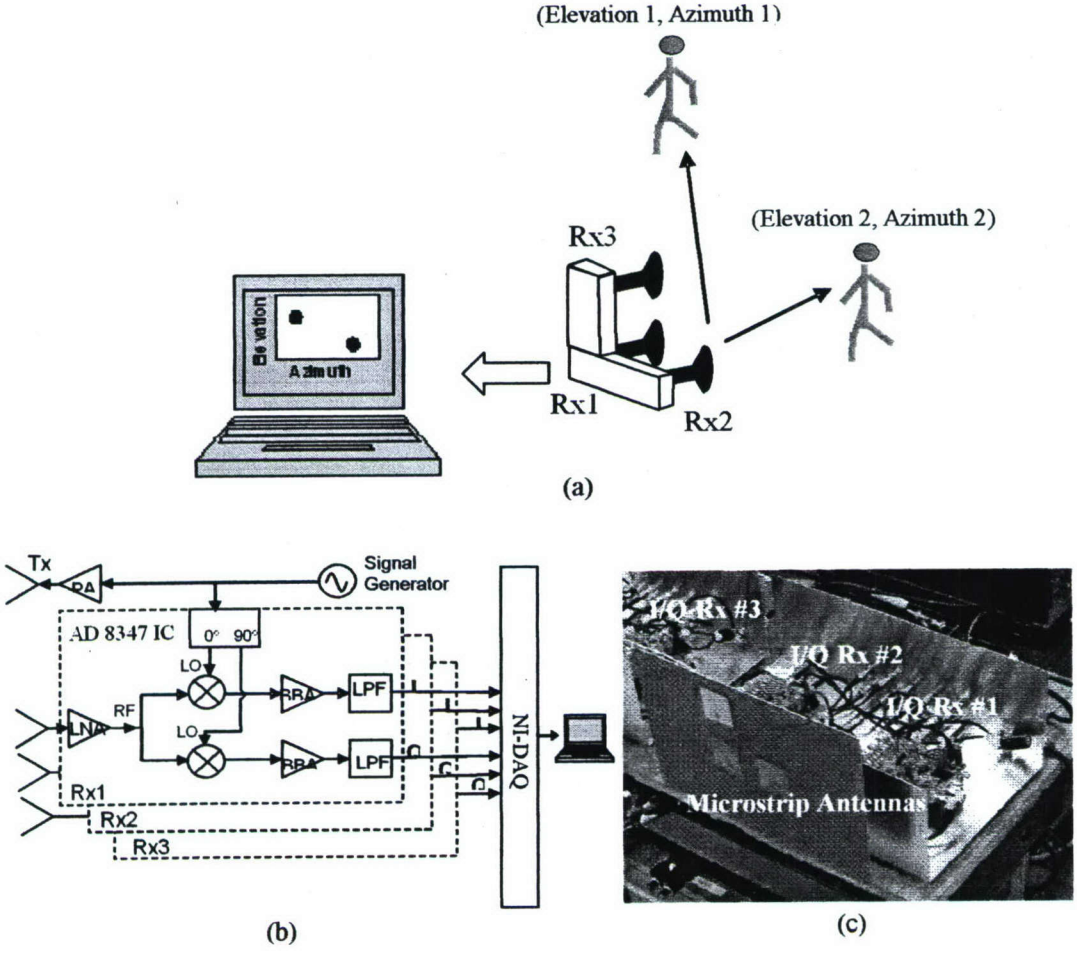

Fig. 9. Two-dimensional human tracking: (a) Basic concept, (b) Radar system block diagram, and (c) Actual hardware implementation.

Fig. 10 shows the results of three loudspeakers driven by 3 different audio tones. A comparison of Figs. 10(a) and 10(d) shows a close correspondence of the DOA results to the frontal perspective of the radar.

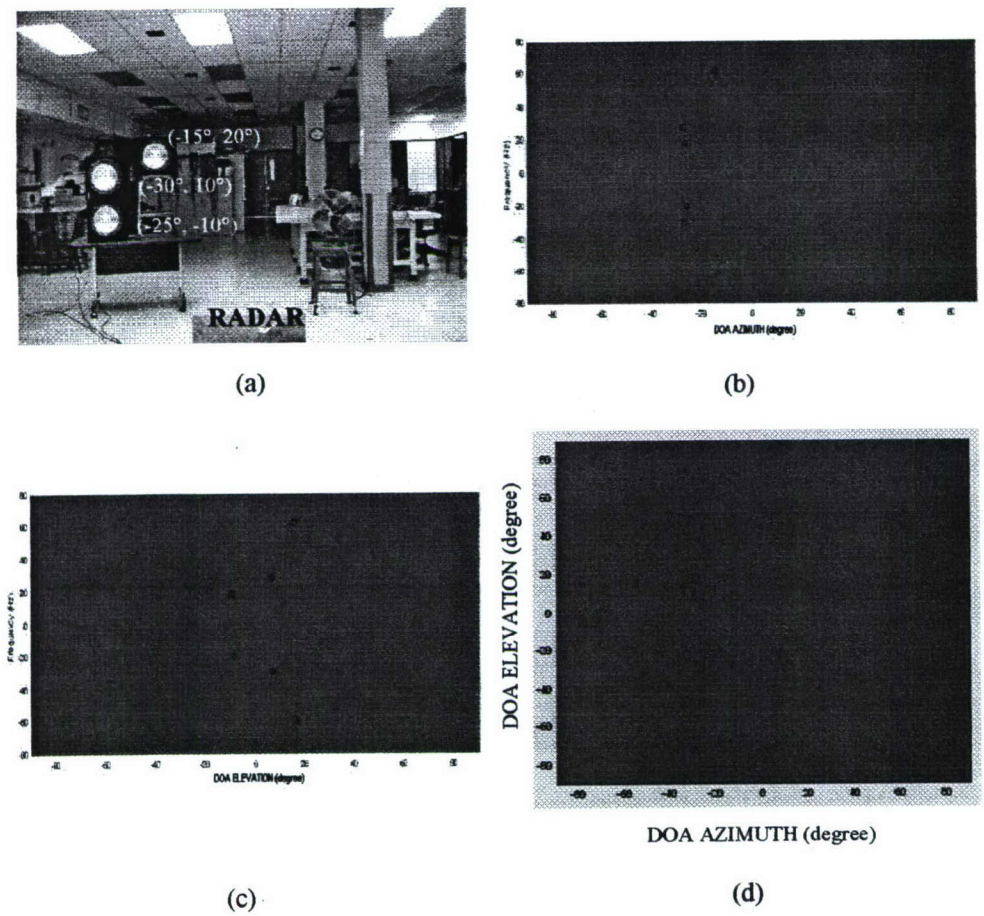

(a) (b)

(c) (d)

Fig. 10. Loudspeaker Doppler and DOA measurements: (a) Setup, (b) Azimuth DOA, (c) Elevation DOA, and (d) Two-dimensional DOA.

Fig. 11 shows the result of two human subjects in front of a building walking in the patterns shown in Fig. 11(a). The subject on the left begins at point A and climbs a staircase to the top at point B. The subject then turns around and descends to the ground level to point A. The subject on the right starts at point C at the ground level and walks to the right until reaching point D. The subject then turns around and walks back to point C. The two-dimensional DOA trajectories are tracked closely by the radar.

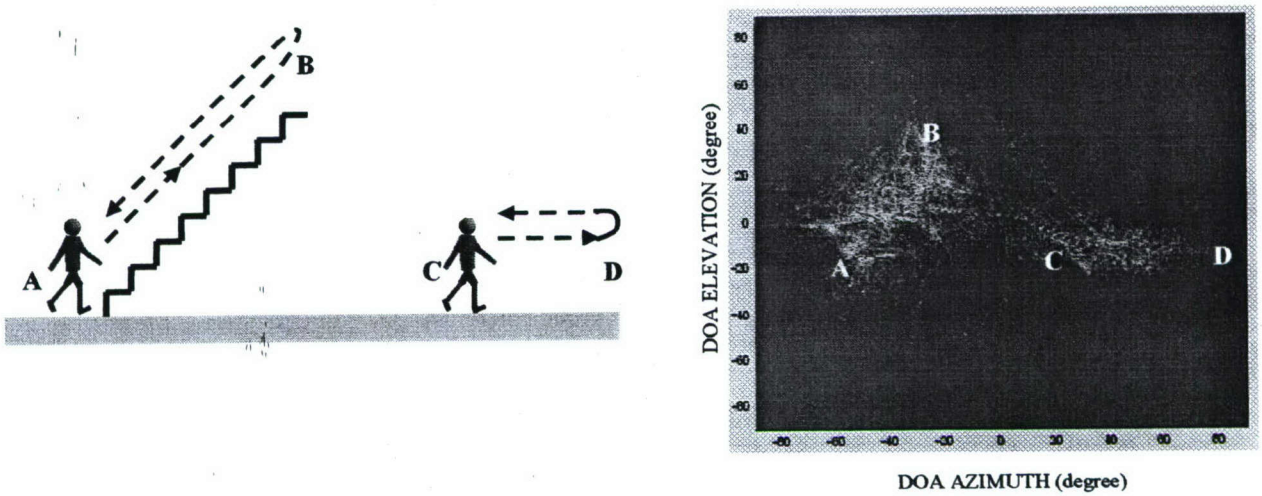

Fig. 11. Tracking two human subjects in the azimuth-elevation plane: (a) Setup, (d) Two-dimensional DOA trajectory.

The idea is explored further for a possible imaging application. In addition to tracking multiple humans, the radar may be employed to generate a two-dimensional image or a frontal view of a human. The concept entails resolving the micro-Doppler frequencies of the returned signals from a moving human, and then measuring the phase difference at each Doppler frequency component to determine the DOA of the various body parts. If each body part gives rise to a different Doppler frequency, then the resulting bearing map should correspond closely to a two-dimensional frontal view of a human. Fig. 12(a) shows such a frontal view of a human subject in a line-of-sight test. During the measurement period, the subject remained standing while moving each body part sequentially. After correlating the azimuth and elevation DOA measurements based on their Doppler information, a two-dimensional or frontal view of the human was constructed. The measured frontal view shows the position of each limb, making an outline of the subject. The dynamic range of the image is 40 dB. The measurement was then repeated in-situ with a 5" thick gypsum/wooden wall in an interior room. Fig. 12(b) shows the measured through-wall view of the human. The image appears to be less focused due to the significant attenuation from the wall. However, the outline of the human is still visible. Of course, this concept is based on the assumption that different body parts give rise to different Doppler frequencies. When this condition is not met in

practice, the resulting bearing information is not accurate. Therefore, the present concept can at best be an "imaging of opportunity" that captures glimpses of the human subject.

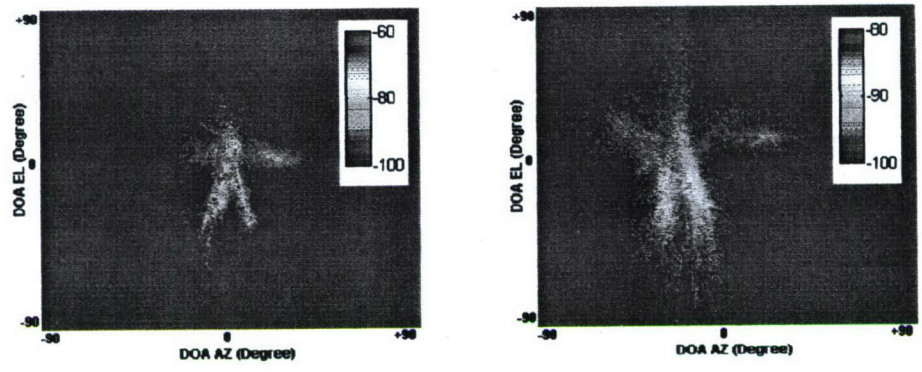

(a) (b)

Fig. 12. Measured frontal view of a human (a) In free-space and (b) Through an indoor wall.

We have also incorporated ranging capability to the radar. In contrast to the pulsed-based or frequency-modulated continuous wave (FMCW) radar, multiple frequency continuous wave (MFCW) radar is a simple and low-cost way to acquire range information. To keep the radar architecture as simple as possible, only two frequencies are used, as shown in Fig. 13. However, a two-frequency system can only acquire the range for a single-target configuration. To overcome this limitation, the Doppler separation among the moving targets is again used as a prefilter before measuring the phase difference to arrive at the range information of the moving targets. Similar to Eq. (1), the range, R, of target n from the radar can then be determined by the phase difference between $F_1(f)$ and $F_2(f)$ at each Doppler bin f_{Di}:

$$R_n = \frac{\angle F_2(f_{Di}) - \angle F_1(f_{Di})}{4\pi\Delta f / c} \tag{2}$$

where $\Delta f = fc_1 - fc_2$. This concept again applies as long as the Doppler frequencies from different targets are sufficiently distinct.

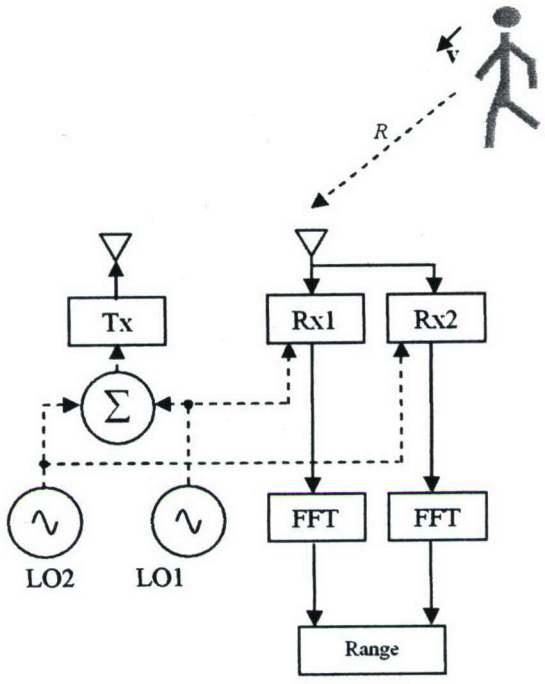

Fig. 13. Basic two-tone radar operation.

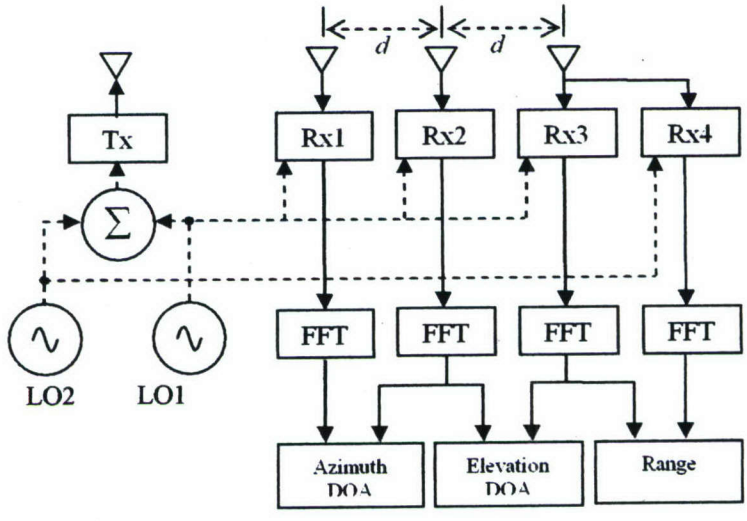

Fig. 14. System block diagram of a three-element and two-frequency Doppler radar.

This two-frequency approach was implemented and integrated to the existing two-dimensional radar to achieve three-dimensional tracking. Fig. 14 shows the overall block diagram of the integrated system. The system operates at two CW frequencies fc_1 (2.4 GHz) and fc_2 (10 MHz below fc_1). The frequency separation is selected to achieve a

maximum unambiguous range of 15 m. Fig. 15 shows the result of the two-loudspeaker test. The measured data show good agreement with the expected Doppler vs. azimuth, elevation and range. The location of each loudspeaker can now be determined after correlating the measured azimuth, elevation and range based on their Doppler information. By using the spherical-to-Cartesian transformation, a three-dimensional location coordinate (cross-range, down-range, elevation) can be constructed accordingly. Figs. 16(a) and (b) show the corresponding top-view, frontal view, and the three-dimensional coordinates of the loudspeakers. Comparing Figs. 15(a) and 16(c), the measured coordinates of the left and right loudspeakers are close to the expected locations.

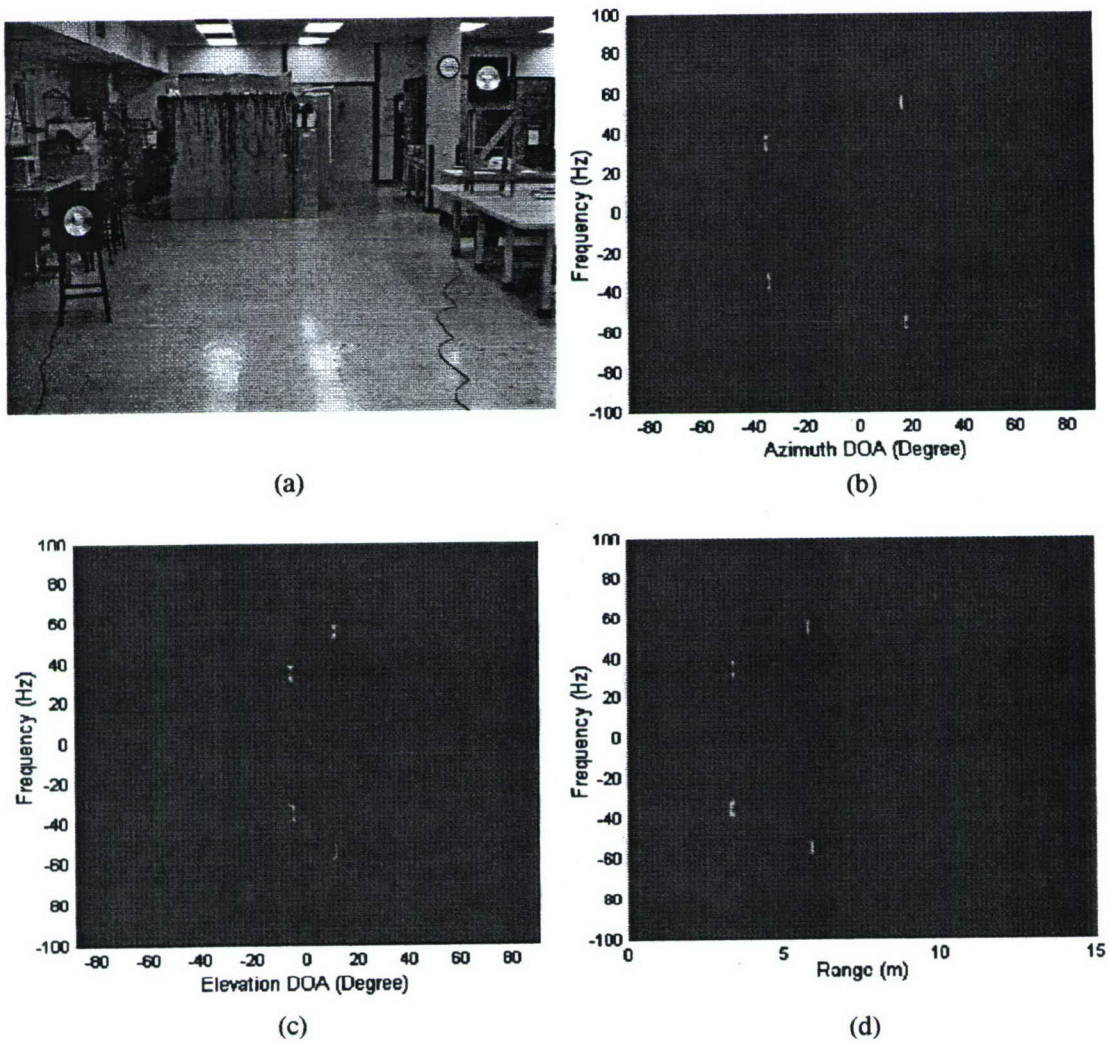

Fig. 15. Two-loudspeaker measurement: (a) Setup, (b) Doppler and azimuth DOA, (c) Doppler and elevation DOA, and (d) Doppler and range

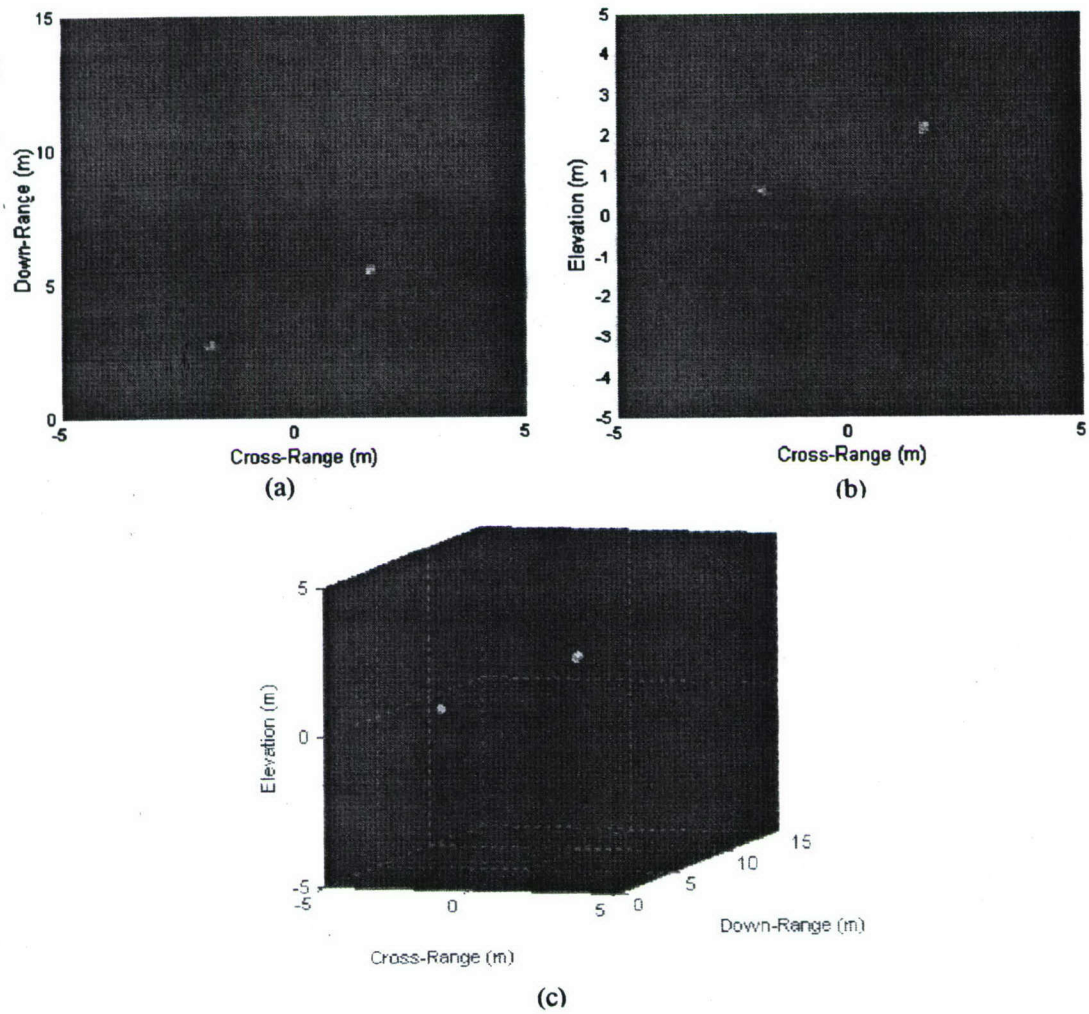

Fig. 16. Three-dimensional tracking of two loudspeakers: (a) Top view, (b) Frontal view, and (c) Three-dimensional coordinate.

Finally, three-dimensional tracking of two human subjects was demonstrated. Two human subjects walked in a straight path at approximately the same speed but in opposite directions (Fig. 17(a)). During the walk, the radar continuously measured and output the bearing and range information of the subjects (Fig. 17(b-d)). The elevation tracks of the two human subjects are not distinguishable in Fig. 17(c) since the subjects walked along the same elevation plane (ground level). The measured range tracks in Fig. 17(d) show a crisscross pattern due to the two subjects moving back and forth. The corresponding top view and frontal view maps are constructed and shown in Figs. 17(e) and (f).

The results of this portion of the research were reported in [J1, J2, C3, C4].

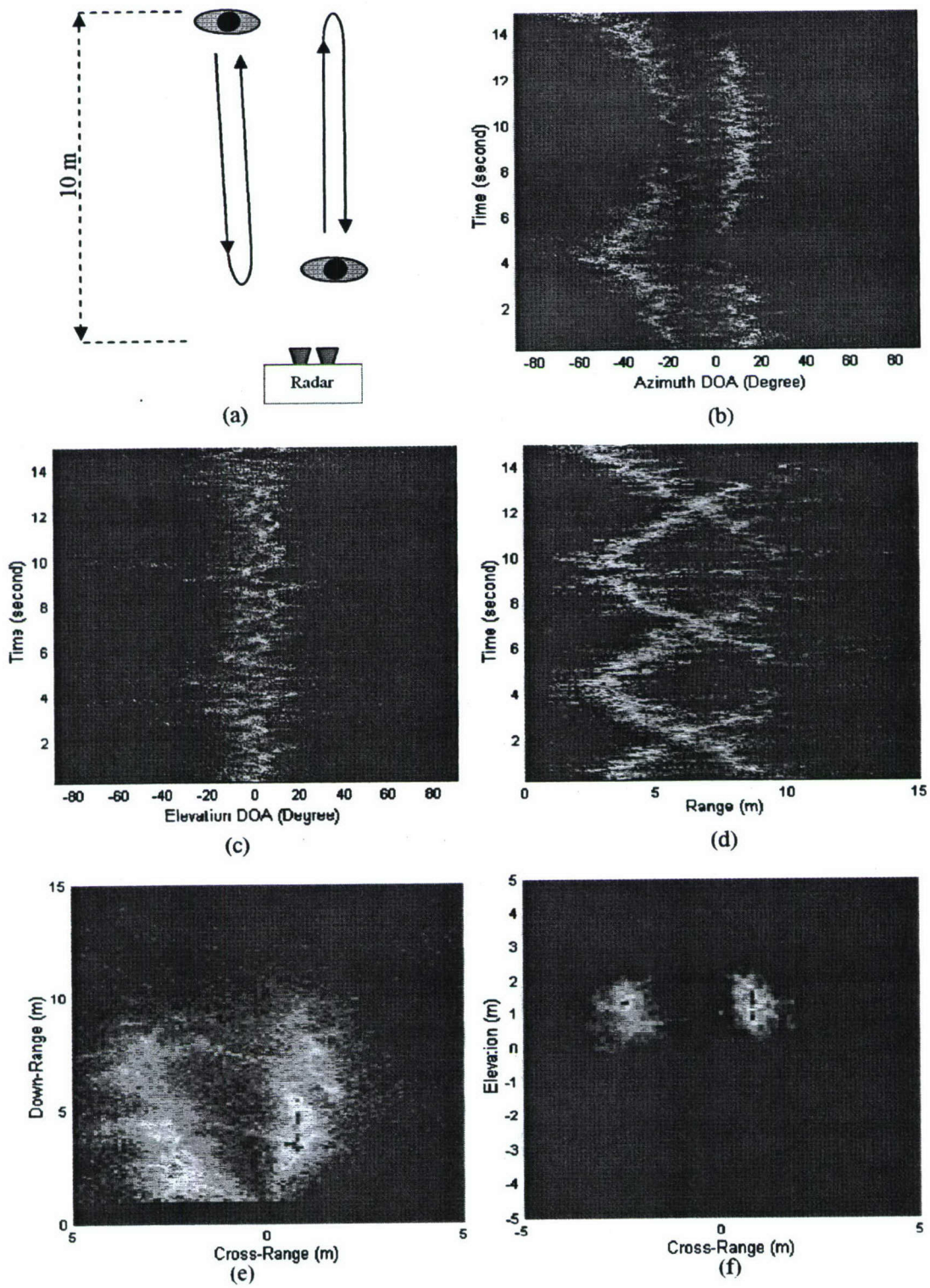

Fig. 17. Three-dimensional tracking of two humans: (a) Set up. (b) Azimuth DOA vs. time. (c) Elevation DOA vs. time. (d) Range vs. time. (e) Top-view. (f) Frontal-view.

B.3. Assessment of system limitations. We have found that one of the major uncertainties in the operation of the radar is the accuracy of the DOA and range measurements under through-wall operations. To better understand the wall propagation phenomenology, we collected the in-situ reflection and transmission data of an exterior brick wall using a vector network analyzer (VNA) from 2 to 6 GHz. The results showed significant variability over different parts of the wall and over the frequency range, indicating multipath. Next, we constructed a cinder block wall in the laboratory and conducted detailed measurements using both a VNA and our radar. The DOA results of the line-of-sight case versus the cinder block wall case (shown in Fig. 18) are compared in Fig. 18. It shows that the DOA accuracy is surprisingly poor for the cinder block wall. The cause of the inaccuracy is not due to lack of power level. To investigate the transmission physics, we carried out a finite-difference time-domain (FDTD) simulation of both a solid homogeneous wall and a cinder block wall structure with air holes. As can be seen in Figs. 19(a) and 19(b), the wavefront transmitted through the solid homogeneous wall remains a well behaved spherical front, while the transmitted wave through the inhomogeneous cinder block wall shows considerable reverberation near the wall. This complex wavefront leads to the poor DOA results using the two element array. We also notice that at a sufficiently far distance from the wall, the wavefront begins to resemble the regular spherical spread. Indeed, we have found in our experiments that the DOA accuracy actually improved at sufficiently far distance away from the wall, provided that the signal strength was not too weak. In summary, our study showed that a wall with interior inhomogeneity causes significant challenge to the present two-element radar concept. The only way to potentially overcome this challenge is with more elements to resolve the different DOA components.

Another potential challenge for the DDOA system is dynamic clutter that can result in false alarm, for example, rotating fans and vibrating structures. The latter has already been well tested using the subwoofer system. We made measurements of a rotating fan and the results are shown in Fig. 20. When the fan is stationary, the spectrogram shows Doppler lines at frequencies corresponding to (the number of blades) times (the number of rotations per second). This phenomenon is very similar to the jet engine modulation (JEM) lines observed in jet aircraft and is well understood. The

(a) Line-of-Sight

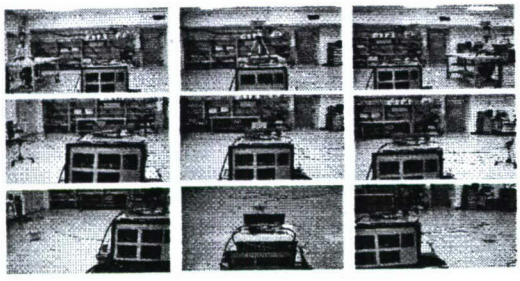

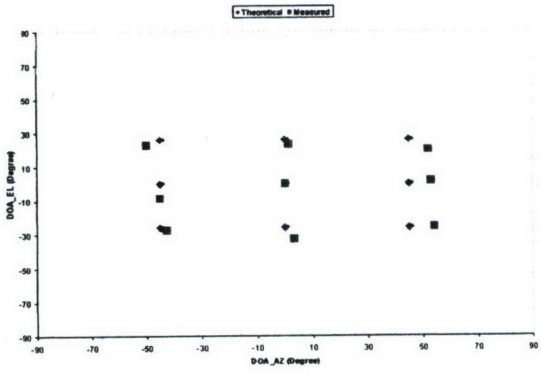

(b) Cinder Block Wall

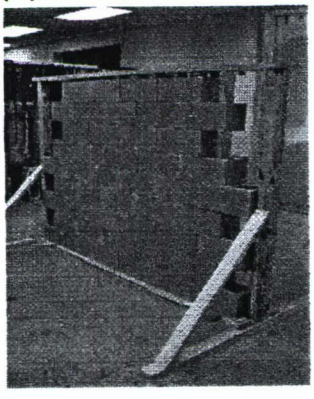

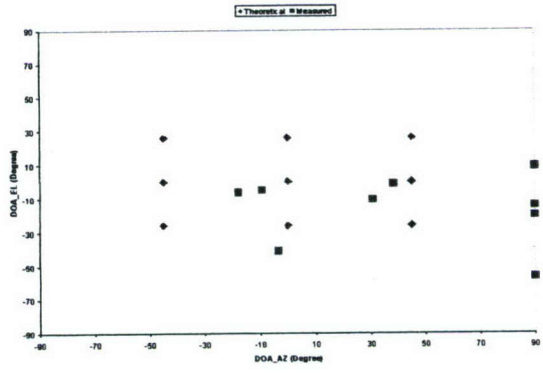

Fig. 18. DOA test for 9 different positions of the transmitter in the (a) line-of-sight case and (b) cinder block wall case. The blue dots are the expected positions of the transmitter while the red dots are the measured DOA in azimuth and elevation.

Solid Homogeneous Wall

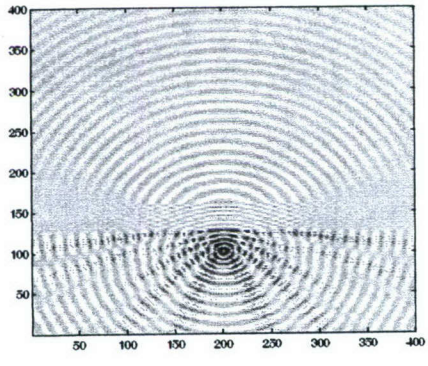

Inhomogeneous Cinder Block Wall

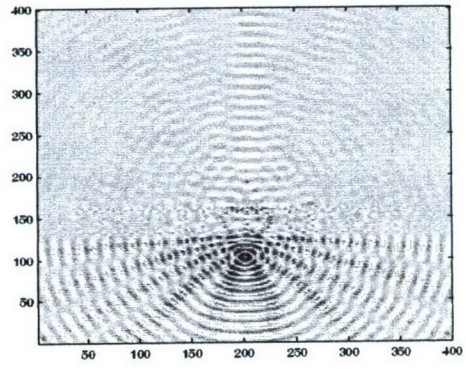

Fig. 19. FDTD simulation results of the wave transmission through a solid homogeneous wall and an inhomogeneous cinder block wall with air holes.

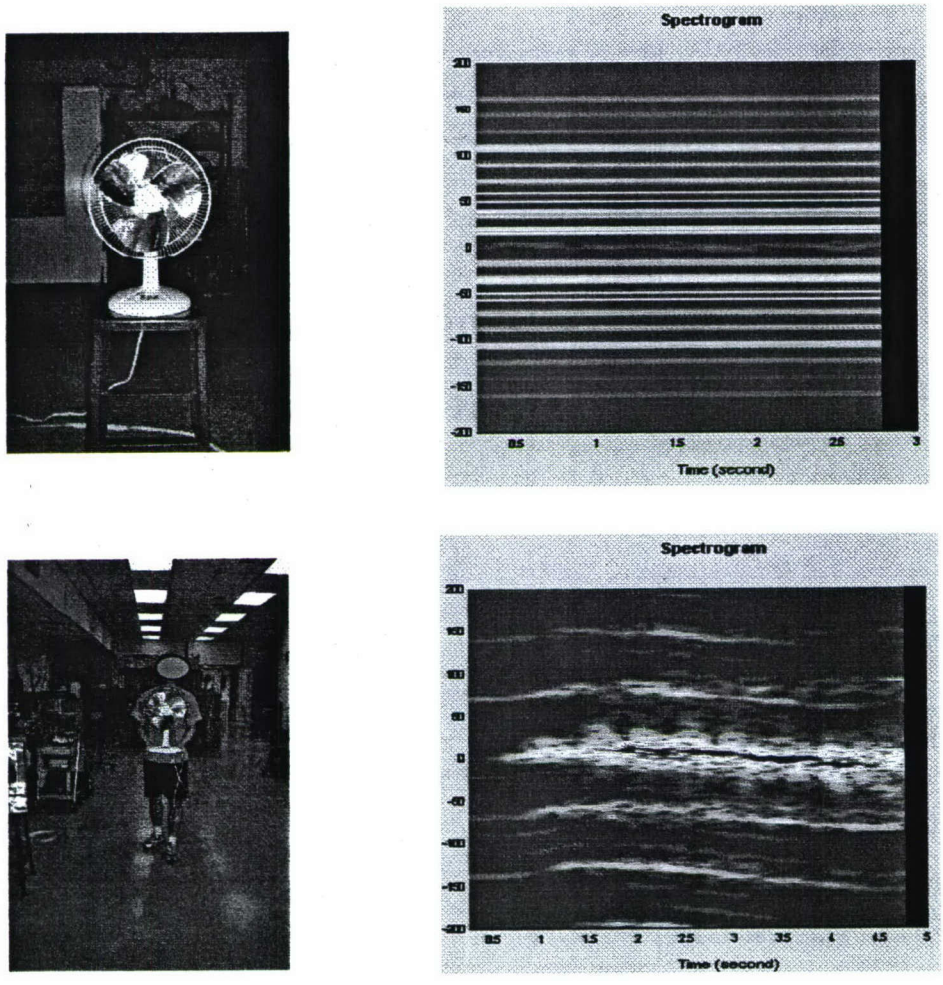

Fig. 20. Spectrogram of a fan in a stationary position and held by a moving subject.

strength of each Doppler line is dictated by the shape of the blade. Another interesting case is when the fan is turned on and held by a walking person. In this case, the Doppler lines are modulated by the movement of the person, as shown in the bottom spectrogram of Fig. 20. This points to an interesting possibility that we might be able to recreate the Doppler lines electronically in an RFID tag, which can be worn by friendly forces. By producing a set of unique Doppler lines, the individual can be readily recognized by the DDOA radar as a friendly target. The way to achieve this goal is to design active RF tags that can electronically create amplitude or phase modulation on the return signal. The basic tag architecture may use an antenna for both transmit and receive, a low-noise amplifier and a passive mixer with an oscillator to create the AM tone. This concept

provides a means by which cooperative and non-cooperative targets can be simultaneously tracked and separately identified by the same sensor.

The main factor that limits the performance of the DDOA radar for multiple human tracking is the overlapping microDoppler returns from the body parts of human targets. We developed a more sophisticated Monte Carlo simulation to establish confidence bounds on the system performance of the radar in tracking multiple movers. Fig. 21 shows the probability of successful DOA determination versus the number of movers for both the point scatterer model (blue) shown earlier in Fig. 8 and a model including human microDoppler (red). As expected, the overlapping micro-Dopplers between movers significantly reduce the Doppler spacing as the number of movers is increased, thus lowering the overall confidence level. Under these parameters, only three targets or fewer can be detected at a success rate of approximately 70%. This result is consistent with the measurement results where successful detection of three movers or higher is harder to achieve.

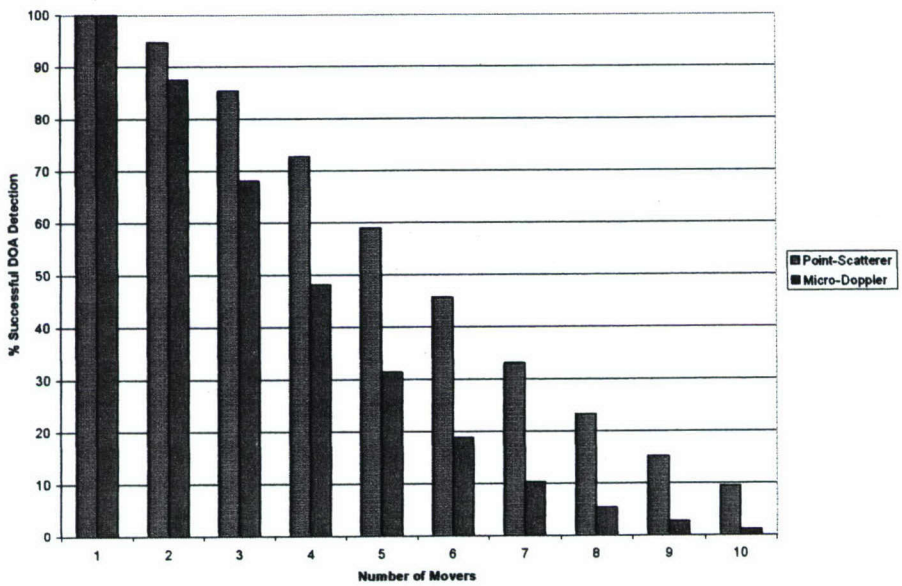

Fig. 21. Probability of successful DOA determination (to a 5° accuracy) versus the number of movers for both the point scatterer model (blue) and a model including human microDoppler (red).

In this program, we have demonstrated a very low-complexity, low-cost radar sensor concept for tracking moving humans. The capabilities of human tracking in one-, two- and three-dimensions were designed, implemented and tested. While the concept was shown to be sound, our results did point out some challenges that should be addressed in future research. In particular, the robustness of the system should be further improved, especially to deal with complex through-wall scenarios, dynamic clutters and human microDoppler phenomenon. Of course, any improvements in performance will need to come at the price of higher complexity and higher cost. We have briefly investigated several potential ideas. One is to increase the number of receiver elements and incorporate software beamforming algorithms into our radar architecture. The other is to use a network of low-cost distributed Doppler sensors, and fuse the resulting data to locate human subjects. These ideas are discussed in [C5, C6]. They should be further researched to ascertain their potential for improving the performance of the current generation of DDOA sensors.

C. FOLLOW-UP STATEMENT:

During this program, we have carried out in-depth research in human detection and tracking in urban environments. We have designed a number of radar sensors, collected a large database of measured data, carried out extensive data analysis and feature interpretation, developed simulation tools and gained a basic understanding of these phenomena. Furthermore, we have carried out signature exploitation efforts to utilize these phenomena in human detection, tracking and imaging. The potential impact of this research to DARPA's Force Multiplier Program is a new low-cost radar sensor technology for personnel tracking and wide-area surveillance in urban areas.

D. PUBLICATIONS:

I. LIST OF JOURNAL ARTICLES (ONR supported in whole or in part)

1. A. Lin and H. Ling, "Frontal imaging of human using a three-element Doppler and direction-of-arrival (DDOA) radar," *Elect. Lett.*, vol. 42, pp. 660-661, May 2006.

2. A. Lin and H. Ling, "Three-dimensional tracking of humans using a very low-complexity radar," *Elect. Lett.*, vol. 42, pp. 67-68, August 2006.

3. A. Lin and H. Ling, "A Doppler and direction-of-arrival (DDOA) radar for multiple-mover sensing based on a two-element array," to appear in *IEEE Trans. Aerospace Electronic Syst.*, June 2007.

II. LIST OF CONFERENCE PROCEEDINGS (ONR supported in whole or in part)

1. A. Lin and H. Ling, "Human tracking using a two-element antenna array," SPIE Defense and Security Symposium, Radar Sensor Technology IX, vol. 5788, pp. 57-64, Orlando, FL, April 2005.

2. A. Lin and H. Ling, "Through-wall measurements of a Doppler and direction-of-arrival (DDOA) radar for tracking indoor movers," International IEEE AP-S Symposium, paper no. S099p03a, 4 pp., Washington, DC, July 2005.

3. A. Lin and H. Ling, "Two-dimensional human tracking using a three-element Doppler and direction-of-arrival (DOA) radar," 2006 IEEE Radar Conference, paper no. 7152, Verona, NY, April 2006.

4. A. Lin and H. Ling, "Location tracking of indoor movers using a two-frequency Doppler and direction-of-arrival (DDOA) radar," International IEEE AP-S Symposium, pp. 1125-1128, Albuquerque, NM, July 2006.

5. S. Sundar Ram, Y. Li, A. Lin and H. Ling, "Human tracking using Doppler processing and spatial beamforming," accepted for presentation at the 2007 IEEE Radar Conference, Boston, MA, April 2007.

6. Y. Kim and H. Ling, "Tracking a moving target with multiple Doppler sensors using artificial neural network," submitted for presentation at the 2007 IEEE AP-S Symposium, Honolulu, HI, June 2007.

III. LIST OF RELATED PRESENTATIONS

1. H. Ling, "Low-cost radar sensors for personnel detection and tracking in urban areas," DARPA Force Multiplier Program Kickoff, Austin, TX, May 17, 2005.

2. H. Ling, "Low-cost radar sensors for personnel detection and tracking in urban areas," Office of Naval Research, Washington, DC, July 8, 2005.

3. H. Ling, "Multiple scattering and microDoppler effects in radar imaging and target recognition," IMA Workshop on Imaging from Wave Propagation, Institute for

Mathematics and its Applications, University of Minnesota, Minneapolis, Minnesota, October 20, 2005.

4. H. Ling, "Low-complexity radar sensors for locating and tracking humans inside buildings," DARPA VisiBuilding Industry Day Briefing, November 14, 2005.

5. H. Ling, "Advanced in scattering center research," Air Force Research Lab, Wright-Patterson Air Force Base, Ohio, December 13, 2005.

6. H. Ling, "Low-cost radar sensors for personnel detection and tracking in urban areas," DARPA Force Multiplier Program Review, Austin, TX, December 16, 2005.

7. H. Ling, "Low-complexity radar sensors for personnel detection and tracking in urban areas," DARPA Force Multiplier Program Briefing, Washington, DC, January 10, 2006.

8. A. Lin, "A low-complexity radar for human tracking," Naval Research Laboratory, Washington, DC, April 17, 2006.

V. LIST OF THESES AND DISSERTATIONS

M.S. Theses

P. Tabrizi, "An adaptive leakage signal canceller for a CW radar," May 2006.

S. Sundar Ram, "Investigation of and improvements to a continuous wave radar system for human detection through walls," May 2006.

Ph.D. Dissertations

A. Lin, "A low-complexity radar for human tracking," May 2006.

VI. RELATED CONTRACTS AND GRANTS

H. Ling, "Exploitation of microDoppler and multiple scattering phenomena for radar target recognition," Office of Naval Research, October 1, 2002 - May 31, 2006.

H. Ling and D. Tanner, "A passive radar sensor exploiting existing wireless infrastructures," Texas Advanced Technology Program, January 1, 2004 – August 31, 2006.

J. Li, E. Banatoski, H. D. Foltz, H. Ling and J. S. Son, "Acquisition of ultra-wideband measurement and modeling facilities for multidisciplinary research," Major Research

Instrumentation Award, National Science Foundation, August 15, 2004 – Aug. 14, 2007.

E. INTERACTIONS/COLLABORATIONS WITH NAVY SCIENTISTS:

Our participation in the Virtual Electromagnetic Design program funded by the High-Performance Computing Office since 2004 is a forum where we come into close contact with a number of Navy scientists, including Dr. Mark Kragalott of Naval Research Laboratory and Dr. John Asvestas of NAVAIR, Patuxent River, MD.

Our graduate student Mr. Adrian Lin presented a talk at Naval Research Laboratory in April 2006 on his dissertation research on human tracking. He was hosted by Dr. Victor Chen of NRL.

F. NEW DISCOVERIES, INVENTIONS, OR PATENT DISCLOSURES:

None.

G. HONORS AND AWARDS:

Mr. Adrian Lin, a graduate research assistant, was a finalist at the student paper competition at the 2006 IEEE Radar Conference held in Verona, NY. Ms. Shohba Sundar Ram will participate in the student paper competition at the 2007 IEEE Radar Conference to be held in Boston, MA.

APPENDIX

Selected Publications Supported by

ONR Research Grant N00014-05-1-0722

Frontal imaging of human using three-element Doppler and direction-of-arrival radar

A. Lin and H. Ling

A two-dimensional Doppler and direction-of-arrival (DDOA) radar concept is proposed for the frontal imaging of humans. The system consists of a three-element receiver array configured to provide simultaneous DOA measurements in the azimuth and elevation planes. An experimental system has been built and tested. Two-dimensional frontal images of a human in free space as well as in a through-wall scenario are generated.

Introduction: Through-wall sensing of humans using radar is a topic of current interest for security, surveillance and search-and-rescue operations. Various aspects of human sensing have been investigated recently, including micro Doppler of humans [1–3] and position tracking and imaging using ultra-wideband systems [4, 5]. Ultra-wideband imagers utilise wideband pulses to gather range information and a one-dimensional aperture to resolve in azimuth. Consequently, the resulting imagery is a top-view of the target. While this type of imaging setup is useful for targets such as airplanes and ground vehicles, for human targets the frontal image may provide more information than the top-view. To acquire the frontal image, a two-dimensional collection aperture is required, leading to a significant increase in complexity.

In this Letter, we present a two-dimensional frontal imager by using only a three-element receiving array and a transmitter. The concept entails resolving the micro Doppler frequencies of the returned signals from a moving human, and then measuring the phase difference at each Doppler frequency component to determine the direction-of-arrival (DOA) of the various body parts. If each body part gives rise to a different Doppler frequency, then the resulting bearing map should correspond closely to a two-dimensional frontal view of the human. An experimental system operating at 2.4 GHz has been designed and constructed to test the concept. The system consists of a three-element receiving array configured to provide simultaneous DOA measurements in both the azimuth and elevation planes. Measurement results on a human subject are presented.

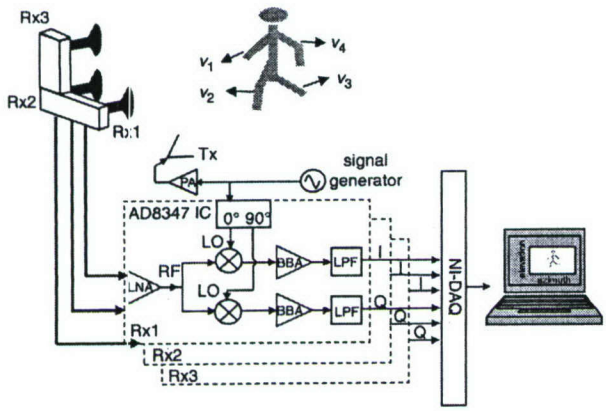

Fig. 1 *Radar system block diagram and conceptual operation*
Moving body parts (arms, legs) of a human produce different Doppler returns and are imaged by the radar

Radar concept: Fig. 1 shows the conceptual operation and the radar system block diagram. Different moving body parts of a human give rise to micro Doppler shifts with respect to the radar. Therefore, by first Doppler processing the data, we can extract the DOA information of the different Doppler frequency bins by measuring the phase difference among the receiver elements. Previously, we have reported on a one-dimensional bearing tracking system for multiple humans in the azimuth plane using a two-element Doppler and DOA radar [6]. The azimuth DOA of the received signals can be obtained from the measured phase difference between the two array outputs, $\Delta\phi = \phi_2 - \phi_1$, using the expression $\theta_{AZ} = \sin^{-1}(\lambda_c \Delta\phi / 2\pi d)$, where d is the spacing between the two antennas. In this work, an additional receiving antenna (Rx3) is placed directly above Rx2. Since Rx2 and Rx3 are placed vertically apart, they form a new array pair to acquire the DOA in the elevation plane, θ_{EL}. By correlating the azimuth and elevation bearing information at each Doppler bin f_{Di}, a data matrix $[A(f_{Di}), \theta_{AZ}(f_{Di}), \theta_{EL}(f_{Di})]$ can be constructed, where $A(f_{Di})$ is the radar return strength at the Doppler bin f_{Di} Provided that each body part gives rise to a different Doppler frequency, the resulting $[A, \theta_{AZ}, \theta_{EL}]$ corresponds to an approximate two-dimensional frontal image of the human.

Radar design: The radar consists of a continuous-wave transmitter operating at a frequency of 2.4 GHz and three receiver elements. Three off-the-shelf quadrature receiver boards from Analog Devices (AD8347 IC) are used. The receiving antennas consist of three microstrip patches fabricated on 1.6 mm FR-4 substrate. The antennas are separated by $\lambda_c/2$, where $\lambda_c = 6.25$ cm, to provide the maximum resolution within the range $-90°$ to $90°$ while avoiding any DOA ambiguity. After downconversion, the received signals are digitised by an NI-DAQ 6024E system. Since human movements produce time-varying Doppler shifts, the digitised signals are processed using a short-time Fourier transform (STFT) for Doppler separation before the DOA calculations are carried out. An integration time of 0.5 s and a Kaiser window with $\beta = 10$ are used in the STFT.

Results: We first use three loudspeakers as stable calibration targets to validate the system. The approximate (azimuth, elevation) co-ordinates of the three loudspeakers are $(-15°, 5°)$, $(-5°, 25°)$ and $(5°, 5°)$ with respect to the radar receivers. The loudspeakers are driven by audio tones of 20, 30 and 66 Hz, respectively. Fig. 2*a* shows the measured azimuth DOA against time. The azimuth DOA of the three loudspeakers are found to be at the expected positions of $-15°$, $-5°$and $5°$. Fig. 2*b* shows the elevation DOA against time, which correspond to the expected elevations of $5°$ and $25°$. After correlating the azimuth and elevation measurements at each of their Doppler bins, a two-dimensional location mapping of the three loudspeakers can be constructed accordingly (Fig. 2*c*), which agrees well with the actual placement of the loudspeakers (Fig. 2*d*).

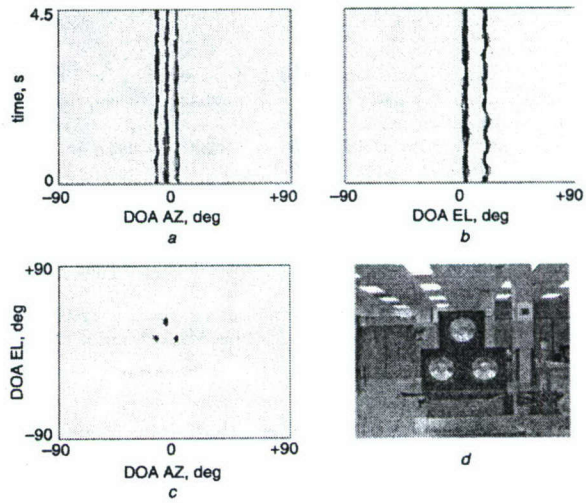

Fig. 2 *Measured data from three loudspeakers driven at three different audio tones*
a Azimuth DOA against time
b Elevation DOA against time
c Resulting frontal image
d Photo of actual loudspeaker placement

Next we use the same setup on a human subject. The subject stands at 2 m from the radar boresight. The height of the subject is approximately 1.8 m. During the measurement period the subject remains at the 2 m distance while moving each body part sequentially. After correlating the azimuth and elevation DOA measurements based on their Doppler information, a two-dimensional or frontal view of the human is

constructed (Fig. 3*a*). The measured frontal view shows the position of each limb, making an outline of the subject. The dynamic range of the image is 40 dB. The measurement is then repeated *in situ* with a 5-inch-thick gypsum/wooden wall in an interior room. The subject stands at approximately 1 m behind the wall while the radar measures the return against time. Fig. 3*b* shows the measured through-wall view of the human. Compared with the free-space image shown in Fig. 3*a*, the through-wall image appears larger since the subject stands closer to the radar. The image also appears to be less focused owing to the significant attenuation from the wall. However, the outline of the human is still visible. The dynamic range of the image is 20 dB and the transmitted power used is −10 dBm.

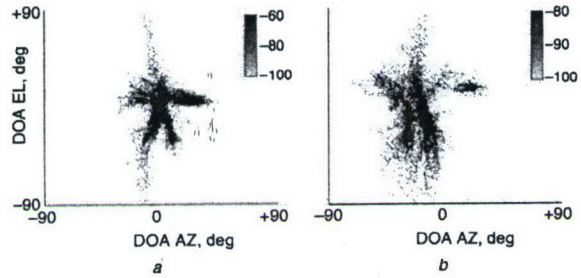

Fig. 3 *Measured frontal view of human in free space and of human through indoor wall*

a Measured frontal view of human in free space
b Measured frontal view of human through indoor wall

Conclusions: A very low complexity radar concept for generating the two-dimensional frontal image of a human is presented. The concept exploits the Doppler separation among the moving body parts, and derives their corresponding two-dimensional DOA using only a three-element receiver array. Measurements were performed using a low-cost, three-element receiver array operating at 2.4 GHz. By correlating the azimuth and elevation DOA measurements based on the Doppler information, the two-dimensional locations of the moving body parts were derived to construct a frontal view of a human in free space. The through-wall measurement result, showed some agreement with the free-space result, albeit at a much lower signal-to-noise ratio. It is worth pointing out that, while the proposed radar has very low complexity, it is based on the assumption that different body parts give rise to different Doppler frequencies. When this condition is not met in practice, the resulting bearing information is not accurate. Therefore, the present radar concept can be termed an 'imaging of opportunity' that captures glimpses of the human subject. This is similar to other types of target-motion induced sensing schemes such as inverse synthetic aperture radar.

Acknowledgments: This work is supported by the Office of Naval Research, the Texas Higher Education Coordinating Board under the Texas Advanced Technology Program and the National Science Foundation Major Research Instrumentation Program.

5 February 2006
Electronics Letters online no: 20060355
doi: 10.1049/el:20060355

A. Lin and H. Ling (*Department of Electrical and Computer Engineering, The University of Texas at Austin, Austin, TX 78712, USA*)
E-mail: adrian.lin@mail.utexas.edu

References

1 Geisheimer, J.L., Greneker, E.F., and Marshall, W.S.: 'High-resolution Doppler model of the human gait', *SPIE Proc., Radar Sensor Technology and Data Visualization*, 2002, **4744**, pp. 8–18
2 Chen, V.C., and Ling, H.: 'Time-frequency transforms for radar imaging and signal analysis' (Artech House, Norwood, MA, 2002), Chap. 8
3 Dorp, P., and Van Groen, F.C.A.: 'Human walking estimation with radar', *IEE Proc., Radar Sonar Navig.*, 2003, **150**, pp. 356–365
4 Hunt, A.R.: 'A wideband imaging radar for through-the-wall surveillance', *SPIE Proc., Sensors, and Command, Control, Communications, and Intelligence (C3I) Technologies*, 2004, **5403**, pp. 590–596
5 Tatoian, J.Z., Franceshetti, G., Lackner, H., and Gibbs, G.G.: 'Through-the-wall impulse SAR experiments'. IEEE Antennas Propagation Society Int. Symp. Dig., July 2005, paper S099p04u
6 Lin, A., and Ling, H.: 'Human tracking using a two-element antenna array', *SPIE Proc., Radar Sensor Technology and Data Visualization*, 2005, **5788**, pp. 57–64

Three-dimensional tracking of humans using very low-complexity radar

A. Lin and H. Ling

A low-complexity radar for human tracking in three-dimensional space is reported. The system consists of a three-element receiving array and two continuous-wave (CW) frequencies configured to provide azimuth bearing, elevation bearing and range measurements. Doppler processing is used for clutter removal as well as to separate multiple moving targets. A radar prototype is constructed and tested. Three-dimensional tracking of multiple humans is performed in both unobstructed and through-wall scenarios.

Introduction: Human detection and tracking is a topic of interest in security and surveillance applications. A popular approach for through-the-wall imaging is to use ultra-wideband (UWB) [1–4], which offers high down-range resolution. To obtain cross-range location information, UWB radars use either a physical or synthetic aperture. High angular resolution is needed for the cross-range localisation of targets at long distances, leading to the requirement of a large aperture. Furthermore, for human detection and tracking in an indoor setting, clutter suppression becomes challenging and requires complex signal filtering algorithms.

In this Letter we present a low-complexity radar architecture capable of tracking multiple humans in three dimensions. The concept entails using Doppler pre-processing to suppress stationary clutter as well as to distinguish multiple movers based on their different Doppler frequencies. A three-element receiver is then used to determine two-dimensional bearing information for each target. The phase difference measurement from the horizontal two-element array is used to obtain the azimuth direction of arrival (DOA), while that from the vertical two-element array is used for the elevation DOA. In addition, the phase difference measured at two CW frequencies is used for target ranging. Therefore, the entire receiver system comprises only three antenna elements and four receiver modules. A radar prototype is designed and constructed to test the concept. Measurement results on human subjects are presented.

Radar concept and design: Fig. 1*a* shows the radar system block diagram. Earlier, we reported on the one- and two-dimensional DOA tracking of multiple movers using a single CW frequency [5, 6]. Here our system operates at two CW frequencies fc_1 (2.4 GHz) and fc_2 (2.39 GHz). The two CW frequencies are combined, amplified and transmitted simultaneously. The scattered wave off a target is received by three antennas connected to the radar receivers. The local oscillator (LO) frequency of receivers Rx_1, Rx_2 and Rx_3 is set to fc_1, and that of Rx_4 is set to fc_2. The downconverted signal for each receiver is lowpass filtered and digitised, and the time-varying Doppler spectrum of the targets is obtained by applying the short-time Fourier transform (STFT). To determine the DOA and the range, we compare the phase differences between the receiver outputs at each Doppler frequency component. The elevation and azimuth DOA are found, respectively, by the formulas $\theta_{EL}=sin^{-1}(\lambda_{c1}\Delta\phi_{32}(f_D)/2\pi d)$ and $\theta_{AZ}=sin^{-1}(\lambda_{c1}\Delta\phi_{21}(f_D)/2\pi d\cos\theta_{EL})$, where λ_{c1} is the wavelength of fc_1, $\Delta\phi_{mn}(f_D)$ is the phase difference between the two array outputs m and n at the Doppler frequency f_D, and d is the spacing between the two horizontal or vertical antennas. The received signal at Rx_3 is also routed into Rx_4, but mixed with LO2 at fc_2. The phase difference, $\Delta\phi_{43}$, is then measured to calculate the target range, R, using the following expression: $R=c\Delta\phi_{43}(f_D)/4\pi\Delta f$, where $\Delta f=fc_1-fc_2$ and c is the speed of light. Since the phase difference $\Delta\phi_{43}$ is modulo 2π, it follows that the maximum unambiguous range is 15 m. By correlating the range and DOA information at each Doppler bin f_D, a data matrix $[A(f_D), \theta_{AZ}(f_D), \theta_{EL}(f_D), R(f_D)]$ can be constructed, where $A(f_D)$ is the radar return strength at the Doppler bin f_D. This resulting map shows the three-dimensional locations and strengths of the targets, provided that the targets have different Doppler frequencies. Fig. 1*b* shows the photo of the radar receivers. The three antennas are microstrip patches with 5 cm spacing between each horizontal and vertical pair. Four off-the-shelf integrated quadrature receivers are used. A window size of 0.5 s is used in the STFT.

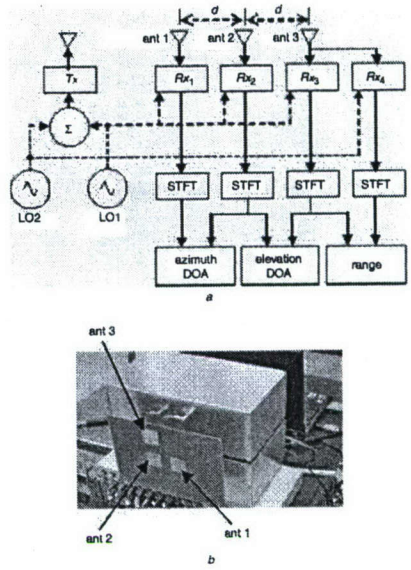

Fig. 1 *Radar system block diagram, and radar receiver prototype photo*
a Radar system block diagram
b Radar receiver prototype photo

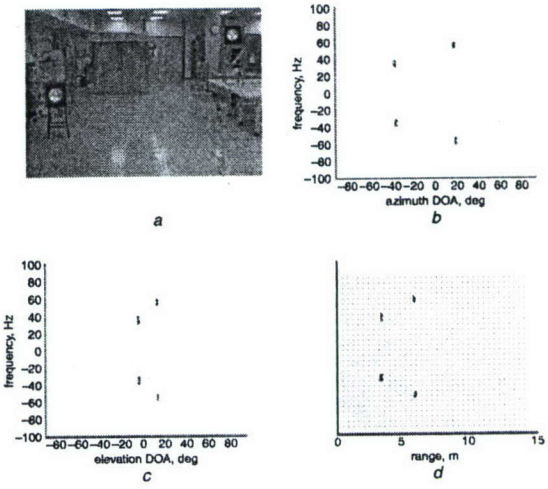

Fig. 2 *Measured data from two loudspeakers driven at two different audio tones*
a Photo of actual loudspeaker placement
b Doppler against azimuth DOA
c Doppler against elevation DOA against time
d Doppler against range

Results: The radar is first tested using loudspeakers driven by audio amplifiers at different monotones. Fig. 2*a* shows the measurement setup and the loudspeakers' locations. The first loudspeaker is located at the approximate (θ_{AZ}, θ_{EL}, R) co-ordinate of (−40°, −5°, 3 m) and driven by a 35 Hz audio tone. The second loudspeaker is positioned at approximately (20°, 15°, 6 m) and driven by a 55 Hz audio tone. Figs 2*b–d* show, respectively, the measured azimuth DOA, the elevation DOA and the range plotted against Doppler frequency. Excellent agreement with the expected locations of the targets in bearing and range is observed. Further, it is seen that the Doppler discrimination allows us to determine the three-dimensional locations of two (or more) targets.

Three-dimensional tracking of two human subjects is shown next. Two human subjects walk back-and-forth along straight paths at approximately the same speed but in opposite directions (Fig. 3*a*). During the walk, the radar continuously measures and outputs the azimuth bearing, the elevation bearing and the range of the subjects (Figs. 3*b–d*). During the first four seconds of the measurement, Fig. 3*b* shows two distinct azimuth-bearing trajectories: the first one progres-

sing from approximately −20° towards −60°, and the second one from 20° to 15°. The elevation tracks of the two human subjects are shown in Fig. 3*c*; however, the tracks are not distinguishable since the subjects walk on the same elevation plane (at ground level). Fig. 3*d* shows the measured range tracks, which criss-cross as the subjects walk back-and-forth. By using the spherical-to-Cartesian transformation, the corresponding front view and top view maps are constructed and shown in Figs. 3*e* and *f*, respectively. The top view in Fig. 3*f* shows good agreement with the actual walking paths in Fig. 3*a*.

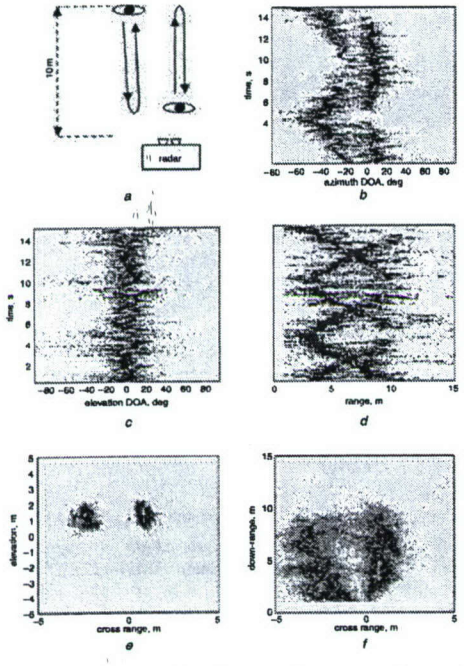

Fig. 3 *Measurement results of two human subjects in unobstructed indoor environment*

a Walking patterns up to 10 m distance
b Azimuth DOA against time
c Elevation DOA against time
d Range against time
e Cross-range against elevation (front view)
f Cross-range against down-range (top view)

A through-wall measurement is also conducted with the radar situated indoors next to an exterior wall while a human subject on the opposite side of the wall walks in a straight path away from and towards the radar. The starting position is approximately 4 m from the radar up to a maximum distance of 35 m (Fig. 4*a*). The wall construction is a 15″-thick double-brick with supporting internal wooden frames and insulation materials. Fig. 4*b* shows the range measurement of the subject during the walk. Since the maximum unambiguous range is 15 m, the measured range repeats whenever the subject walks past an integer multiple of 15 m of distance from the radar. During the first 17 seconds, the subject travels twice the 15 m distance plus the remaining 5 m, as evidenced by the three distinct range tracks during the time interval 0 to 5 s, 5 to 14 s, and 14 to 17 s. Thus, the radar is capable of measuring a human subject at least up to 35 m away through this wall. The transmitter output power used is +11 dBm.

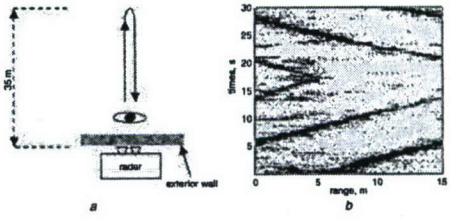

Fig. 4 *In situ range measurement of walking human through 15-inch-thick exterior brick wall*

a Setup
b Measured range track of up to 35 m

Conclusion: A low-complexity radar concept for tracking multiple humans in three-dimensional space (azimuth, elevation and range) has been presented. Measurements using a prototype consisting of three antenna elements and four integrated receivers operating at 2.4 and 2.39 GHz have been performed to validate the concept. The three-dimensional tracking of moving humans is realised by correlating the range, azimuth and elevation DOA measurements based on their Doppler information. The in situ measurement result through a 15-inch thick exterior brick wall showed tracking up to a distance of 35 m.

Acknowledgments: This work is supported by the Office of Naval Research, the Texas Higher Education Coordinating Board under the Texas Advanced Technology Program and the National Science Foundation Major Research Instrumentation Program.

8 May 2006
Electronics Letters online no: 20061432
doi: 10.1049/el:20061432

A. Lin and H. Ling (*Department of Electrical and Computer Engineering, The University of Texas at Austin, Austin, TX 78712, USA*)

E-mail: adrian.lin@mail.utexas.edu

References

1 Attiya, A.M., *et al.*: 'UWB applications for through-wall detection'. IEEE Antennas Propagation Society Int. Symp. Dig., April 2000, Vol. 3, pp. 1868–1875
2 Hunt, A.R.: 'A wideband imaging radar for through-the-wall surveillance', *SPIE Proc., Sensors, and Command, Control, Communications, and Intelligence (C3I) Technologies*, September 2004, **5403**, pp. 590–596.
3 Tatoian, J.Z., *et al.*: 'Through-the-wall impulse SAR experiments'. IEEE Antennas Propagation Society Int. Symp. Dig., July 2005, Paper no. S099p04u
4 Yang, Y., and Fathy, A.E.: 'See-through-wall imaging using ultra wideband short-pulse radar system'. IEEE Antennas Propagation Society Int. Symp. Dig., July 2005, Vol. 3B, pp. 334–337
5 Lin, A., and Ling, H.: 'Human tracking using a two-element antenna array'. Proc of. SPIE, Radar Sensor Technology IX, Orlando, FL, USA, April 2005, Vol. 5788, pp. 57–64
6 Lin, A., and Ling, H.: 'Two-dimensional human tracking using a three-element Doppler and direction-of-arrival (DDOA) radar'. Proc. IEEE Radar Conf., April 2006, Paper no. 7152

A Doppler and Direction-of-Arrival (DDOA) Radar for Multiple-Mover Sensing Based on a Two-Element Array

Adrian Lin and Hao Ling

Department of Electrical and Computer Engineering
The University of Texas at Austin
Austin, TX 78712

Abstract

A low-cost, two-element receiving array concept is investigated for detecting multiple moving targets in indoor surveillance applications. Conventional direction of arrival (DOA) detection requires the use of an antenna array with multiple elements. Here we investigate the use of only two elements in the receiver array. The concept entails resolving the Doppler frequencies of the returned signals from the moving targets, and then measuring the phase difference at each Doppler frequency component to calculate the DOA of the targets. Simulations are performed to demonstrate the concept and to asses the DOA errors for multiple movers. An experimental system is designed and constructed to test the concept. The system consists of a two-element receiver array operating at 2.4 GHz. Measurement results of human subjects in indoor environments are presented, including through-wall scenarios.

Keywords: Doppler, direction of arrival, radar, human tracking, through-wall

1 Introduction

The need for detecting moving targets (such as humans) and their locations is becoming one of the key necessities in security and surveillance systems, especially for law enforcement, counter-terrorism and urban warfare. Information such as the number of combatants and their locations can aid in decision making. Therefore, the capability of detecting multiple targets is an important feature in such systems. Recent work on radar detection of humans has focused mainly on the Doppler characteristics from a single human [1-5], or the ultra-wideband imaging of an entire scene [6-9].

Multiple target detection using a Doppler radar system has been explored in [10]. The system uses a superheterodyne receiver architecture operating at a 10.53 GHz carrier frequency to detect the velocity and acceleration of a rocket-driven flare. The Doppler returns are downconverted, digitized and processed using the short-time Fourier transform (STFT) [11, 12]. Multiple targets can then be detected as long as they move at different velocities, and their accelerations can be calculated by observing the rate of Doppler changes with respect to time as the result of the STFT process. The system, however, does not provide the bearing information of the targets.

In order to acquire the bearing information or the direction of arrival (DOA) of multiple targets, the standard approach is to use multiple receiving elements and to apply a direction finding algorithm such as MUSIC or ESPRIT [13, 14]. Such methods require the number of elements to be at least one greater than the maximum number of targets. That is, they require at least N + 1 elements to detect N targets. However, increasing the number of elements leads to an increase in the physical size, cost and complexity of the overall system.

In this paper, we explore the use of a low-cost, two-element receiving array for detecting multiple moving targets. The DOA of a mover is obtained from the phase difference of the reflected waves arriving at the two receiving antennas. However, a two-element receiving array is not able to resolve the DOA from multiple targets due to multiple wavefronts arriving simultaneously at the two receiving antennas. We exploit the fact that the different moving targets typically give rise to different Doppler shifts with respect to the radar. Therefore, by processing the data via Doppler discrimination, we can extract the DOA information by measuring the phase difference at each Doppler frequency component.

Numerical simulations are first conducted to test the concept. Detection of two movers is simulated to analyze factors influencing the DOA accuracy such as the Doppler separation between movers. A Monte Carlo simulation is then performed to predict the DOA error resulting from the reduced Doppler separation due to multiple movers. The confidence level of correctly detecting the DOA versus the number of movers is generated accordingly.

An experimental radar system is designed and constructed to test the concept. The system consists of a two-element antenna array, dual-quadrature integrated receivers (Analog Devices AD8347 ICs) and a transmitter operating at a frequency of 2.4 GHz. Since this IC is targeted for the consumer wireless market, it is extremely low cost. Microstrip antennas are used, resulting in a small form factor. The receiver uses a direct conversion architecture [15], eliminating the need of the second mixing process and filtering as in the superheterodyne architecture. The received signals are downconverted, digitized and processed for Doppler and DOA calculations. Measurement results of the

DOA from multiple targets are presented. The limitations of the proposed system resulting from DOA ambiguity of multiple moving targets are studied. The performance of the system under through-wall scenarios is also reported.

2 Basic Theory

To obtain the DOA information, consider a two-element receiver array as shown in Fig. 1(a). Assuming the far-field case, the incoming wave scattered off the target arrives at the two antennas with a path length difference x of:

$$x = d \sin \theta \tag{1}$$

where d is the spacing between the two antennas and θ is the DOA of the target. The measured phase difference $\Delta\psi$ of the two array outputs can be expressed in terms x by:

$$\Delta\psi = \frac{2\pi}{\lambda_c} x \tag{2}$$

where λ_c is the wavelength of the carrier frequency. Therefore, the DOA of the target can be obtained by:

$$\theta = \sin^{-1}\left(\frac{\Delta\psi}{2\pi d / \lambda_c} \right) \tag{3}$$

However, this scheme works when only one target is present. When multiple targets are present, the incoming signal at the two antennas is the summation of the scattered waves from all the targets. The individual phase information of each target is no longer available and therefore their corresponding DOA are not resolvable.

To obtain the DOA of multiple targets, we take advantage of the Doppler discrimination that is possible for moving targets. Referring to Fig. 1(b), consider the

signals arriving at the two receivers, $s_1(t)$ and $s_2(t)$. For the sake of simplicity, we assume that the scattered waves arriving at the receivers have the same strength. After the demodulation, the signals can be expressed as:

$$s_1(t) = e^{j\psi_1(t)} + e^{j\psi_2(t)} \tag{4}$$

$$s_2(t) = e^{j(\psi_1(t)+\Delta\psi_1)} + e^{j(\psi_2(t)+\Delta\psi_2)} \tag{5}$$

The phase term $\psi_n(t)$ of target n can be expressed as:

$$\psi_n(t) = -2\pi\left(\frac{2R_{0n}}{\lambda_c} - \frac{2v_n t}{\lambda_c}\right) \tag{6}$$

where R_{0n} and v_n are respectively the initial distance and the radial velocity of target n with respect to the radar. Similar to equation (2), the term $\Delta\psi_n$ is the phase delay due to the position of the antenna elements and the direction of the incident wavefront for target n.

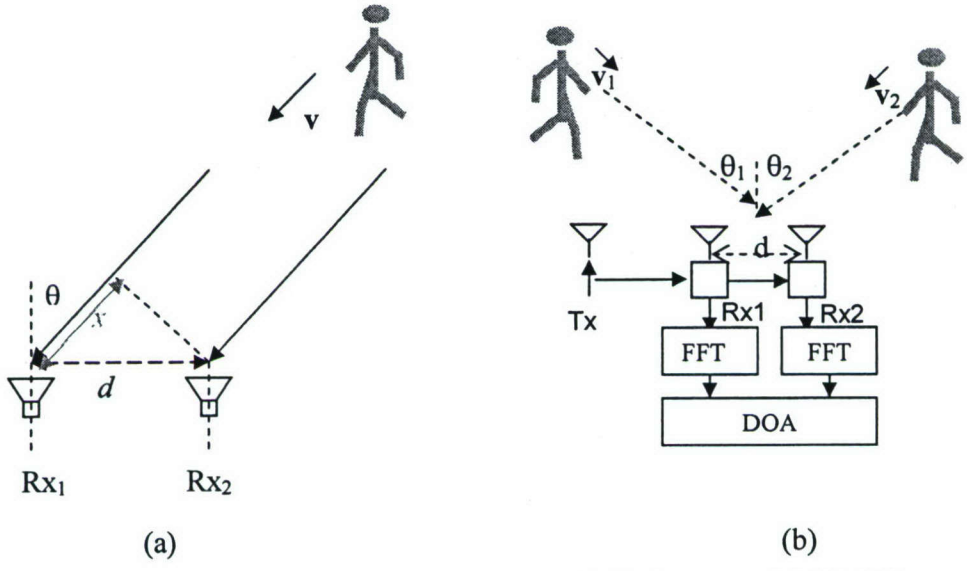

Figure 1. DOA detection using a two-element array: (a) Single target and (b) Multiple targets.

Next, we process each signal by the Fourier transform. By assuming infinite integration time and ignoring the constant term, the signals become:

$$S_1(f_D) = \delta(f_D - f_{D_1}) + \delta(f_D - f_{D_2}) \tag{7}$$

$$S_2(f_D) = \delta(f_D - f_{D_1})e^{\Delta\psi_1} + \delta(f_D - f_{D_2})e^{\Delta\psi_2} \tag{8}$$

where $f_{Dn} = 2v_n/\lambda_c$ is the Doppler frequency of target n. The phase difference $\Delta\psi_n$ at Doppler bin f_{Dn} for target n can be calculated as:

$$\Delta\psi_n(f_{Dn}) = \angle S_1(f_{Dn}) - \angle S_s(f_{Dn}) \tag{9}$$

If the targets generate different Doppler frequencies due to the difference in their radial velocities with respect to the radar, then the DOA of target n with respect to the receiver array boresight can be determined by:

$$\theta_n = \sin^{-1}\left(\frac{\angle S_1(f_{D_n}) - \angle S_2(f_{D_n})}{2\pi d/\lambda_c}\right) \tag{10}$$

which is similar to equation (3). It can be seen from equation (10) that this concept applies as long as the Doppler frequencies from different targets are sufficiently distinct.

3 Simulations

Two simulations are performed to test the concept. The first simulation is used to evaluate the DOA calculation result as the Doppler spacing between the two movers is reduced. The second simulation is used to assess the DOA error as the result of reduced Doppler spacing for more than two movers.

Fig. 2(a) shows the simulation result of the Doppler frequency versus DOA from two moving targets. The Doppler of the first target is 8 Hz with a DOA of -20° while the second target has 80 Hz Doppler and +20° DOA. An FFT integration time of 0.25 second and Kaiser windowing with $\beta = 1$ are used in the Doppler processing. Under this

Doppler spacing (8:80), the algorithm produces the correct DOA information for both targets. The Doppler of the first target is then increased to 76 Hz while its DOA is kept at -20°. With the reduced Doppler spacing (76:80), the DOA of the two targets become hard to identify and are erroneous (as shown in Fig. 2(b)). This is expected since the minimum resolvable Doppler separation is 4 Hz due to the 0.25 second integration time.

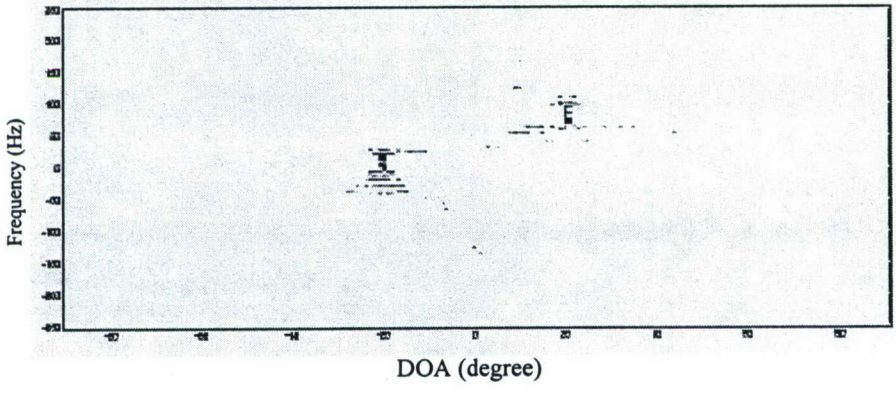

(a)

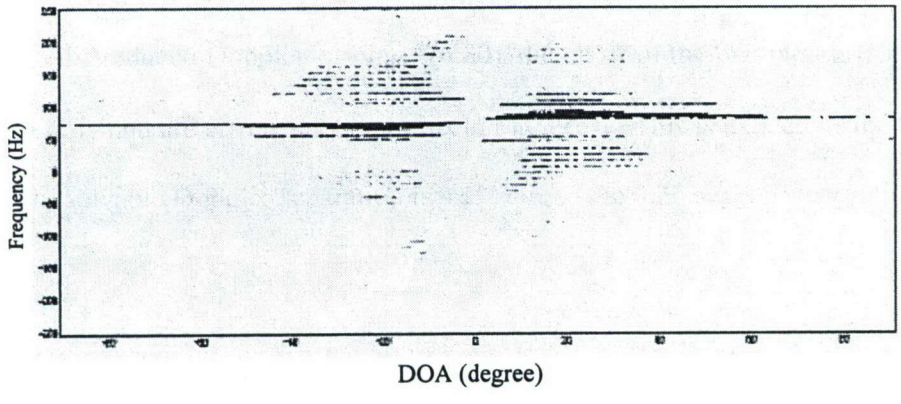

(b)

Figure 2. Simulations for two targets: (a) Doppler spacing 8:80 and (b) Doppler spacing 76:80

To predict the DOA error behavior as the result of reduced Doppler spacing for two or more movers, we run a more exhaustive Monte-Carlo simulation with more realistic

input parameters. The simulations input parameters include a spatial boundary of 10 m by 10 m, moving targets with speeds with uniform distributions from 0 m/s to 6 m/s, and a direction that is uniformly distributed from 0 to 2π. A carrier frequency of 2.4GHz is assumed. Two or more moving targets are placed inside the boundary with the selected velocities. These parameters are used to mimic people in a typical indoor environment. Amplitude decay as a function of $1/r^4$, where r is the distance of the target from the radar, is also accounted for in the simulation. The decay calculation is included to evaluate the effect of the received signal strengths of the two targets on the DOA calculation. Fig. 3(a) illustrates the simulation setup. The Monte Carlo simulations use the monostatic configuration where both the receiver and transmitter are co-located at the (0,0) coordinate. One hundred thousand realizations are generated. The DOA errors with respect to the Doppler separation of multiple moving targets are calculated. However, only the worst DOA error of all targets is recorded in each realization. The recorded DOA errors are then plotted at the end of all realizations.

Figs. 3(b)-(d) show the simulation results for multiple moving targets, for two, five and seven movers. The worst case DOA error is plotted versus the Doppler separation between the targets. For each Monte Carlo sample, the target with the worst DOA error is identified first. The minimum Doppler separation between that target and the others is obtained next. The DOA error of that target is then plotted versus the minimum Doppler separation. The grey scale indicates the relative signal strengths between the targets, with the darker grey shades representing more similar strengths and the lighter ones representing a difference in strengths of more than 50 dB. As seen by the trend in Fig. 3(b), the DOA error generally gets larger when there is smaller Doppler separation

between the two targets, and vice versa. However, there are also cases that contain large DOA errors even though the Doppler separations are large. From their lighter shading, we know that they correspond to cases where there is a significant difference in the signal strengths of the two targets (more than 50 dB). This corresponds to the case when one target is located much closer to the radar (thus a much larger reflected signal) than the other. This phenomenon is referred to as the close-far effect, where the side-lobe energy from the stronger, close-in target contaminates the phase of the much weaker signal from the far-away target in its frequency bin.

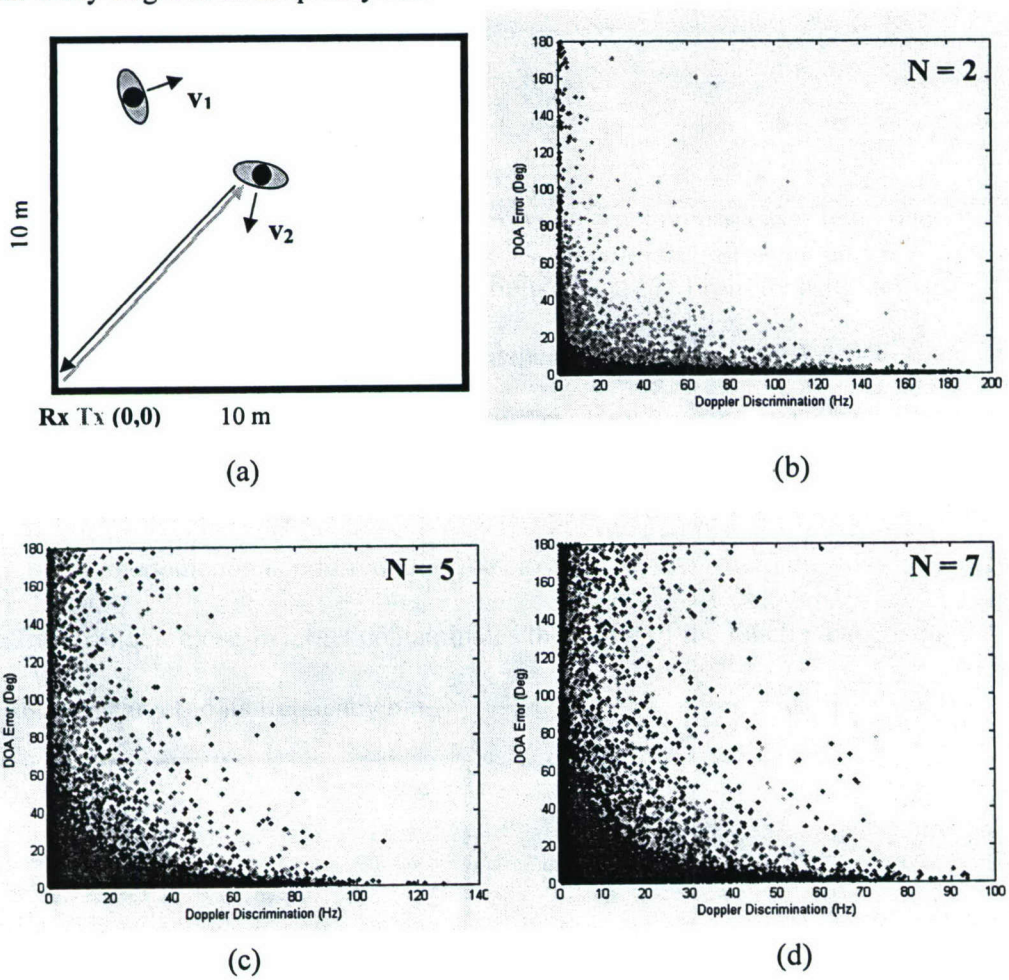

Figure 3. Monte Carlo simulations for N movers: (a) Setup and (b-d) Worst DOA errors vs. Doppler separation for N = 2,5 and 7, respectively.

As N increases, the DOA error increases, as observed in Figs. 3(c) and (d). At the end of the simulations, we count the number of successful DOA detections for a given number of movers. If the difference between the calculated and the expected DOA is less than 5° then the sample is considered a success. A profile of the percentages of successful DOA detections can be generated accordingly. As shown in Fig. 4, the percentage of successful cases decreases as the number of movers is increased. This is expected since a larger number of movers result in more occurrences of close Doppler spacing (similar velocities). From the simulation, it can be concluded that the DOA accuracy of the two-element system is affected by the number of movers. Nevertheless, a success rate of 70% can be maintained for four targets or fewer.

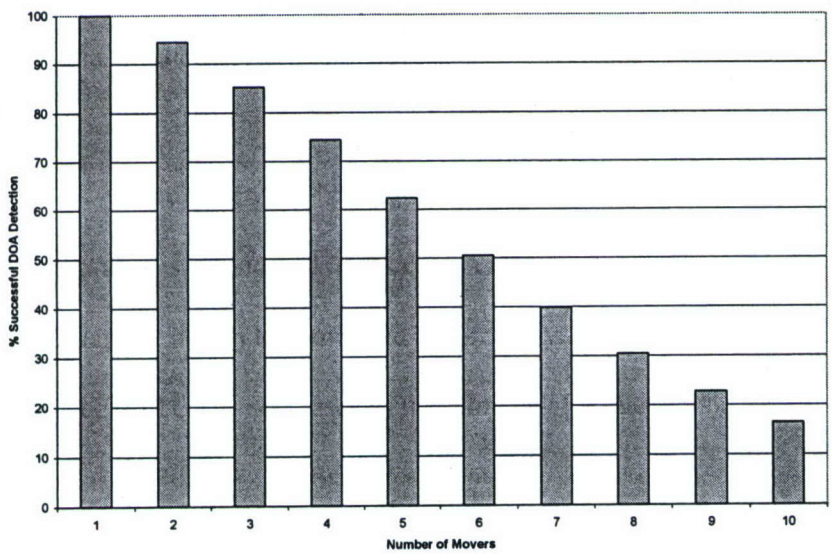

Figure 4. Successful DOA detection profile with 5° failure threshold.

The above simulation uses a point-scatterer model to study the system behavior as the number of movers is increased. In the actual case of human tracking, however, the Doppler spacing is further reduced by the overlapping micro-Doppler returns from the

body parts of each mover. Therefore, a more realistic model should be used to account for the micro-Doppler effects. In [16], we incorporated the micro-Doppler effects for human limbs in a similar simulation and found that the successful DOA detection rate is around 70% for *three* movers. This is more consistent with our observations on the actual measurement results.

It is also worthwhile to compare the performance of our two-element system to that of a multi-element array here. Our analysis has shown that the performance of the two-element system depends on the Doppler separation among multiple targets. The performance is worst when the targets have the same Doppler return, in which case the phase information from each target is not resolvable, leading to erroneous bearing determination. In a conventional multiple-element system, spatial beamforming can be utilized to obtain the locations of multiple targets. However, the bearing accuracy depends on the beamwidth of the array. Higher accuracy requires the use of a larger aperture (for narrower beamwidth) and correspondingly more array elements. Hence the implementation complexity and cost of such a system will be higher than that of the two-element system.

4 System Design and Implementation

An experimental radar system is designed and constructed to test the concept. Our radar receiver consists of a two-element direction-finding array, each with full quadrature detectors, to determine both the Doppler shift and the DOA of the target. The transmitter uses a continuous wave (CW) operating at 2.4 GHz carrier frequency. Two microstrip antennas are used as receiving antennas. The antennas are fabricated on a 1.6 mm thick FR-4 substrate with a dielectric constant of 4.3. Each patch is of dimensions 3 cm by 3

cm and follows the conventional half-wavelength microstrip antenna design [17]. The antennas are configured to receive the vertical polarization, since the human body is predominantly vertical (height is greater than width). The spacing between the feed points is 5 cm (slightly less than $\lambda_c/2$) to avoid DOA ambiguity while providing good sensitivity in the scanning range from -90° to 90°.

Two low-cost, off-the-shelf integrated boards manufactured by Analog Devices (AD8347) are used as the quadrature (or I/Q) receivers. Each receiver has the low-noise amplifier (LNA), I/Q mixers, gain control, and baseband amplifications all integrated on one chip. The chip allows a direct conversion from RF to baseband, eliminating the need for special analog filtering as in the superheterodyne conversion. Fig. 5 shows the radar system block diagram and the actual hardware implementation. Appendix A describes the range estimate of the system based on the radar equation. Appendix B discusses the procedure used to correct for the I/Q imbalance in the system.

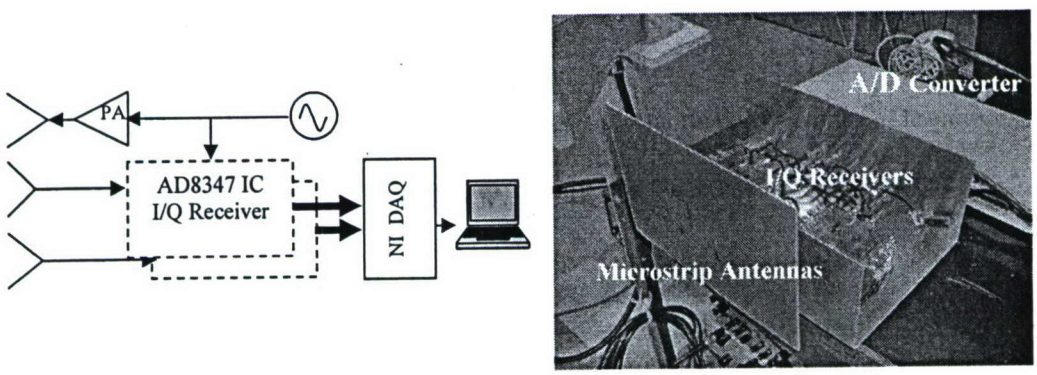

(a) (b)

Figure 5. Radar hardware: (a) System block diagram and (b) Hardware implementation

After being received and downconverted, the reflected signals from the moving targets are digitized by a 12-bit analog to digital converter (ADC) from National Instruments. The signals are sampled at a 500 Hz sampling rate, which is sufficient to sample humans movement data at 2.4 GHz. The sampled data are then logged into a computer and further processed using Matlab software. The signal processing is performed on the time domain data using the FFT to obtain the Doppler spectrum for each channel. By comparing the phase difference between the two Doppler spectra at each Doppler bin, we can then generate the DOA information one Doppler frequency at a time using Eq. (10).

5 Measurements

A series of measurements are conducted using the radar hardware to validate the simulations. The first measurement series is performed using loudspeakers driven by audio tones. The loudspeakers are chosen as calibration targets since they produce very stable and repeatable results. The next measurement series is carried out with human subjects.

5.1 Loudspeakers Measurements

To demonstrate multiple target detection, two loudspeakers are used. The vibrating membrane of each loudspeaker is covered by aluminum tape to enhance its return. The back-and-forth vibration of the membrane results in a radar return that is frequency modulated. The two loudspeakers are placed at -25°and -15° to the radar boresight and driven by a 55 Hz and a 35 Hz audio tone, respectively. Both loudspeakers are located at

about 4.5 m away from the radar and separated by 0.6 m from each other (Fig. 6(a)). Their expected Doppler returns are +/- 55 Hz and +/- 35 Hz with the DOA of -25° and -15°, respectively. The two-sided nature of the Doppler is due to the frequency modulation. The measured data are plotted in Fig. 6(b) and clearly show the expected returns.

To investigate the effect of Doppler separation on the DOA accuracy, the 55 Hz audio tone is lowered in 1 Hz decrement approaching the 35 Hz tone. Since the length of the FFT integration time used in this measurement is 1 s, the corresponding minimum resolvable Doppler separation is 1 Hz. Therefore, the DOA calculation is expected to be accurate up to about 1 Hz. The measured data is plotted in Fig. 6(c) and clearly shows that the DOA accuracy is still maintained for a 1 Hz Doppler separation. Both audio tones are then set to 35 Hz. Fig. 6(d) shows the measured data with the incorrect DOA as the result of zero Doppler separation.

(a)

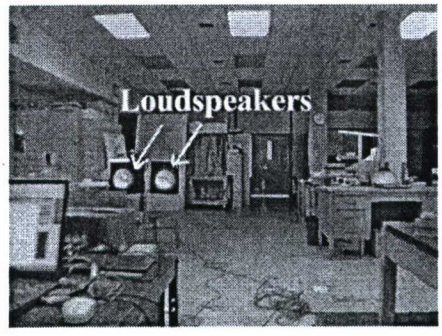

(b)

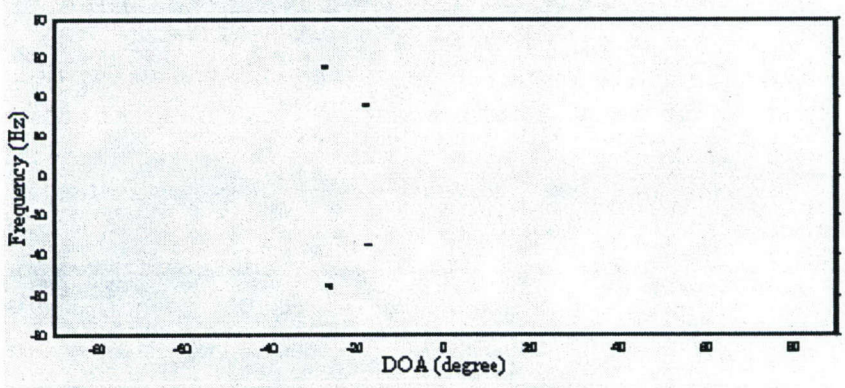

(c)

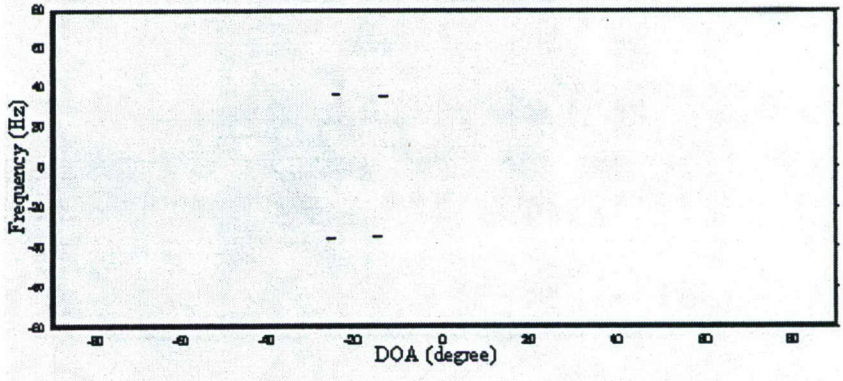

(d)

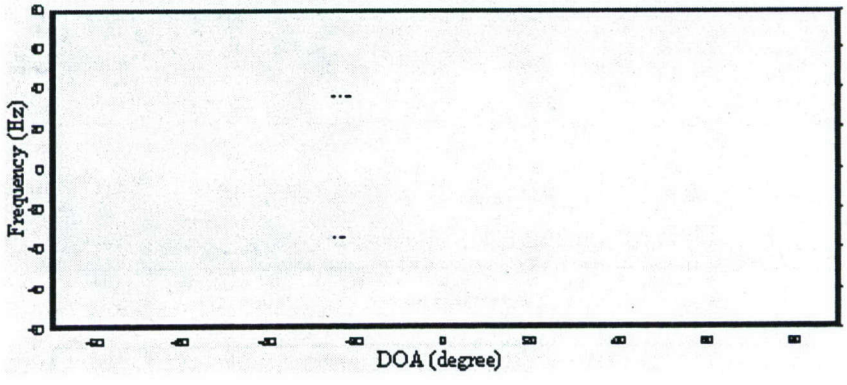

Figure 6. Two loudspeakers measurement: (a) Setup, (b) Doppler spacing (55:35), (c) Doppler spacing (36:35) and (d) Doppler spacing (35:35)

The next measurement involves three loudspeakers driven at different audio tones: 55, 75, and 35 Hz. The purpose is to demonstrate detection of more than two movers with using only a two-element array. They are placed at approximately -50°, -20° and +55° to the radar boresight at about 6.5, 10 and 2 m away from the radar (Fig 7(a)). Their expected Doppler returns are +/- 55 Hz, +/- 75 Hz and +/- 35 Hz with the DOA of -50°, -20° and +55°, respectively. The measured data are plotted in Fig. 7(b) and clearly show the expected returns. Also note from Fig. 7(a) that the environment is full of stationary clutter. However, they do not contaminate the DOA results due to the Doppler processing.

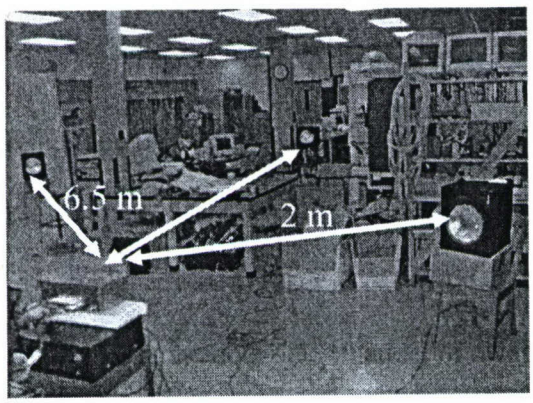

(a)

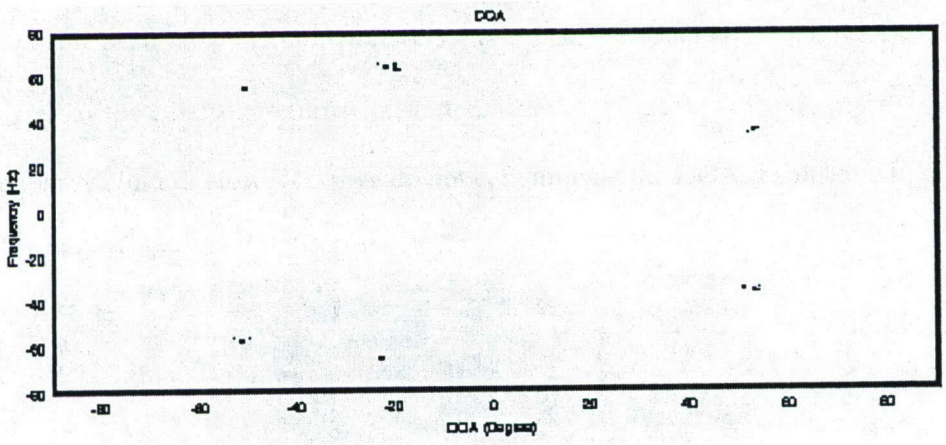

(b)

Figure 7. Three loudspeakers measurement: (a) Setup and (b) Measured Doppler and DOA.

It can be summarized from the loudspeaker measurements that the DOA accuracy can be maintained as long as there is sufficient Doppler separation. One of the factors influencing the Doppler separation is the integration time. Longer integration results in better Doppler resolution. However, long integration time might introduce other issues, especially for fast moving targets. This is similar to photography when shooting fast moving objects with a low shutter speed. In particular, Doppler returns from humans contain complex higher-order motions of body parts such as arms, legs, etc. The higher-order information is contained in the so-called micro Doppler returns [1-5]. The next set of measurements is taken on moving humans to analyze such phenomena affecting the DOA accuracy.

5.2 Human Measurements

Since radar returns from humans contain time-varying micro Doppler features, the measured data should be processed using the short-time Fourier Transform (STFT). The STFT is well-suited for analyzing a non-stationary signal. For a signal *s(t)*, its STFT is defined as:

$$STFT_s(t,f) = \int_{-\infty}^{+\infty} s(\tau)h(t-\tau)e^{-j2\pi f\tau}d\tau \qquad (11)$$

where *h(t)* is the sliding analysis window. Windowing the signal leads to a tradeoff in time resolution versus frequency resolution. Good time resolution requires a short duration sliding window, while good frequency resolution requires a long duration window. For the human measurements, we empirically determined that a good sliding

window duration to be around 1 second. The result of the STFT is then presented as a spectrogram, which is the squared modulus of its STFT.

Figure 8 shows the spectrogram of a human walking toward and away from the radar. As shown in the spectrogram, the micro Doppler modulation results in higher overall Doppler frequencies than the main body returns. For a 2.4 GHz carrier frequency the main body return of a human walking at 1.5 m/s produces a 24 Hz Doppler shift; however, the body parts produce much higher Doppler shifts up to one hundred Hertz.

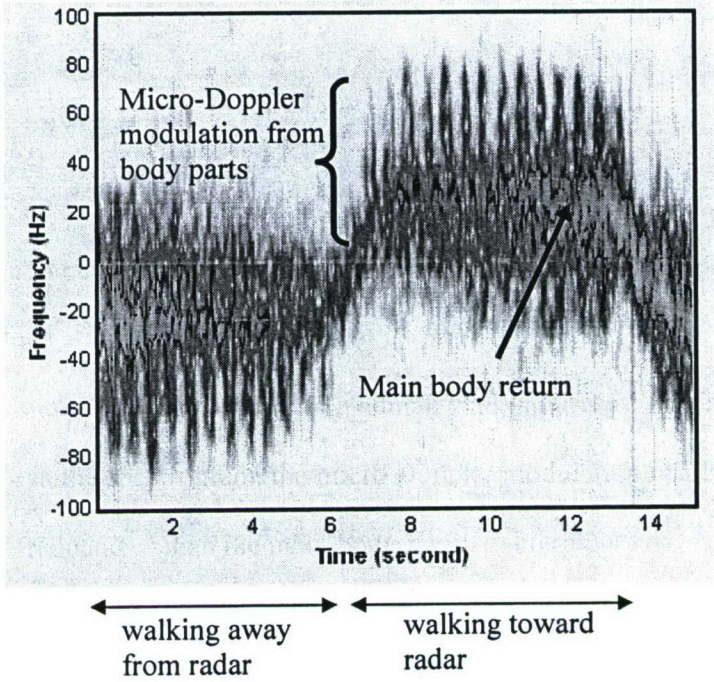

Figure 8. Spectrogram of a walking human.

If there are multiple humans walking simultaneously then there is a possibility that their micro Doppler returns will overlap with each other. The overlapping micro Doppler returns degrade the Doppler discrimination, which could lead to an increase in the DOA error.

Figure 9(a) shows the measurement setup for a walking human. The walking path starts at about 20° to the left of the radar. The subject walks in a straight path away from and then returns toward the radar. The turning point is approximately 10 m away from the radar. During the walk, the radar continuously measures and outputs the DOA of the subject (Fig. 9(b)). The grey scale indicates the strength of the returned signal, from black (strongest) to white (weakest). As expected, as the subject walks farther away from the radar the return signal gets weaker as indicated by the grey shades. The plot also shows that the signal fades out at approximately t = 4.5 second, when the subject stops and turns around toward the radar. When the subject stops the corresponding Doppler return falls into the zero Doppler bin and is filtered out by the software. Hence the signal appears to fade out the most during this time interval. The round-trip walking trajectory appears to be curved since it is plotted at the perspective or angular view of the radar.

The next measurement scenario involves a human walking from the right to the left of the radar as shown in Fig. 10(a). The starting position is approximately 40° to the right of the radar. As in the previous human measurement, the radar continuously collects and plots the DOA while the subject walks across the radar (Fig. 10(b)). As expected, the walking trajectory spans approximately ± 40° of the radar boresight. The DOA trace also shows detailed movements of the body parts as indicated by the arrows corresponding to the right and left feet of the subject. Through the time sequence, it is possible to identify that the subject's left foot reaches -20° at t = 2.5 s first. In the subsequent stride, the right foot reaches -40° at t = 4 s. Since the left foot is also closer toward the radar, its return is stronger than the right foot, as indicated by the arrow pointing to the darker shaded area on the plot.

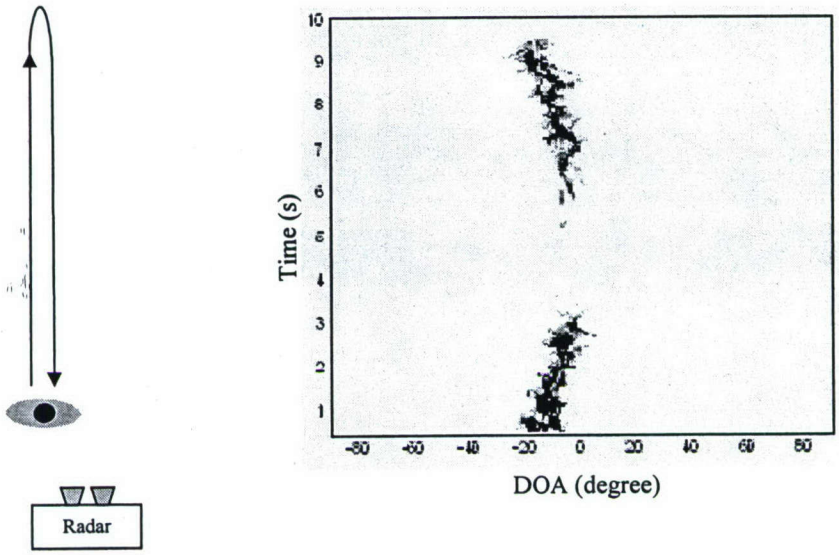

Figure 9. Measurement of a human walking away and towards the radar: (a) Setup and (b) DOA vs. time

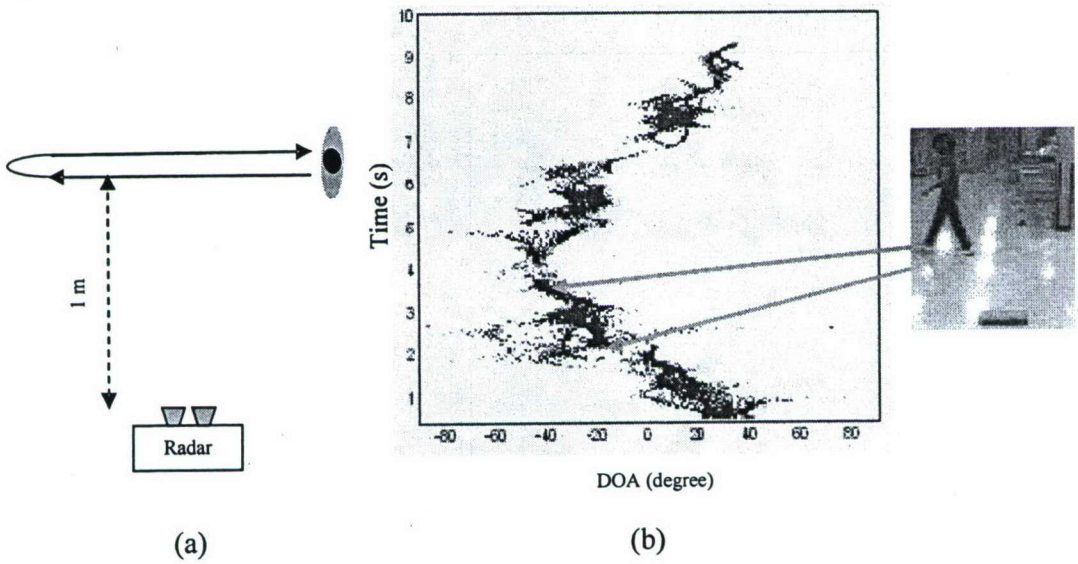

Figure 10. Measurement of a human walking across the radar: (a) Setup and (b) DOA vs. time

To demonstrate DOA detection of multiple targets, the next set of measurements involves multiple human subjects. Fig. 11(a) shows the setup for two humans walking at

the same speed but in opposite directions. As expected, the measured DOA vs. time plot (Fig. 11(b)) shows two traces corresponding to the angular positions of the two subjects as they walk during the data acquisition.

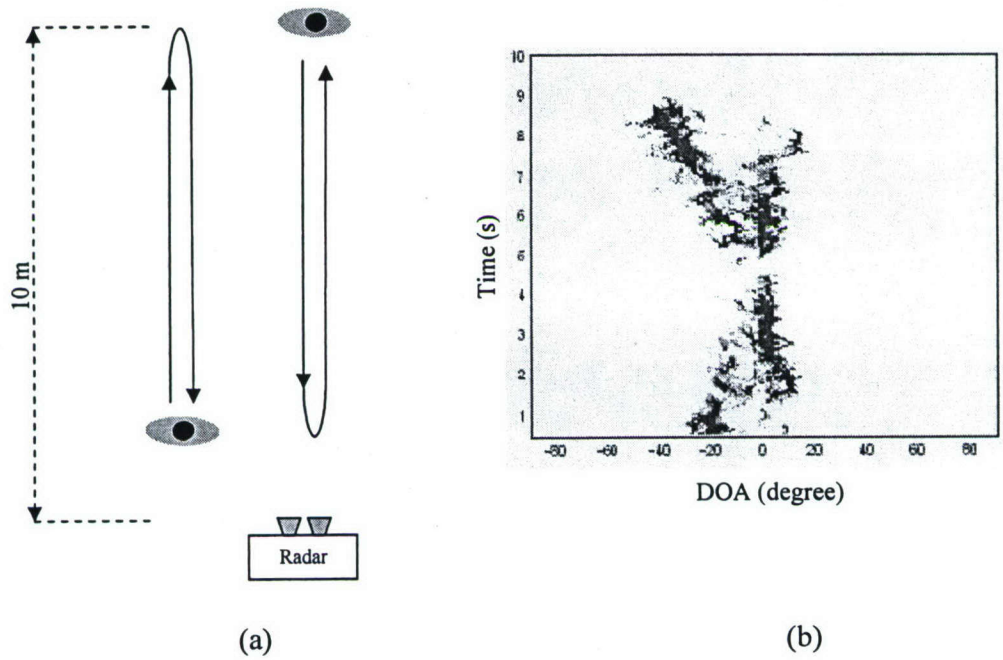

Figure 11. Measurement of two humans walking in opposite direction: (a) Setup and (b) DOA vs. time

In the next scenario, the two humans walk in the same direction, first away and then toward the radar (Fig. 12(a)). Since they move at about the same speed, their Doppler returns overlap significantly thus resulting in DOA error. As shown in Fig. 12(b), the overlapping instances appear as lines bridging across the two correct traces, as indicated by the arrow. This DOA behavior due to overlapping Doppler returns is similar to the earlier simulation result of Fig. 2(b). The system basically produces incorrect DOA under this condition. This is an intrinsic limitation of this radar, which we have addressed earlier in the simulation.

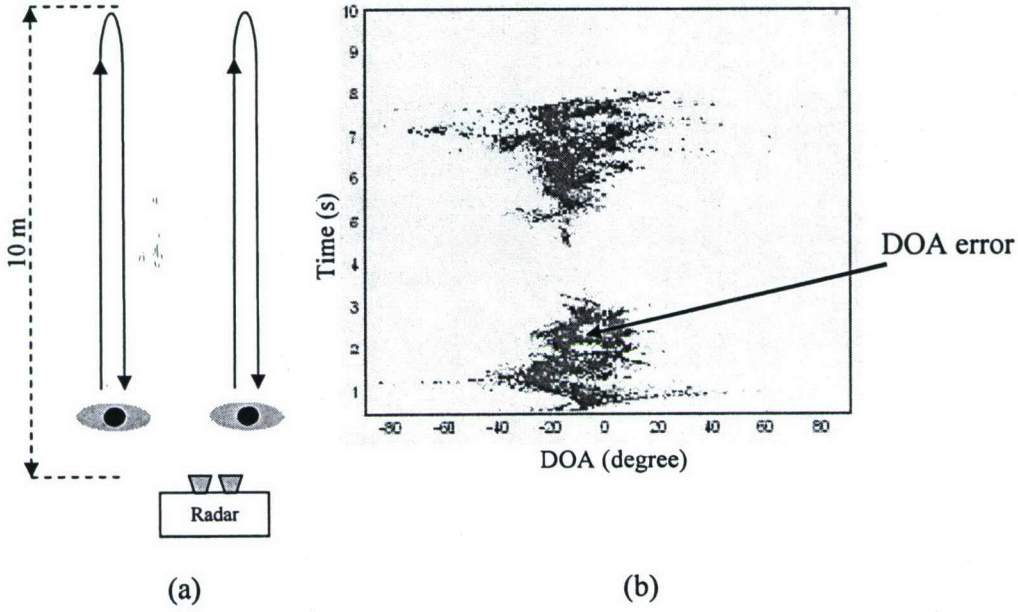

Figure 12. Measurement of two humans walking at the same speed: (a) Setup and (b) DOA vs. time

The last measurement set involves three human subjects. Two of the subjects walk at the same speed but in opposite directions while the third one walks sideways with respect to the radar boresight (Fig. 13(a)). The measured DOA vs. time plot (Fig. 13(b)) shows three traces corresponding to the angular positions of the three subjects as they walk during the data acquisition. Again, there are some instances where line features bridging across the three correct traces appear in the figure due to the overlapping Doppler returns. Such appearance is rather similar to the cross term effects in the Wigner-Ville distribution [11]. However, the radar is still capable of capturing three distinct targets over a large portion of the time intervals.

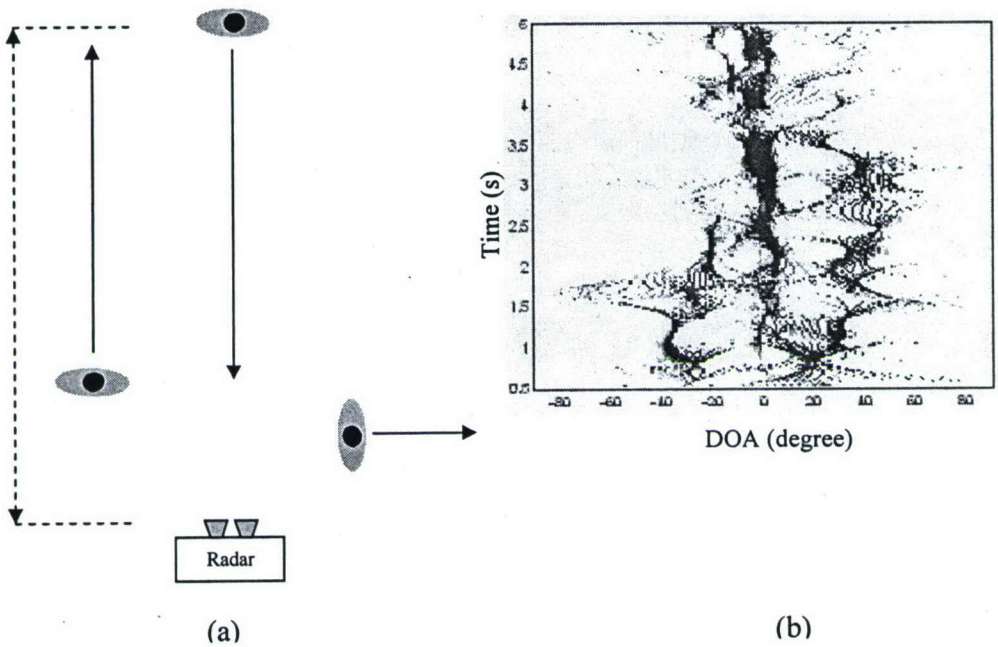

Figure 13. Measurement of three humans: (a) Setup and (b) DOA vs. time

6 Through-wall Measurements

Next, we evaluate the system performance in through-wall scenarios. Since a Doppler shift can only be induced by a moving target, Doppler sensing provides very good stationary clutter suppression. In through-wall scenarios, the returns from the wall itself fall into the DC bin and are filtered out while the Doppler frequency components are passed through, although attenuated. From [18], significant wall penetration is expected at 2.4 GHz compared to the higher frequencies.

Figure 14(a) shows the through-wall measurement setup where the radar is placed against a 15-inch exterior brick wall. Figure 14(b) shows the DOA vs. time of a human walking away and towards the radar on the opposite side with approximately a 10 m

maximum walking distance from the wall. In this scenario, the human walks in a straight path along the radar boresight. As expected, the corresponding trajectory is approximately straight at 0° DOA as shown in the measured data. We have also tested the through-wall performance using two loudspeakers placed at different locations off boresight (reported earlier in [19]). We found that the wall did not produce any noticeable effect on the DOA accuracy.

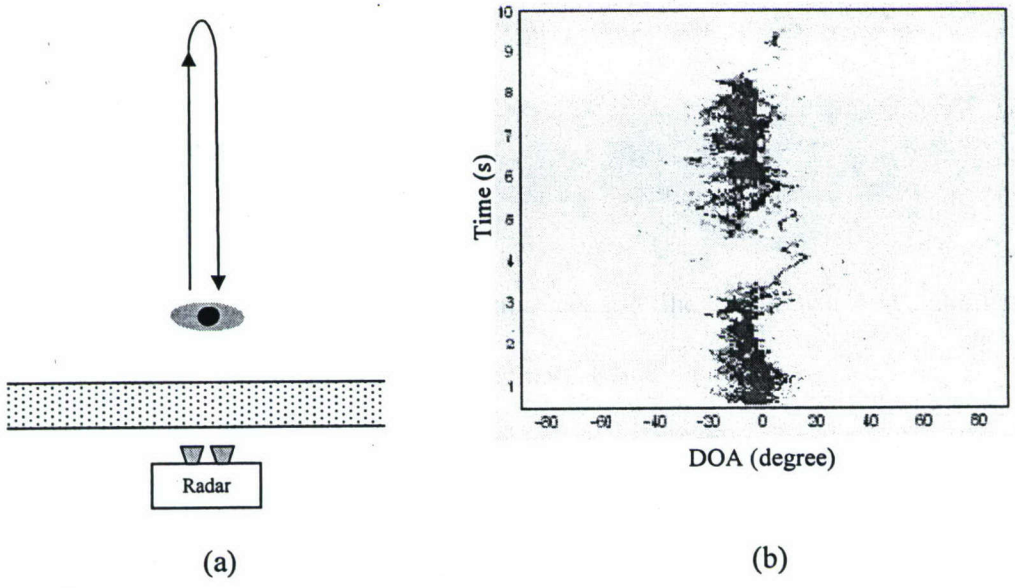

Figure 14. Through-wall measurement of a walking human: (a) Setup and (b) DOA vs. time

Measurements are also performed to evaluate the wall attenuation on the radar returns for different types of walls. A loudspeaker is used again as a test target, positioned at 4 m away from the radar boresight.

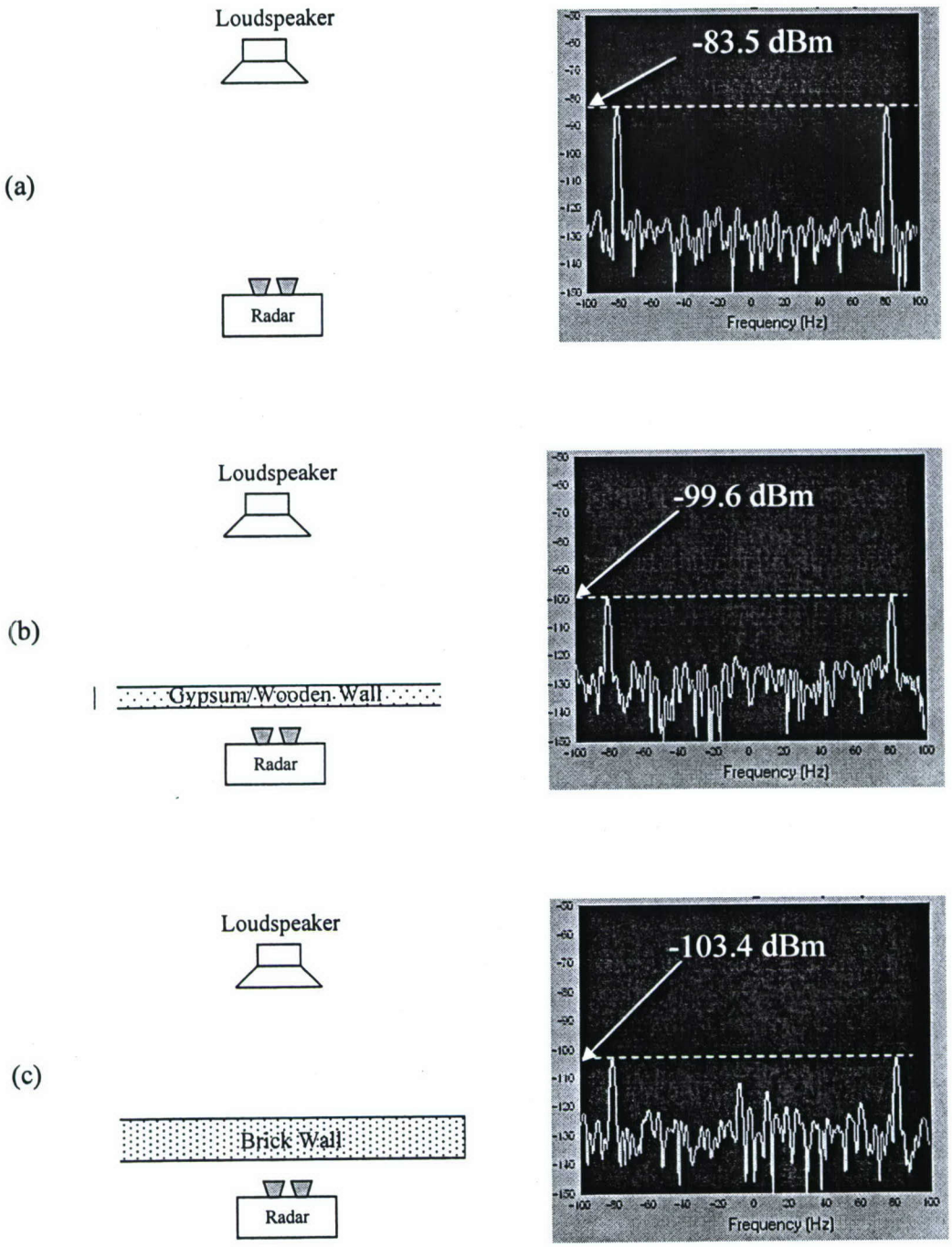

Figure 15. Wall attenuation measurements: (a) Free space, (b) 5" Gypsum/wooden wall and (c) 15" Brick wall

Three measurements are carried out: in free space (no wall), in-situ with a gypsum/wooden wall in an interior room, and in-situ with an exterior brick wall. As shown in Fig. 15, the processed radar returns are -83.5 dBm, -99.6 dBm and -103.4 dBm for the free space, the 5" gypsum/wooden wall and the 15" brick wall, respectively. Therefore, it can be concluded that the attenuations of the gypsum/wooden wall and brick wall are respectively 16 dB and 20 dB.

7 Conclusions

Simulation and measurement results of a Doppler and DOA radar for detecting multiple moving targets have been studied. The measurements were performed using a low-cost, two-element receiver array operating at 2.4 GHz. Based on the measurement results, it has been shown that simultaneous DOA detection of multiple movers using a two-element array is feasible. Our study also showed that the system could be used in indoor and through-wall scenarios due to the use of Doppler processing to suppress stationary clutters. Future work includes additional studies of through-wall scenarios. Extension of the concept to gather two-dimensional bearing and three-dimensional location information has also been investigated and reported in [21-24].

Acknowledgements

This work is supported by the Office of Naval Research, the Texas Higher Education Coordinating Board under the Texas Advanced Technology Program and the National Science Foundation Major Research Instrumentation Program. The authors thank S. Sundar Ram, Y. Yang and M. Starosta for their help in the data collection.

References

[1] J. L. Geisheimer, E. F. Greneker and W. S. Marshall, "High-resolution Doppler model of the human gait," *SPIE Proc., Radar Sensor Technology and Data Visualization*, vol. 4744, pp. 8-18, July 2002.

[2] V. C. Chen, "Analysis of radar micro-Doppler with time-frequency transform", *Proc. of the 10th IEEE Workshop on Statistical Signal and Array Processing*, pp. 463-366, Pocono Manor, PA, Aug. 2000.

[3] J. Li and H. Ling, "ISAR feature extraction from non-rigid body targets using adaptive chirplet signal representation," *IEE Proc. – Radar, Sonar and Navigation*, vol. 150, pp. 284-291, Aug. 2003.

[4] P. van Dorp and F. C. A. Groen, "Human walking estimation with radar," *IEE Proc. – Radar, Sonar and Navigation*, vol. 150, pp. 356-365, Oct. 2003.

[5] G. Greneker, "Very low cost stand-off suicide bomber detection system using human gait analysis to screen potential bomb carrying individuals," *SPIE Proc., Radar Sensor Technology and Data Visualization*, vol. 5788, p. 46-56, May 2005.

[6] A. M. Attiya, A. Bayram, A. Safaai-Jazi and S. M. Riad, "UWB applications for through-wall detection," *IEEE Antennas Propagat. Soc. Int. Symp. Digest*, vol. 3, pp. 1868-1875, Apr. 2000.

[7] S. Nag, H. Fluhler and M. Barnes, "Preliminary interferometric images of moving targets obtained using a time-modulated ultra-wideband through-wall penetration radar," *Proc. 2001 IEEE Radar Conf.*, pp. 64-69, May 2001.

[8] J. Z. Tatoian, G. Franceshetti, H. Lackner and G. G. Gibbs, "Through-the-wall impulse SAR experiments," *IEEE Antennas Propagat. Soc. Int. Symp. Digest,* paper no. S099p04u, July 2005.

[9] Y. Yang and A. E. Fathy, "See-through-wall imaging using ultra wideband short-pulse radar system," *IEEE Antennas Propagat. Soc. Int. Symp. Digest,* vol. 3B, pp. 334-337, July 2005.

[10] C. P. Bodenstein, W. C. Venter, G. J. Kahl, "A Doppler radar for multiple targets," *IEEE Trans. Instrumentation Measurement*, vol. 43, pp. 706-710, Oct.1994.

[11] S. Qian and D. Chen, *Introduction to Joint Time-Frequency Analysis – Methods and Applications*, Prentice Hall, Englewood Cliffs, NJ, 1996.

[12] V. Chen and H. Ling, *Time-Frequency Transforms for Radar Imaging and Signal Analysis*, Artech House, Norwood, MA, 2002.

[13] R. Schmidt, "Multiple emitter location and signal parameter estimation," *IEEE Trans. Antennas Propagation*, vol. 34, pp. 276-280, Mar. 1986.

[14] R. Roy, A. Paulraj and T. Kailath "ESPRIT – A subspace rotation approach to estimation of parameters of cissoids in noise," *IEEE Trans. Acoust., Speech, Signal Processing*, vol. ASSP-34, pp. 1340-1342, Oct.1986.

[15] B. Razavi, *RF Microelectronics*, Prentice-Hall, NJ, 1998.

[16] A. Lin, "A Low-complexity radar for human tracking," Ph.D. Dissertation, The University of Texas at Austin, May 2006.

[17] C. A. Balanis, *Antenna Theory*, John Wiley & Sons, 2nd Edition, 1997.

[18] T. B. Gibson and D. C. Jenn, "Prediction and measurement of wall insertion loss", *IEEE Trans. Antennas Propagation*, vol. 47, pp. 55-57, Jan. 1999.

[19] A. Lin and H. Ling, "Through-wall measurements of a Doppler and direction-of-arrival (DDOA) radar for tracking indoor movers," *IEEE Antennas Propagat. Soc. Int. Symp. Digest,* vol. 3B, pp. 322-325, July 2005.

[20] H. G. Park, C. Park, H. Oh and M. G. Kyeong, "RF gain/phase and I/Q imbalance error correction technique for multi-channel array antenna systems," *Proc. IEEE Vehicular Tech. Conf.*, vol. 1, pp. 175-179, May 2001.

[21] A. Lin and H. Ling, "Frontal imaging of human using a three-element Doppler and Direction-of-Arrival (DDOA) radar," *Electronics Letters*, vol. 42, pp. 660-661, May 2006.

[22] A. Lin and H. Ling, "Two-dimensional human tracking using a three-element Doppler and Direction-of-Arrival (DOA) radar," *Proc. 2006 IEEE Radar Conf.*, pp. 248-251, April 2006.

[23] A. Lin and H. Ling, "Location tracking of indoor movers using a two-frequency Doppler and Direction-of-Arrival (DDOA) radar," *IEEE Antennas Propagat. Soc. Int. Symp. Digest*, paper no. 1125, July 2006.

[24] A. Lin and H. Ling, "Three-dimensional tracking of humans using a very low-complexity radar," *Electronics Letters*, vol. 42, pp. 1062-1064, Aug 2006.

Appendix A. Radar Range Estimate

The radar equation is used to estimate the maximum operating range of our radar:

$$R_{\max} = \left(\frac{P_T G_T G_R \lambda_c^{\,2} \sigma}{(4\pi)^3 S_{NF} (S/N_{\min})} \right)^{1/4} \tag{12}$$

where

P_T = transmitter output power = -10.3 dBm
G_T = transmitter antenna (horn) gain = 7 dBi
G_R = receiver antenna (microstrip) gain = 1 dBi
λ_c = carrier frequency wavelength = 0.125 m
σ = human body radar cross-section = 0 dBsm
S_{NF} = system noise floor = -130 dBm
S/N_{min} = minimum signal-to-noise ratio = 10 dB

Using Eq. (12) with the parameters above, we estimate the maximum operating range of our radar for human detection in free-space to be 46.4 m. This free-space range estimate agrees fairly well with our outdoor measurements on human subjects. For the wall attenuations of 16 dB (gypsum/wooden wall) and 20 dB (brick wall), the estimated maximum operating ranges become 18.5 m and 14.7 m, respectively.

Appendix B. Correction for I/Q Imbalance

Since our radar uses the homodyne architecture, it is inherently sensitive to the hardware gain and phase errors of the in-phase and quadrature (I/Q) downconversion mixers [15]. The I/Q gain and phase errors introduce signals at the image frequencies of the actual downconverted signal, and may interfere with other target returns at those

frequencies. A correction algorithm is therefore needed to correct the I/Q gain and phase errors.

During the calibration, a known sinusoidal tone at a frequency of f_{dcal} above the carrier frequency f_c is injected at the RF input terminal. The signal level of the calibration tone is set to maximize the system dynamic range while avoiding input saturation. This level is typically 10 dB below the 1 dB input compression point of the system. After the calibration tone is downconverted, the actual I/Q gain and phase errors are measured at the frequency f_{dcal}.

The following equations are then used to represent the actual measured downconverted I and Q signals:

$$I = A(1+\varepsilon)\cos(\omega_{d_{cal}} t) \tag{13}$$

$$Q = A\sin(\omega_{d_{cal}} t + \psi) \tag{14}$$

where A is the signal amplitude, ε and ψ are the I/Q gain and phase errors respectively. The errors can then be corrected by the following equation [20]:

$$\begin{bmatrix} I_{corr} \\ Q_{corr} \end{bmatrix} = \begin{bmatrix} E & 0 \\ P & 1 \end{bmatrix} \begin{bmatrix} I \\ Q \end{bmatrix} \tag{15}$$

$$E = \frac{\cos\psi}{1+\varepsilon} \tag{16}$$

$$P = \frac{-\sin\psi}{1+\varepsilon} \tag{17}$$

The corrected I and Q signals then become:

$$I_{corr} = EI = A\cos(\omega_{d_{cal}} t)\cos\psi \tag{18}$$

$$Q_{corr} = PI + Q = A\sin(\omega_{d_{cal}} t)\cos\psi \tag{19}$$

As shown in Eqs. (18) and (19), the corrected I and Q signals are of equal amplitude and 90° of each other. Note that this algorithm works as long as the errors do not vary as a function of frequency. Since our radar has a very narrow bandwidth (250 Hz) and the errors are relatively stable throughout the bandwidth, the algorithm can therefore be employed. We typically use f_{dcal} of 40 Hz for the calibration.

Human Tracking Using a Two-Element Antenna Array

Adrian Lin and Hao Ling
Department of Electrical and Computer Engineering
The University of Texas at Austin
Austin, TX 78712

ABSTRACT

We investigate the use of a low-cost, two-element receiving array for tracking human movements in indoor surveillance applications. Conventional direction of arrival (DOA) detection requires the use of an antenna array with multiple elements. Here we investigate the use of only two elements in the receiver array. The concept entails simultaneously resolving the Doppler frequencies of the returned signals from the moving targets and the DOA of the targets. Simulation is performed to demonstrate the concept. Both the monostatic and the bistatic scenario where the transmitter and the receiving array are placed at different locations are investigated. DOA errors and tolerances are analyzed for each scenario. An experimental system is constructed to test the concept. The system consists of a two-element receiver array operating at 2.4 GHz. Measurement results of various collection scenarios are presented.

Keywords: Doppler, direction of arrival, radar, human tracking

1. INTRODUCTION

We explore the use of a low-cost, two-element receiving array for tracking human movements. The direction of arrival (DOA) of a moving human is obtained from the phase difference of the reflected waves arriving at the two receiver antennas. However, a two-element receiving array is unable to resolve individual DOA from multiple moving humans due to multiple phase differences arriving simultaneously at the two receiving antennas. Conventional methods are to increase the number of receiving elements and to apply direction finding algorithms such as MUSIC [1-3]. We investigate a way to overcome this issue while maintaining the use of a two-element receiving array for human tracking.

The basic concept of our approach is to detect both the Doppler frequency and the DOA information of the movers. Under a monostatic scenario, Doppler discrimination allows the detection of multiple movers, depending on the unique combination of speed and direction of each mover. An extra degree of discrimination freedom can be achieved in a bistatic scenario since the incident and reflected wave vectors of each mover are different, depending on the transmitter and receiver placement.

Extensive Monte Carlo simulation is performed to demonstrate the concept. Both the monostatic scenario and the bistatic scenario where the transmitter and the receiving array are placed at different locations are investigated. DOA errors resulting from the imperfect Doppler discrimination are analyzed for each scenario.

An experimental system is constructed to test the concept. The system consists of a two-element antenna array, dual-quadrature integrated receivers (Analog Devices AD8347 ICs) and a transmitter operating at a frequency of 2.4 GHz. Microstrip antennas are used, resulting in a small form factor. The received signals are downconverted, digitized and processed using the FFT for Doppler and DOA calculations.

Measurement results of the DOA from multiple targets are presented. The limitations of the proposed system resulting from DOA ambiguity of multiple moving targets are studied.

2. METHODOLOGY

Our radar receiver consists of a two-element direction-finding array, each with full quadrature detectors, to determine both the Doppler shift and the direction of arrival of the target. The transmitter uses a continuous wave (CW) operating at 2.4 GHz carrier frequency. The position of the transmitter and receiver can be arranged in a monostatic or a bistatic configuration.

In the monostatic configuration, the radar transmitter and receiver are co-located with Doppler shift given by $f_D = 2v/\lambda_c$. In the bistatic configuration, the radar transmitter and receiver are not located at the same position and the Doppler shift is given by $f_D = (\mathbf{u}_r - \mathbf{u}_i) \bullet \mathbf{v}/\lambda_c$. The bistatic radar Doppler frequency is related to the component of target velocity **v** along the difference of the reflected and incident unit vectors, $(\mathbf{u}_r - \mathbf{u}_i)$, and λ_c is the wavelength of the transmitted carrier. Since the Doppler shift is only induced for a moving target, Doppler sensing provides very good clutter suppression in a highly cluttered environment such as indoors.

The DOA of the received signal can be obtained by the measured phase difference of the two array outputs, $\Delta\phi = \phi_2 - \phi_1$, as follows: $\theta = \sin^{-1}(\lambda_c \Delta\phi / 2\pi d)$ where d is the spacing between the two antennas (Fig. 1). To provide the maximum resolution while avoiding DOA ambiguity within the scanning range of θ from -90° to 90°, the distance between the two antennas is set to $\lambda_c/2$.

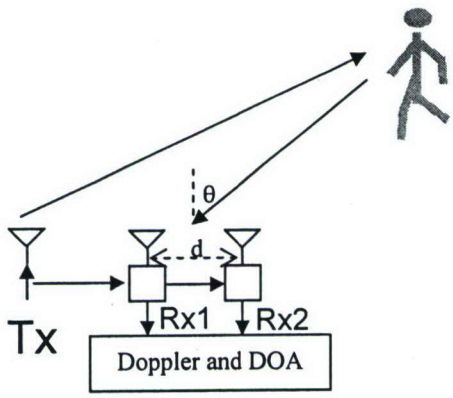

Figure 1. Basic radar operation.

For proof-of-concept, we have constructed a low-cost system that consists of a transmitter and a two-element direction-finding array. For the transmitter, an RF signal generator capable of outputting CW frequency at 2.4 GHz is utilized. For the receiver, an off-the-shelf IC receiver manufactured by Analog Devices (AD8347) is used. This integrated receiver has all the required features including low-noise amplifier (LNA), I/Q mixers, gain control, and baseband amplification. Low-pass filtering with a cut-off frequency of 250 Hz is used for anti-aliasing before the A/D converter. The National Instruments NI-DAC 6024E is used for digitizing the receiver output. Fig. 2 shows the system block diagram and the actual radar implementation.

The signals reflected from the moving targets are received, downconverted, digitized and processed using the FFT for Doppler discrimination. By measuring the phase difference at each Doppler frequency component, we can obtain the DOA information of multiple targets. This scheme works as long as their Doppler frequencies are sufficiently distinct. We discuss in the following section several cases where erroneous DOA information might occur as the result of poor Doppler discrimination.

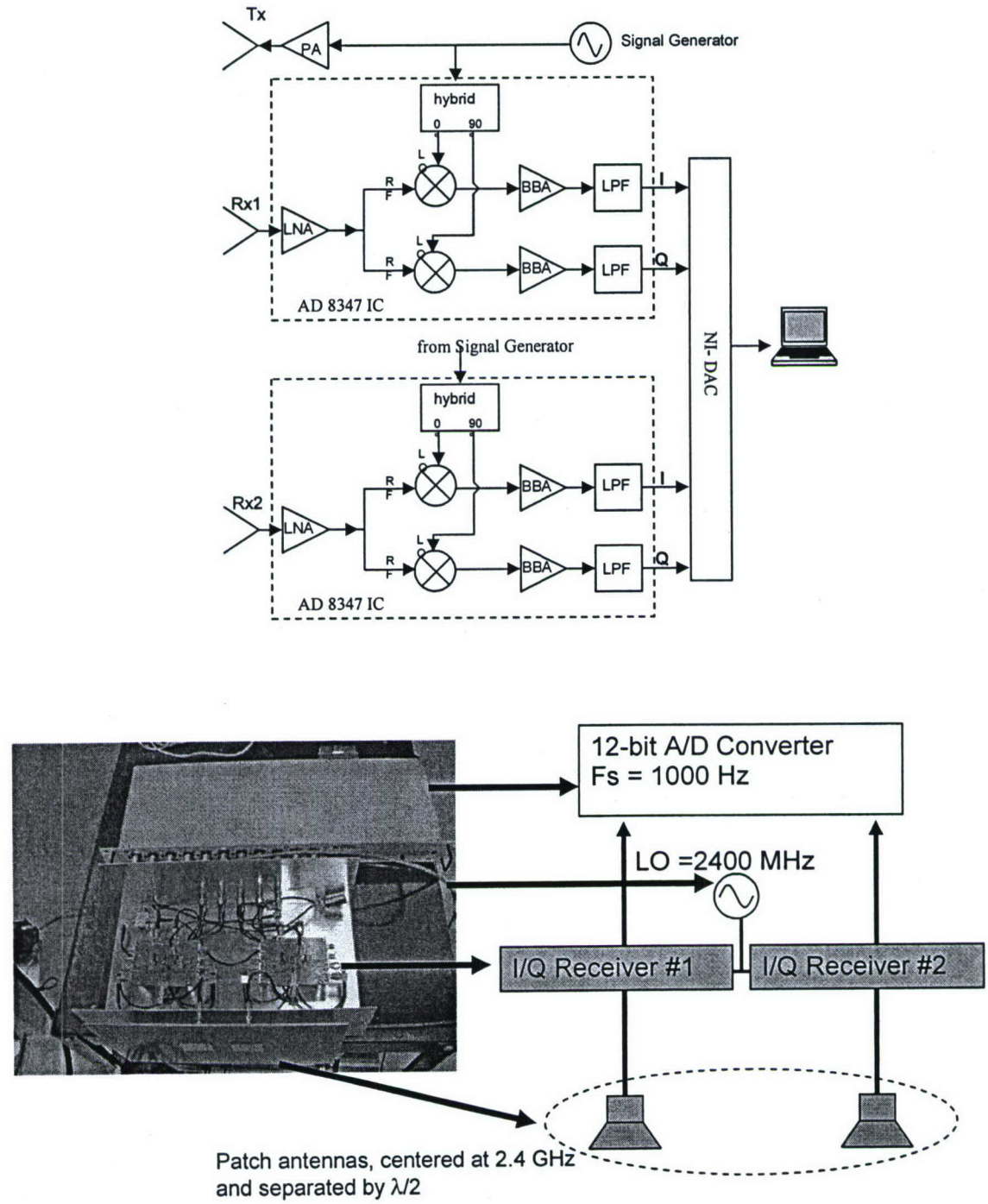

Figure 2. Radar system block diagram and actual hardware implementation.

3. SIMULATION DATA

Fig. 3 shows the simulation result of the Doppler and DOA from two moving targets. The Doppler of the first target is 8 Hz with a DOA of -20° while the second target has 80 Hz Doppler and +20° DOA. Both Doppler returns have the same received power level. Under this Doppler spacing (8:80), the detection algorithm produces the correct DOA information for both targets. The Doppler of the first target is then increased to 76 Hz while its DOA is kept at -20°. With the reduced Doppler spacing (76:80), the DOA of the two targets become hard to identify and are erroneous (as shown in Fig. 4). To predict the DOA error behavior as the result of reduced Doppler discrimination, we run a more exhaustive Monte-Carlo simulation with more realistic input parameters.

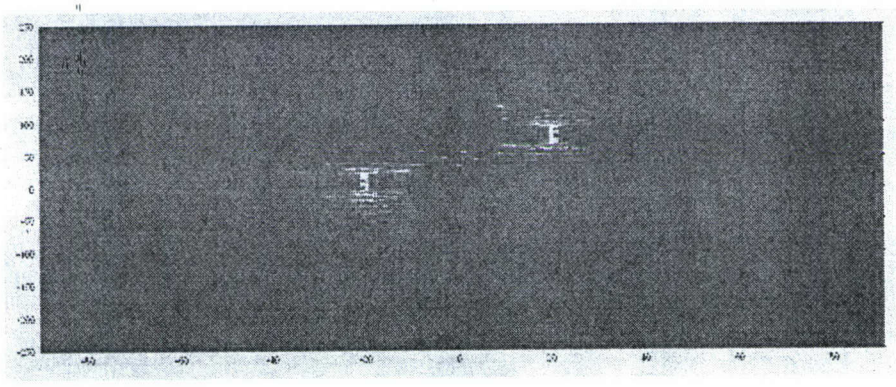

Figure 3. Doppler and DOA simulation result of two moving targets (Doppler spacing 8:80).

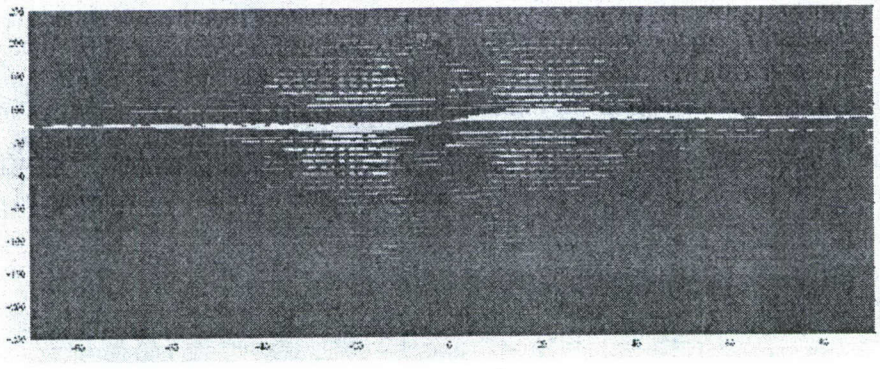

Figure 4. Doppler and DOA simulation result of two moving targets (Doppler spacing 76:80).

The simulations input parameters include a spatial boundary of 10 m by 10 m, moving speed with a uniform distribution from 0 m/s to 6 m/s, and a velocity direction that is uniformly distributed from 0 to 2π. Two moving targets are placed inside the boundary with the given speed and velocity range. These parameters are used to mimic a typical office environment of 10 m by 10 m with two moving humans. Amplitude decay as a function of distance is also calculated and accounted for in the simulation to evaluate the effect of the received signal strengths of the two targets. Fig. 5 illustrates the simulation setup. The receiver and transmitter coordinates are shown for the monostatic and bistatic configurations.

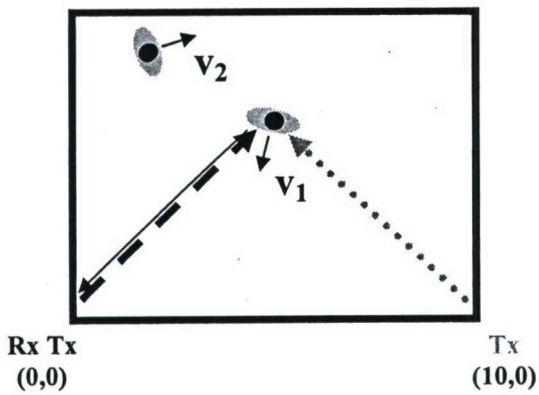

Figure 5. Simulation setup for two moving targets in a spatial boundary of 10 m by 10 m.

The first simulation case uses the monostatic configuration where both the receiver and transmitter are co-located at the (0,0) coordinate. One hundred thousand realizations are generated. The DOA errors with respect to the Doppler discrimination of the two moving targets are calculated and plotted. Fig. 6(a) shows the simulation result using the Kaiser window with the smallest main-lobe setting (but the highest side-lobes). The different color/grey shades indicate the relative signal strengths between the two targets, with the lighter shades representing more similar strengths. As expected, the DOA error is the largest when the Doppler separation between the targets is the smallest, and vice versa.

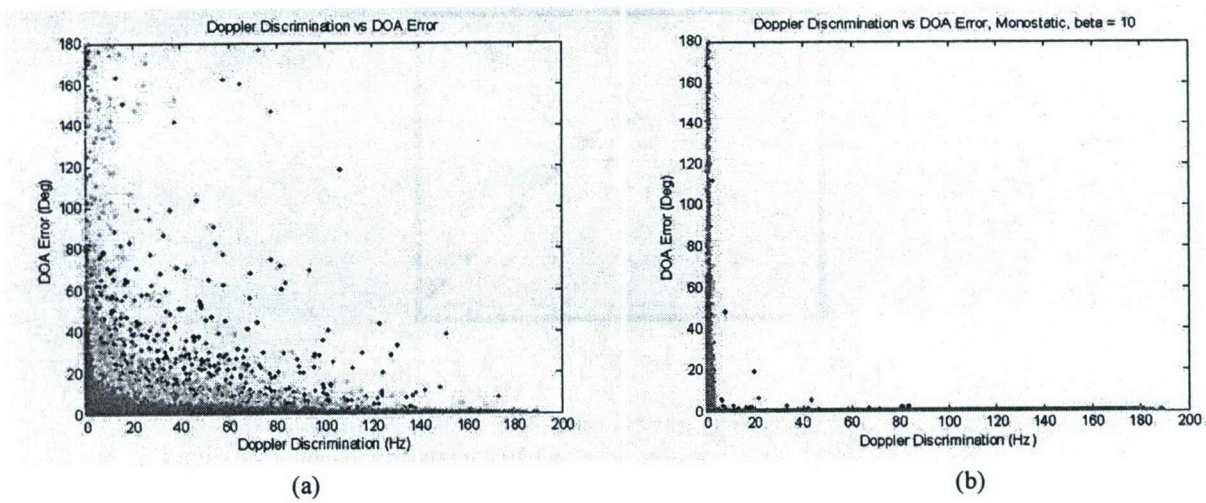

Figure 6. Monostatic simulation results using a Kaiser window with: (a) Highest side-lobes and (b) Reduced side-lobes.

However, there are also cases that contain large DOA errors even though the Doppler separations are large. From the darkness of the points, we also know that they correspond to cases where there is a significant difference in signal strengths (larger than 50 dB). This is caused by one target located much closer to the radar (thus much larger signal strength) than the other. This phenomenon is referred to as the close-far effect, where the side-lobe energy from the stronger, close-in target contaminates the much weaker, far-away target in its frequency bins. One way to mitigate the close-far effect is to decrease the side-lobe energy by setting the Kaiser window parameter accordingly. Fig. 6(b) shows the simulation result with the lower side-lobe window. This time there are much fewer occurrences of the DOA error due to the close-far effect.

We repeat the simulations above for the bistatic configuration where the radar receiver is located at (0,0) and the transmitter is at (10,0). Fig. 7(a) shows the simulation result with the highest side-lobe window setting. The DOA error trend is very similar to the monostatic case, but there are fewer occurrences of the close-far effect. With a lower side-lobe window setting, the close-far effect is hardly noticeable, as shown in Fig. 7(b). We verify the simulation cases above by measurements and discuss the results in the following section.

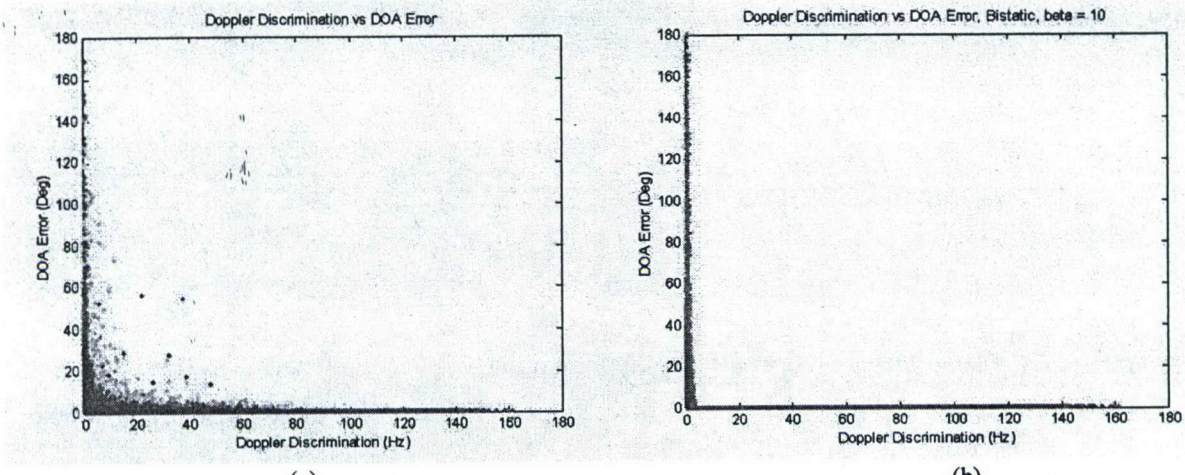

(a) (b)

Figure 7. Bistatic simulation results using a Kaiser window with: (a) Highest side-lobes and (b) Reduced side-lobes.

4. MEASUREMENT RESULTS

To demonstrate the multiple target detection, we use two loudspeakers as stable test targets. The vibrating membrane of each loudspeaker is covered by aluminum tape to enhance its return. The audio tone causes the loudspeaker membrane to vibrate back and forth and the radar return is an FM signal. The two loudspeakers are placed at -25°and +15° to the radar boresight and driven by a 55 Hz and a 35 Hz audio tone, respectively. Both loudspeakers are located at about 15 feet away from the radar (Fig. 8(a)). Their expected Doppler returns are +/- 55 Hz and +/- 35 Hz with the DOA of -25° and +15°, respectively. The measured data are plotted in Fig. 8(b) and clearly show the expected returns.

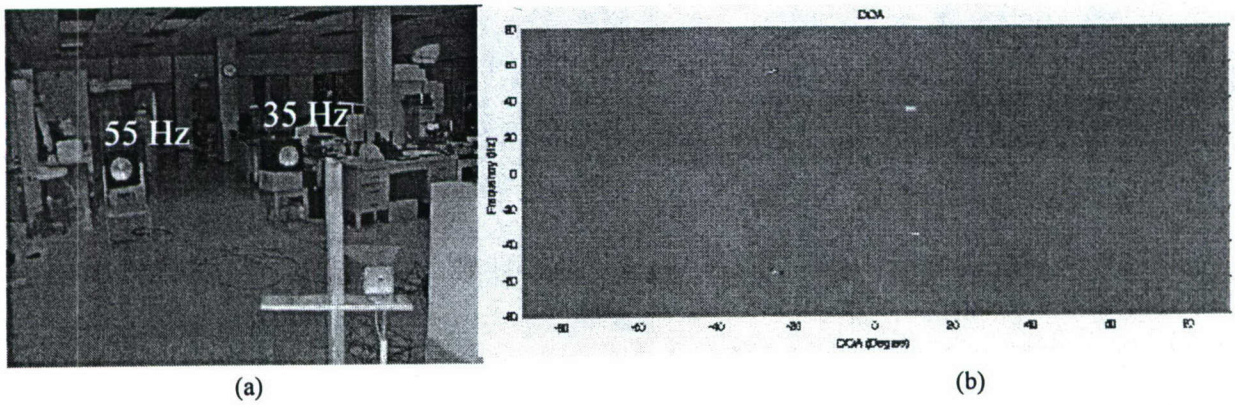

(a) (b)

Figure 8. Measurement results of two loudspeakers: (a) Setup and (b) Measured Doppler and DOA.

Moving human detection is next demonstrated. Two people move in the room with the person on the left (-15°) moving away and the person on the right (+20°) moving toward the radar. The measured Doppler and DOA returns are shown in Fig. 9. The wider Doppler spread is caused by the higher-order movements (arm/leg swings). These higher-order movements result in microDoppler returns [4, 5]. The measurement is taken with 0.5 second refresh time resulting in a wider DOA angle spread depicting the accumulated Dopplers during the 0.5 second duration. This is analogous to when a fast moving object is photographed with slow shutter speed.

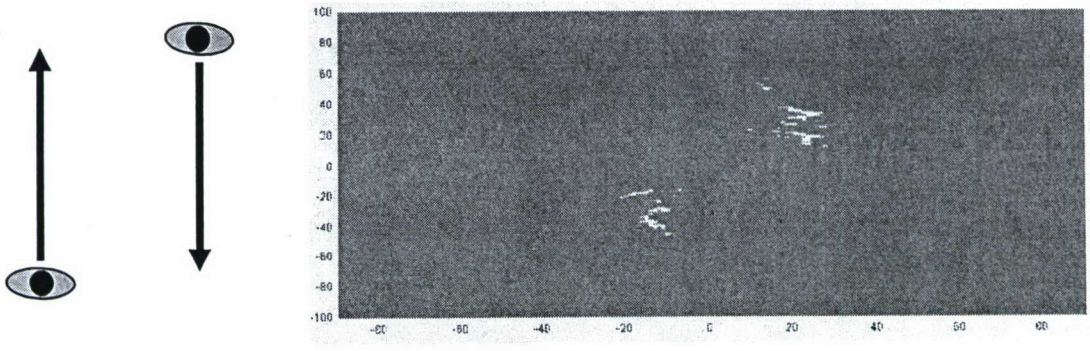

Figure 9. Doppler and DOA measurement results of two people walking in opposite directions.

The next set of measurement results shows the close-far phenomenon. First the monostatic configuration is used in an outdoor setting (Fig. 10(a)). The two loudspeakers are placed at -20°and -10° to the radar boresight and driven by 75 Hz and 55 Hz audio tones, respectively. The loudspeaker at -20° is located at 3 feet from the radar while the other one (at -10°) is at 42 feet away. As predicted by the simulation, the monostatic case clearly shows the close-far effect where the incorrect DOA is measured for the far-away target as shown in Fig. 10(b). The closer loudspeaker dominates the Doppler return of the far-away one, causing both DOA to be -20° (instead of -20°and -10°). In the bistatic configuration (Fig. 11(a)), the transmitter is placed at equidistance from the two loudspeakers. As shown in Fig. 11(b), this time the correct DOA are measured for both targets (-20°and -10°).

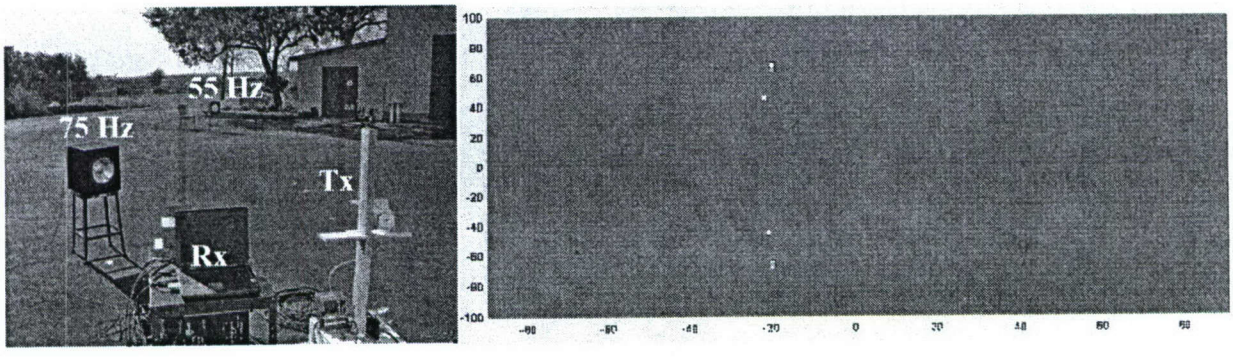

(a) (b)

Figure 10. Close-far monostatic measurement of two loudspeakers: (a) Setup and (b) Measured Doppler and DOA.

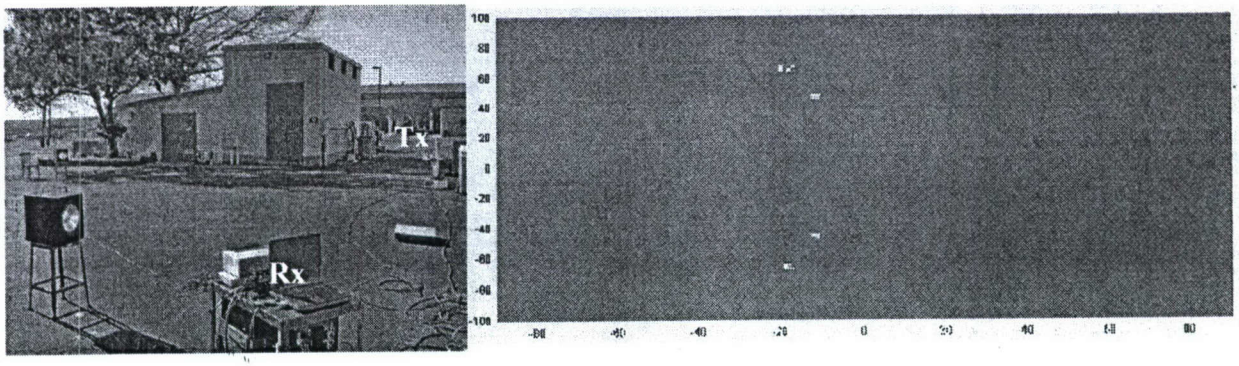

a) (b)

Figure 10. Close-far bistatic measurement of two loudspeakers: (a) Setup and (b) Measured Doppler and DOA.

5. CONCLUSIONS

Doppler and DOA simulation and measurement results of multiple moving targets have been presented. The measurements were performed using a low-cost, two-element receiver array operating at 2.4 GHz. Based on our measurement results, it is shown that simultaneous DOA detection of multiple movers using a two-element array is feasible. Our study also shows that the DOA accuracy is influenced by the Doppler separation and the close-far effect. Both our simulation and measurement results show that the bistatic radar configuration can be used to mitigate the close-far effect thus improving the DOA accuracy.

ACKNOWLEDGMENT

This work is supported by the Office of Naval Research and the Texas Higher Education Coordinating Board under the Texas Advanced Technology Program.

REFERENCES

[1] H. Mewes, J.L. ter Haseborg, F. Wolf, "A multichannel direction finding system", *Proc. IEEE Antennas Propagat. Soc. Int. Symp.*, pp 682-685, June 28-July 2 1993.

[2] T. Svantesson, M. Wennstrom, "High-Resolution direction finding using a switched parasitic antenna", *Proc. 11th IEEE Sig. Processing Workshop on Statistical Sig. Processing*, pp 508-511, Aug 6-8, 2001.

[3] J.G. Worms, "RF direction finding with a reduced number of receivers by sequential sampling", *Proc. IEEE Int. Conf. on Phased Array Sys. and Tech.*, pp 165-168, May 21-25 2000.

[4] J. L. Geisheimer, E. F. Greneker and W. S. Marshall, "High-resolution Doppler model of the human gait," *SPIE Proc., Radar Sensor Technology and Data Visualization*, vol. 4744, pp. 8-18, July 2002.

[5] H. Ling, "MicroDoppler exploitation: data collection and analysis," Naval International Cooperative Opportunities in Science and Technology (NICOP) program on Time-Frequency ISAR and NCTI, London, England, June 2004.

Through-Wall Measurements of a Doppler and Direction-of-Arrival (DDOA) Radar for Tracking Indoor Movers

Adrian Lin* and Hao Ling
Department of Electrical and Computer Engineering
University of Texas at Austin
Austin, TX 78712, USA

Introduction

Increasing demands on security and surveillance systems in military and law enforcement applications have prompted studies on through-wall detection of moving targets such as humans [1,2]. Recent developments show implementations of through-wall radars employing ultra-wideband (UWB) [3] and pulsed-Doppler signals [4]. UWB-based radars use very short pulses thus can provide high spatial resolution for through-wall imaging. However, certain wall materials such as bricks have significant dispersion and loss effects, causing only the lower portion of the signal band to be useful. For concrete walls, UWB radar is not suitable for through-wall detection [5]. Pulsed-Doppler based through-wall radars use Doppler shifts for motion detection and pulse timing for target ranging information. Using a carrier frequency of 5.8 GHz, the radar in [4] can provide a range accuracy of approximately 30 cm with minimum target velocity of 4 cm/sec. However, the range of the system is limited to 4 m.

In this paper, we demonstrated the use of a low-cost, two-element receiving array for tracking human movements in indoor surveillance applications. The concept entails simultaneously resolving the Doppler frequencies and the directions of arrival (DOA) of the returned signals from moving targets. The carrier frequency is 2.4 GHz as it provides significant through-wall penetration [6-8]. Moving target detection up to 30 feet distance through a 15-inch brick wall is demonstrated. Through-wall data of multiple movers is also collected using our system.

DDOA Radar

The system consists of a two-element receiver array operating at 2.4 GHz. Two microstrip antennas spaced a half wavelength apart are used as receiving antennas. Two low-cost, off-the-shelf integrated boards manufactured by Analog Devices (AD8347) are used as the quadrature receivers. Each receiver has the low-noise amplifier (LNA), I/Q mixers, gain control, and baseband amplifications all integrated on one board. After the down-converted signals are digitized, the fast Fourier transform is applied for Doppler discrimination and the phase difference between the two channels is used to calculate the DOA. Figure 1 illustrates the basic radar concept.

Through-Wall Measurement Results

Figure 2 shows the spectrogram results of through-wall Doppler measurements of a person walking toward the radar. The left figure was taken from a 5 GHz system built earlier [9]. The right figure shows the result from the present 2.4 GHz radar under approximately the same setup. The radar is placed against a 15-inch exterior brick wall while a person walks toward the wall on

the opposite side. The data show that the person is visible only during the last 3 seconds of the walk for the 5 GHz system, whereas the person is visible over the entire 10-second duration for the 2.4 GHz system. As expected, the 2.4 GHz carrier offers a longer detection range due to better wall penetration than at higher frequencies.

To measure the maximum through-wall detection distance, we use a loudspeaker driven by a 55 Hz audio tone as a stable test target. The vibrating membrane of the loudspeaker is covered by aluminum tape to enhance its return. The tone causes the loudspeaker membrane to vibrate back and forth and the radar return is an FM signal with fundamentals at +/- 55 Hz. Figure 3 shows the measurement setup and the results. First the loudspeaker is placed at approximately 20° to the left of the radar boresight at 30 feet distance from the other side of the wall. The return from this distance has sufficient power such that the correct Doppler and DOA can be measured (+/- 55 Hz and -20° respectively as shown in Fig. 3(b)). The loudspeaker is then moved to a 40 feet distance. This time erroneous DOA is measured due to the weaker signal, although the Doppler return is still vaguely recognizable (Fig. 3(c)). Therefore, we approximate the maximum through-wall detection range of our radar to be about 30 feet at a transmit power level of 23 dBm.

Multiple targets detection is next demonstrated. Two loudspeakers are placed at 10°and 30° to the left of the radar boresight and driven by 75 Hz and 55 Hz audio tones, respectively. Both loudspeakers are located at about 12 feet away from the wall (Fig. 4(a)). Their expected Doppler returns are +/- 75 Hz and +/- 55 Hz with the DOA of -10° and -30°, respectively. The measured data are plotted in Fig. 4(b) and clearly show the expected returns. Moving human data will be presented.

Conclusion

Doppler and DOA through-wall measurement results have been presented. The measurements were performed using a low-cost, two-element receiver array operating at 2.4 GHz. Based on our measurement results, our system is capable of detecting an indoor mover from outside a 15-inch brick wall with a range of 30 feet. Through-wall Doppler and DOA detection of multiple movers in a highly cluttered indoor environment was also demonstrated using our system.

Acknowledgment

This work is supported by the Office of Naval Research and the Texas Higher Education Coordinating Board under the Texas Advanced Technology Program.

References

[1] L. M. Frazier, "Surveillance through walls and other opaque materials," *Proc. IEEE National Radar Conference Electronic Systems*, pp. 27-31, May 1996.

[2] L. M. Frazier, "Motion detection radar (MDR) for law enforcement," *IEEE Potentials*, vol. 16, Issue 5, pp. 3079-3082, June 20-25, 2004.

[3] A. M. Attiya, A. Bayram, A. Safaai-Jazi and S. M. Riad, "UWB applications for through-wall detection," *IEEE Antennas Propagat. Soc. Symp.*, vol. 3, pp. 1868-1875, April 2000.

[4] D. G. Falconer, R. W. Ficklin and K.G. Konolige, "Robot-mounted through-wall radar for detecting, locating, and identifying building occupants," *Proc. IEEE Int. Conf. Robotics Automations*, vol. 2, pp. 1868-1875, April 2000.

[5] S. M. Riad, A. Muqaibel and A. Bayram, "Ultra-wideband propagation measurements and channel modeling," *DARPA NETEX Program, Report on Through-the-Wall Propagation and Material Characterization*, Nov. 2002.

[6] S. Todd, M. El-Tanany, G. Kalivas and S. Mahmoud, "Indoor radio path loss comparison between the 1.7 GHz and 37 GHz bands," *IEEE Int. Conf. Universal Personal Comm.*, vol. 2, pp. 621-625, Oct. 1993.

[7] W. Mohr, "Radio propagation for local loop applications at 2 GHz," *IEEE Third Annual Int. Conf. Universal Personal Comm.*, pp. 119-123, 27 Sept. 1994.

[8] D.I. Axiotis and M.E. Theologou, "Building penetration loss at 2 GHz for mobile communications at high elevation angles by HAPS," *IEEE Int. Symp. Wireless Personal Multimedia Comm.*, vol. 1, pp. 282-285, Oct. 2002.

[9] H. Ling, "MicroDoppler exploitation: data collection and analysis," Naval International Cooperative Opportunities in Science and Technology (NICOP) program on Time-Frequency ISAR and NCTI, London, England, June 2004.

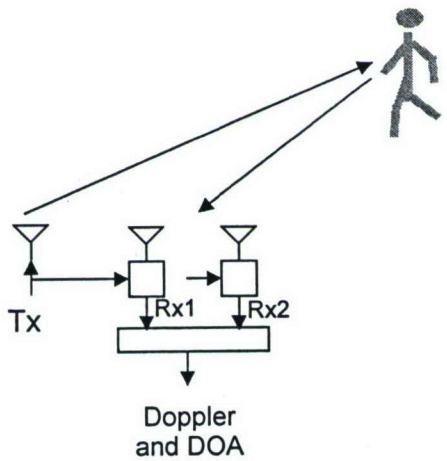

Figure 1. Basic radar operation.

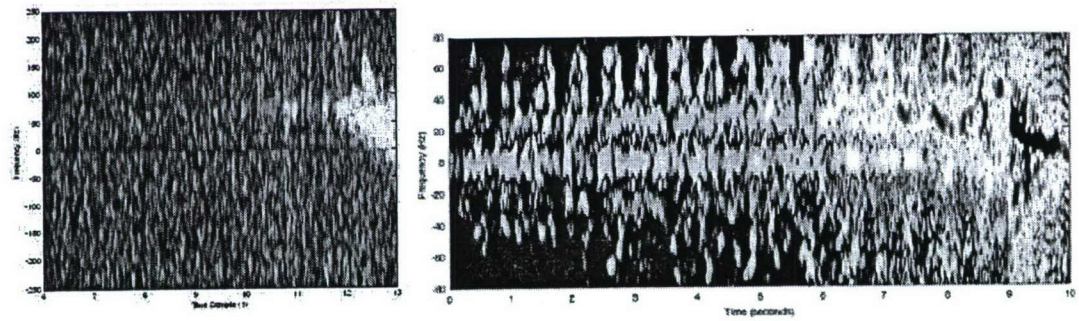

(a) (b)

Figure 2. Through-wall Doppler of a walking person: (a) 5 GHz and (b) 2.4 GHz.

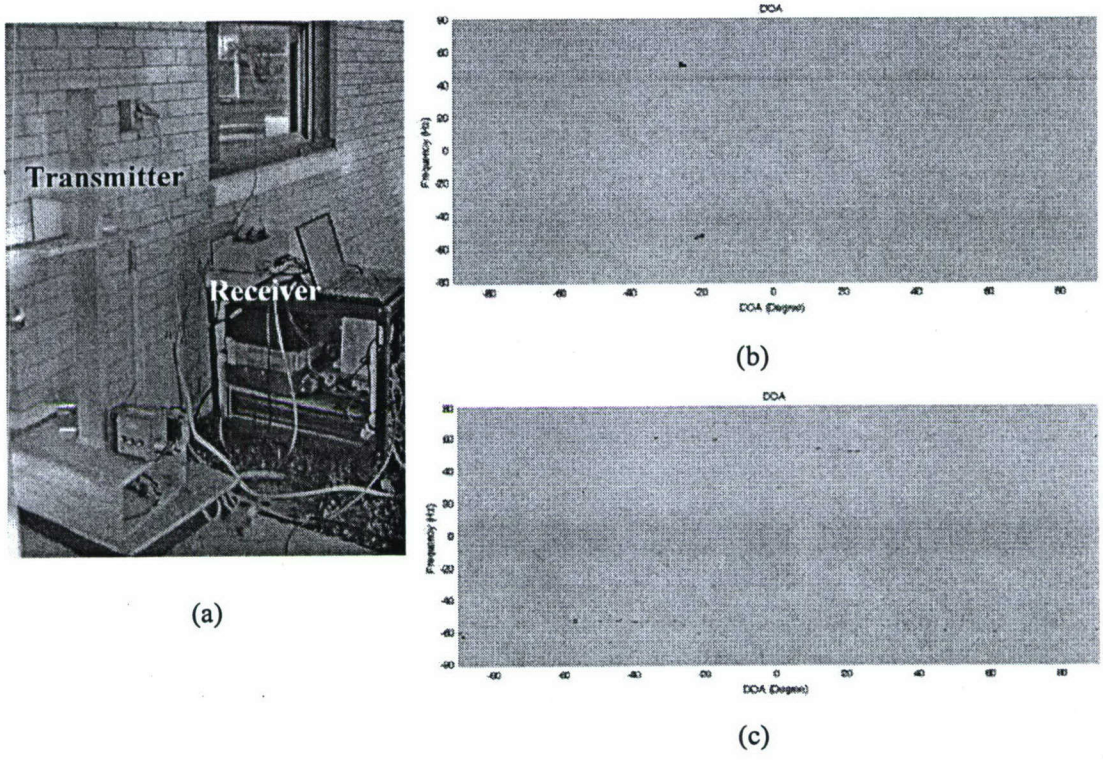

Figure 3. Through-wall Doppler of a single loudspeaker: (a) Radar system. (b) DDOA of the loudspeaker at 30' distance. (c) DDOA of the loudspeaker at 40' distance.

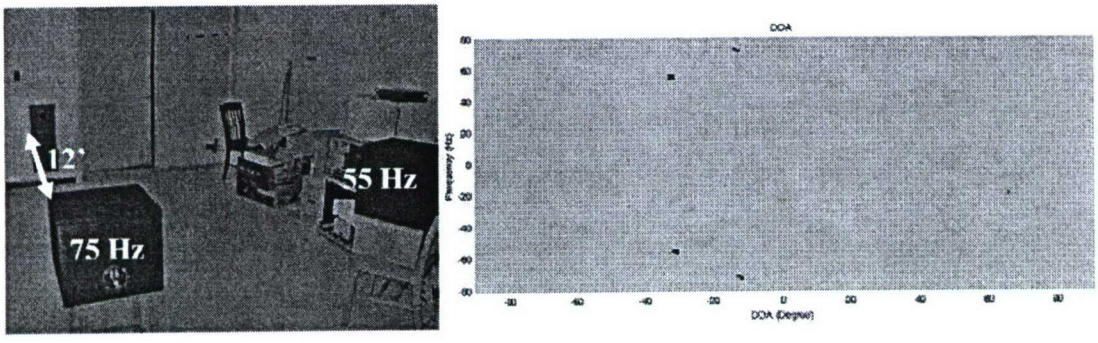

Figure 4. Through-wall Doppler of two loudspeakers: (a) Loudspeakers placement. (b) DDOA of the two loudspeakers.

Two-Dimensional Human Tracking Using a Three-Element Doppler and Direction-of-Arrival (DDOA) Radar

Adrian Lin and Hao Ling
Department of Electrical and Computer Engineering
University of Texas at Austin
Austin, TX 78712, USA
Email: adrian.lin@mail.utexas.edu

Abstract—**We investigate the use of a low-cost, three-element receiving array for two-dimensional direction-of-arrival (DOA) sensing of multiple movers. The concept entails resolving the Doppler frequencies of the returned signals from the moving targets, and then measuring the phase difference at each Doppler frequency component to calculate the DOA of the targets. The three-element receiving array is configured to provide simultaneous DOA measurements in both the azimuth and elevation planes. An experimental system is constructed to test the concept and measurement results of multiple movers are presented.**

I. Introduction

Increasing demands on security and surveillance systems in military and law enforcement applications have prompted studies on human detection using radar. Information such as the number of humans and their locations in a high clutter environment is crucial for counter-terrorism, urban warfare and disaster search. Recent work on human detection includes both investigations on the Doppler characteristics from human movements [1-3] and the development of ultra-wideband imagers [4-6].

For Doppler detection, which is attractive for stationary clutter suppression, a directional receiving antenna can be used to provide the additional bearing information or the direction of arrival (DOA) of a moving target. Conventional DOA sensing of multiple targets requires the use of an antenna array with multiple elements, in combination with the use of direction finding algorithms. Such methods require the number of elements to be at least one greater than the number of targets. However, increasing the number of elements leads to an increase in the physical size, cost and complexity of the overall system.

In [7, 8], we reported on the DOA sensing of multiple moving targets from a two-element receiver array by utilizing Doppler discrimination. The phase difference of the reflected waves arriving at two receiver antennas are measured at each Doppler bin to allow for the DOA determination of multiple movers with sufficient Doppler separation. The two antennas are spatially separated in the horizontal dimension. Thus one-dimensional DOA sensing in the horizontal (azimuth) plane can be achieved.

In this paper, we extend the idea to the two-dimensional (azimuth and elevation) tracking of multiple movers by using a receiving array consisting of three elements. The receiver array is implemented using three commercial off-the-shelf integrated receivers. With two-dimensional information, it becomes possible to track multiple humans moving at different elevations of a structure such as in a multi-storied building.

II. Basic Theory

Different moving targets typically give rise to different Doppler shifts with respect to the radar. Therefore, by processing the data via Doppler discrimination, we can extract their DOA information by measuring the phase difference at each Doppler frequency component. More explicitly, if we assume the time signals received at the two antenna elements to be $f_1(t)$ and $f_2(t)$, then after the Doppler processing the signals become $F_1(f_D)$ and $F_2(f_D)$, respectively. If the targets of interest generate different Doppler frequencies f_{Di} due the difference in their velocities with respect to the radar transceiver, then the DOA of target i with respect to the array boresight is given by:

$$\theta_i = \sin^{-1}\left[\frac{\angle F_1(f_{Di}) - \angle F_2(f_{Di})]}{(2\pi d/\lambda_c)}\right] \qquad (1)$$

where d is the spacing between the elements and λ_c is the RF wavelength. Referring to Fig. 1(a), if the two receiving

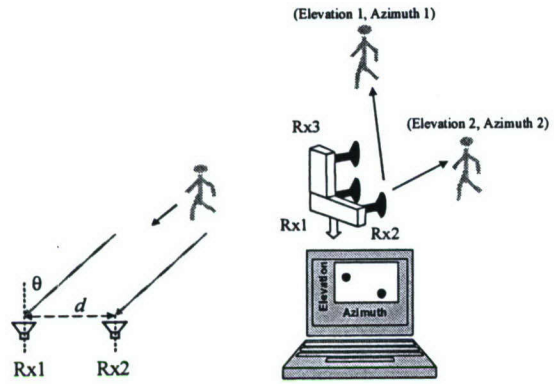

Fig 1. DOA sensing in: (a) One-dimensional (azimuth) and (b) Two-dimensional (azimuth, elevation)

elements (Rx1 and Rx2) are placed horizontally apart, they provide DOA (θ_{AZ}) information in the horizontal (azimuth) plane.

To obtain the bearing information in the elevation direction, an additional receiving antenna (Rx3) is placed directly above Rx1 as shown in Fig. 1(b). The additional receiver Rx3 and the existing receiver Rx1 form a new pair of elements to provide the DOA in the elevation plane, θ_{EL}. The Doppler and DOA processing in Eq. (1) is then repeated for the Rx1 and Rx3 signals. Finally, by correlating the DOA results based on their associated Doppler, it is possible to construct the data matrix $[A(f_{Di}), \theta_{AZ}(f_{Di}), \theta_{EL}(f_{Di})]$, where $A(f_{Di})$ is the signal strength at the Doppler component f_{Di}. Hence, the two-dimensional bearing sensing of multiple movers can be achieved, provided that the movers have different Doppler frequencies.

III. Radar Design

An experimental system is designed and constructed to test the concept. The system consists of a three-element antenna array, three dual-quadrature integrated receivers (Analog Devices AD8347 ICs) and a transmitter operating at a frequency of 2.4 GHz. Since the IC is targeted for the consumer wireless market, it is very low cost (less than $100 per evaluation board assembly). Three microstrip patch antennas on a 1.6 mm thick FR-4 substrate are used. To provide the maximum resolution while avoiding DOA ambiguity within the scanning range from -90° to 90°, the distances between the two antennas in both the azimuth and elevation planes are set to $\lambda_c/2$. The received signals are downconverted, digitized by the NI-DAQ 6024E and processed using the FFT for Doppler discrimination before the DOA calculations are carried out. Fig. 2 shows the system block diagram and a photo of the radar hardware.

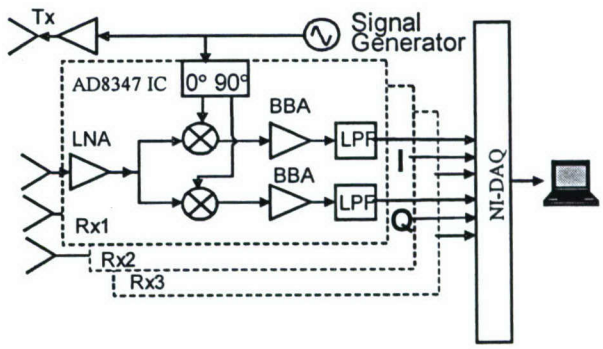

(a)

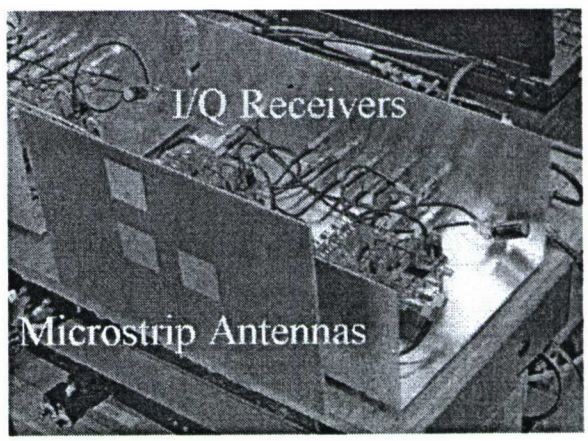

(b)

Fig 2. Radar (a) system block diagram and (b) actual hardware implementation.

IV. Measurement Results

1) Loudspeakers. We use three loudspeakers driven by 20 Hz, 30 Hz and 66 Hz audio tones as stable test targets. The vibrating membrane of each loudspeaker is covered by aluminum tape to enhance its return. The tones cause the loudspeaker membrane to vibrate back and forth and the radar returns are FM signals with fundamentals at +/-20 Hz, +/-30 Hz and +/-66 Hz. The three loudspeakers are placed at the approximate (azimuth, elevation) coordinates of (-28°, -10°), (-30°, 10°) and (-15°, 18°) respectively. The measurement setup and results are shown in Fig 3. As expected, Fig. 3(b) shows that the Doppler and azimuth DOA of the three loudspeakers are (+/-20 Hz, -28°), (+/-30 Hz, -30°) and (+/-66 Hz, 18°). Fig. 3(c) shows the Doppler and elevation DOA of (+/-20 Hz, -10°), (+/-30 Hz, 10°) and (+/-66 Hz, 18°), which correspond to the expected elevations. By correlating the two measurements based on the Doppler information, a two-dimensional DOA plot can be constructed accordingly. Fig. 3(d) shows the resulting azimuth and elevation coordinates of the three loudspeakers.

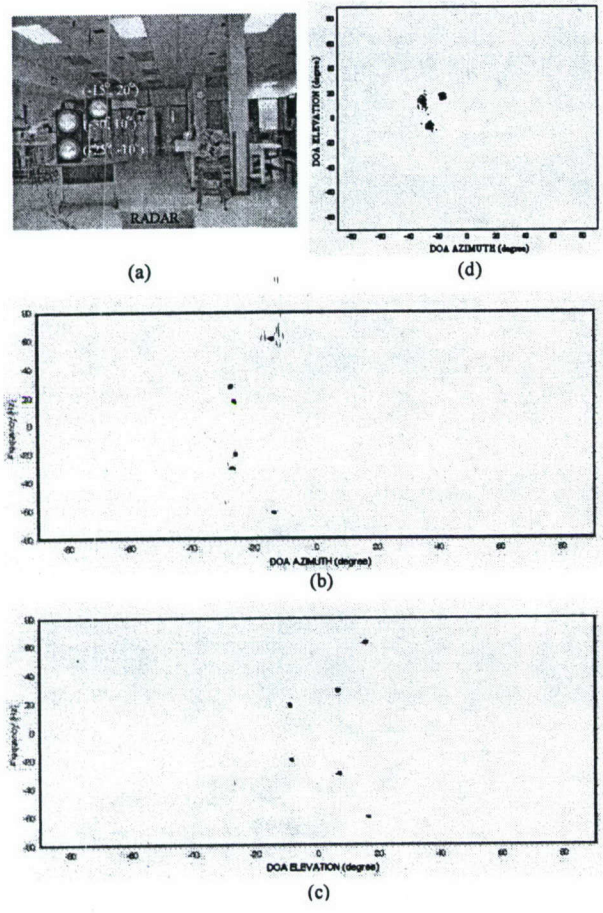

Fig 3. Loudspeakers measurement: (a) Setup, (b) Doppler and azimuth DOA, (c) Doppler and elevation DOA and (d) Two-dimensional DOA (azimuth, elevation)

A comparison of Figs. 3(a) and 3(d) shows a close correspondence of the DOA results to the frontal perspective of the radar.

2) Bouncing Ball. To show two-dimensional trajectory tracking we use a bouncing basketball as a moving target. The ball is also covered by aluminum tape to enhance its return. The ball is launched from the left side of the radar toward the radar boresight and bounces on the floor three times during its trajectory. Fig. 4 shows the measurement setup and results. The short-time Fourier transform [9, 10] is used to process the measured data to extract the Doppler components of the moving target with respect to time. The corresponding DOA versus time plots are used to show the motion trajectory of the ball in the azimuth and elevation planes, as shown in Figs. 4(b) and (c). After correlating the DOA information from both planes according to the Doppler, a two-dimensional DOA trajectory is generated (Fig. 4(d)). It shows the entire time that the ball is in motion.

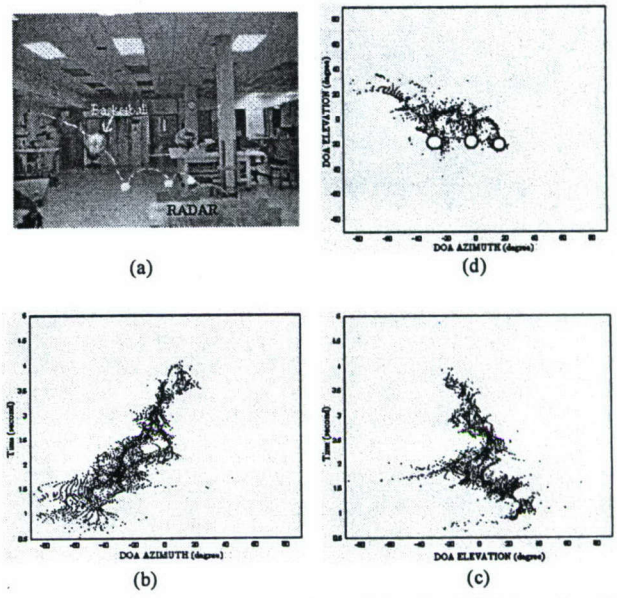

Fig 4. Bouncing basketball: (a) Setup, (b) Azimuth DOA vs. time, (c) Elevation DOA vs. time and (d) Two-dimensional DOA trajectory.

The gray shading indicates the signal strength. The measured trajectory result agrees with the actual trajectory: the first bounce is at approximately (-30°, -20°), followed by subsequent bounces at (-10°, -20°) and (15°, -20°) as indicated by the three white dots.

3) Human Walking. The next measurement involves human subjects. Two human subjects in front of a building walk in the patterns shown in Fig. 5(a). The subject on the left begins at point A (at approximately (-60°, -20°) with respect to the radar) and climbs a staircase to the top at point B (-20°, 40°). The subject then turns around and descends to the ground level back to point A. The subject on the right starts at point C (at approximately (20°, -20°) at the ground level) and walks to the right until reaching point D at (85°, -20°). The subject then turns around and walks back to point C. The radar is placed approximately 10 m away from the building. Since a directional horn is used as the radar transmitter, the measurable angular range in the azimuth plane is limited to approximately +/-70°. Figs. 5(b), (c) and (d) show the measured azimuth, elevation and two-dimensional DOA trajectories, respectively. As we can see from Fig. 5(d), the measured walking trajectories span from point A to point B for the person on the left, and from point C to point D for the person on the right.

V. CONCLUSION

Two-dimensional DOA sensing of multiple movers using a Doppler and DOA (DDOA) radar has been presented. Measurements were performed using a low-cost, three-element receiver array operating at 2.4 GHz. By correlating the azimuth and elevation DOA measurements based on the

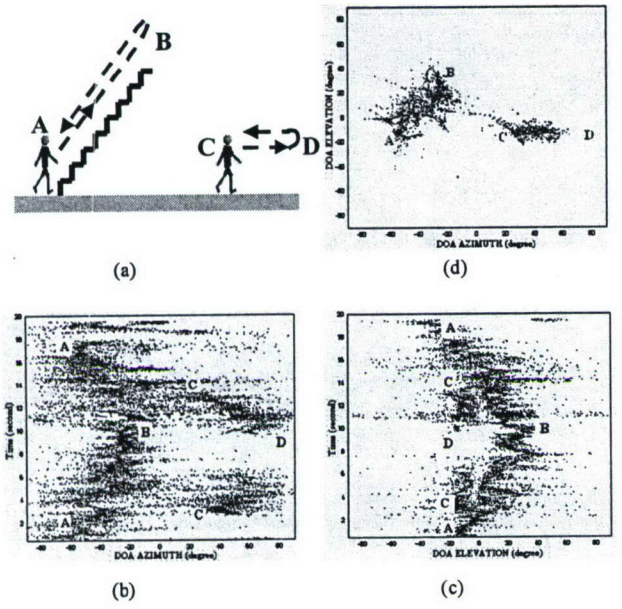

Fig 5. Two humans tracking: (a) Setup, (b) Azimuth DOA vs. time, (c) Elevation DOA vs. time and (d) Two-dimensional DOA trajectory.

Doppler information, the two-dimensional locations of multiple moving targets can be derived accordingly. Preliminary measurement results show good agreement with the actual setup. Improvement in the signal processing and more extensive data collection will be carried out next in our research.

VI. ACKNOWLEDGMENT

This work is supported by DARPA, the Office of Naval Research, Texas Higher Education Coordinating Board under the Texas Advanced Technology Program and the National Science Foundation Major Research Instrumentation Program.

VII. REFERENCES

[1] J. L. Geisheimer, E. F. Greneker and W. S. Marshall, "High-resolution Doppler model of the human gait," *SPIE Proc., Radar Sensor Technology and Data Visualization*, vol. 4744, pp. 8-18, July 2002.

[2] V. C. Chen, "Analysis of radar micro-Doppler with time-frequency transform", *Proc. of the 10th IEEE Workshop on Statistical Signal and Array Processing*, pp. 463-366, Pocono Manor, PA, Aug. 2000.

[3] P. van Dorp and F. C. A. Groen, "Human walking estimation with radar," *IEE Proc. – Radar, Sonar and Navigation*, vol. 150, pp. 356-365, Oct. 2003.

[4] S. Nag, H. Fluhler and M. Barnes, "Preliminary interferometric images of moving targets obtained using a time-modulated ultra-wideband through-wall penetration radar," *Proc. 2001 IEEE Radar Conf.*, pp. 64-69, May 2001.

[5] A. R. Hunt, "Image formation through walls using a distributed radar sensor network," *SPIE Proc., Sensors, and Command, Control, Communications, and Intelligence (C3I) Technologies*, vol. 5778, pp. 169-174, May 2005.

[6] J. Z. Tatoian, G. Franceshetti, H. Lackner and G. G. Gibbs, "Through-the-wall impulse SAR experiments," *IEEE Antennas Propagat. Soc. Int. Symp. Digest*, July 2005.

[7] A. Lin and H. Ling, "Human tracking using a two-element antenna array," *SPIE Proc., Radar Sensor Technology and Data Visualization*, vol. 5788, p. 57-64, May 2005.

[8] A. Lin and H. Ling, "Through-wall measurements of a Doppler and direction-of-arrival (DDOA) radar for tracking indoor movers," *IEEE Antennas Propagat. Soc. Int. Symp. Digest*, July 2005.

[9] S. Qian and D. Chen, *Introduction to Joint Time-Frequency Analysis – Methods and Applications*, Prentice Hall, Englewood Cliffs, NJ, 1996.

[10] V. Chen and H. Ling, *Time-Frequency Transforms for Radar Imaging and Signal Analysis*, Artech House, Norwood, MA, 2002.

Location Tracking of Indoor Movers Using a Two-Frequency Doppler and Direction-of-Arrival (DDOA) Radar

Adrian Lin* and Hao Ling
Department of Electrical and Computer Engineering
University of Texas at Austin
Austin, TX 78712, USA

Introduction

Two-dimensional location tracking of humans is useful for physical security applications. Previously, we reported on a two-element Doppler and Direction-of-Arrival (DDOA) radar for a bearing tracking of multiple humans [1, 2]. In this paper, we add the ranging capability to the radar to achieve two-dimensional location tracking. In contrast to conventional pulsed-based or frequency-modulated continuous wave (FMCW) radar, multiple frequency continuous wave (MFCW) radar is a simple and low-cost way to acquire range information [3, 4]. To keep the radar architecture as simple as possible, we use only two frequencies. However, a two-frequency system can only acquire the range for a single-target configuration. To overcome this limitation, we take advantage of the Doppler separation among the moving targets as a prefilter before measuring the phase difference to arrive at the range information of the moving targets. This two-tone approach in conjunction with the two-element DDOA radar can then provide the two-dimensional locations of humans. Multiple human location tracking results are collected using our system.

Two-Frequency DDOA Radar

Figure 1(a) illustrates the basic radar architecture. The system operates at two CW frequencies fc_1 (2.4 GHz) and fc_2 (10 MHz below fc_1). The frequency separation is selected to achieve a maximum unambiguous range of 15 m. The two CW frequencies are combined and transmitted simultaneously. The scattered wave off a target is received by two microstrip antennas spaced a half wavelength apart. Three low-cost, off-the-shelf integrated boards manufactured by Analog Devices (AD8347) are used as the quadrature receivers. Each receiver has a low-noise amplifier (LNA), I/Q mixers, gain control, and baseband amplifiers all integrated on one board. The actual radar hardware is shown in Fig. 1(b). The local oscillator (LO) frequency of receivers Rx_1 and Rx_2 is set to fc_1, and that of Rx_3 is set to fc_2. The down-converted signals are digitized and the Doppler frequencies of the target are extracted after applying the sliding-window fast Fourier transform. The phase difference $\Delta\Phi_{21}$ at each Doppler bin from Rx_1 and Rx_2 is measured to obtain the bearing information θ using the following equation:

$$\theta = \sin^{-1}\left(\frac{\lambda_{c1}\Delta\Phi_{21}}{2\pi d}\right) \tag{1}$$

where d is the spacing between the receiving antennas and λc_1 is the wavelength of fc_1. The received signal at Rx_2 is also routed into Rx_3 and the phase difference $\Delta\Phi_{32}$ at each Doppler bin from Rx_2 and Rx_3 is measured to calculate the target range R using the following equation:

$$R = \frac{c\Delta\Phi_{32}}{4\pi\Delta f} \tag{2}$$

where $\Delta f = fc_1 - fc_2$ and c is the speed of light. By correlating the bearing and range information based on their associated Doppler, it is possible to assemble the data matrix $[A(f_{Di}), \theta(f_{Di}), R(f_{Di})]$, where $A(f_{Di})$ is the signal strength at the Doppler bin f_{Di}. The two-dimensional range and bearing information of multiple movers can then be obtained accordingly as long as the movers have different Doppler frequencies.

Measurement Results

We first use two loudspeakers as stable test targets. The vibrating membrane of each loudspeaker is covered by aluminum tape to enhance its return. Fig. 2(a) shows the measurement setup and the loudspeakers locations. The first loudspeaker is located at approximately 20° to the left of the radar boresight at 4 m distance, driven by a 40 Hz audio tone. The second loudspeaker is positioned at approximately 20° to the right of the radar at 5.5 m distance, driven by a 50 Hz audio tone. The measured data are plotted in Fig. 2(b), and show good agreement with the expected bearings of -20° and +20°. Fig. 2(c) shows the range measurements which agree with the expected ranges of 4 m and 5.5 m. By using the polar-to-Cartesian transformation $(R\sin\theta, R\cos\theta)$, a location map can be constructed and is shown in Fig. 2(d). The coordinates of the left and right loudspeakers are close to the expected locations at (-1.4 m, 3.8 m) and (1.8 m, 5.2 m).

Preliminary human location tracking measurements are described next. Two human subjects walk in a straight path at approximately the same speed but in opposite directions (Fig. 3(a)). During the walk, the radar continuously measures and outputs the bearing and range information of the subjects (Fig. 3(b, c)). During the first five seconds of the measurement, Fig. 3(b) shows two distinct bearing trajectories: the first one progressing from approximately -20° toward 0°, and the second one from 0° toward 20°. These measured bearing trajectories are expected since they are plotted based on the perspective of the radar. As the subject to the left walks in a straight path away from the radar, the measured bearing angle advances toward the radar boresight. The opposite happens for the subject on the right: the measured bearing angle advances away from the radar boresight as the subject walks closer to the radar.

Fig. 3(c) shows the measured range tracks. In the first five seconds of the measurement, there are two distinct range tracks: the first one starts at about 1 m and ends at 10 m while the second one progresses from approximately 10 m to 1 m. The first range track is associated with the subject to the left of the radar, who walks away from the radar during this time. The second range track belongs to the subject to the right, who walks closer toward the radar during the time interval. At approximately t = 5 sec, both subjects turn around and walk back to their original starting positions. This is clearly shown in Figs. 3(b) and 3(c) as changes in the bearing and range tracks at t = 5 sec. The corresponding two-dimensional location map is constructed and shown in Fig. 3(d).

Conclusion

Two-dimensional bearing and range tracking of multiple indoor movers using a two-frequency Doppler and DOA radar have been presented. Measurements were performed using a low-cost, two-element receiver array operating at two CW tones. The

attractiveness of the system is that it has very low complexity. However, its performance is dependent on the Doppler separation between the targets.

Acknowledgment

This work is supported by the Office of Naval Research, the Texas Higher Education Coordinating Board under the Texas Advanced Technology Program and the National Science Foundation Major Research Instrumentation Program.

References

[1] A. Lin and H. Ling, "Human tracking using a two-element antenna array," *SPIE Proc., Radar Sensor Technology and Data Visualization*, vol. 5788, p. 57-64, May 2005.

[2] A. Lin and H. Ling, "Through-wall measurements of a Doppler and direction-of-arrival (DDOA) radar for tracking indoor movers," *IEEE Antennas Propagat. Soc. Int. Symp. Digest,* paper no. S099p03a, July 2005.

[3] M. A. Solano, J. S. Ipina, J. M. Zamanillo and C. Perez-Vega, "X-band Gunn diode oscillator for a multiple-frequency continuous-wave radar for educational purposes," *IEEE Trans. on Education*, vol. 45, No. 4, pp. 316-322, Nov. 2002.

[4] M. G. Anderson, "Multiple frequency continuous wave radar design for micro-Doppler extraction," Master Thesis, The University of Texas at Austin, May 2005.

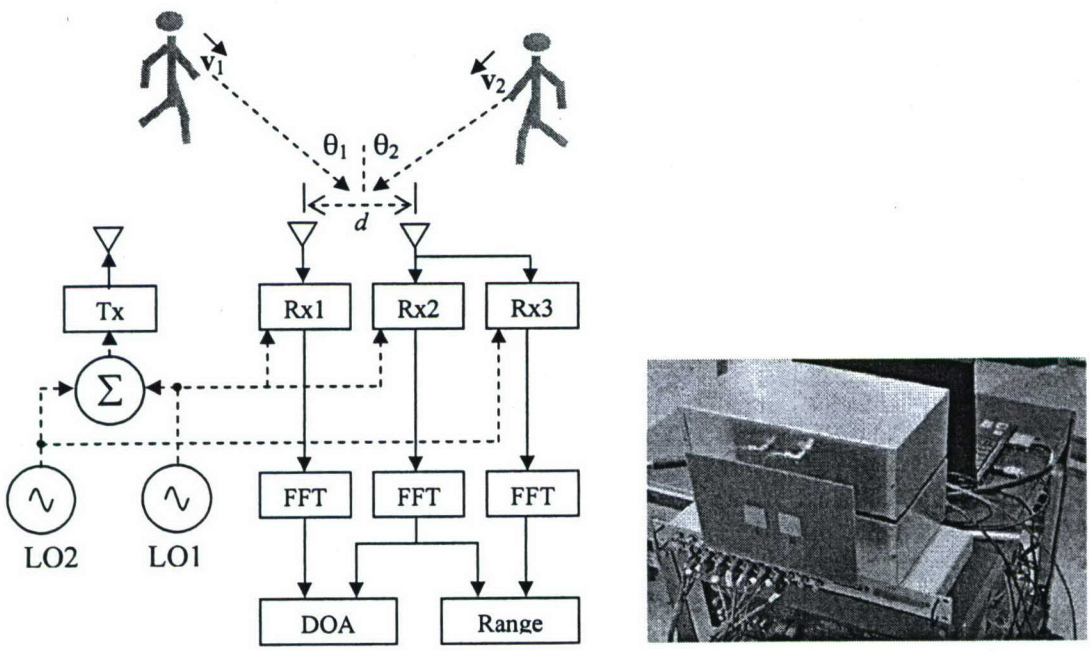

Figure 1. (a) Basic radar operation and (b) actual radar hardware.

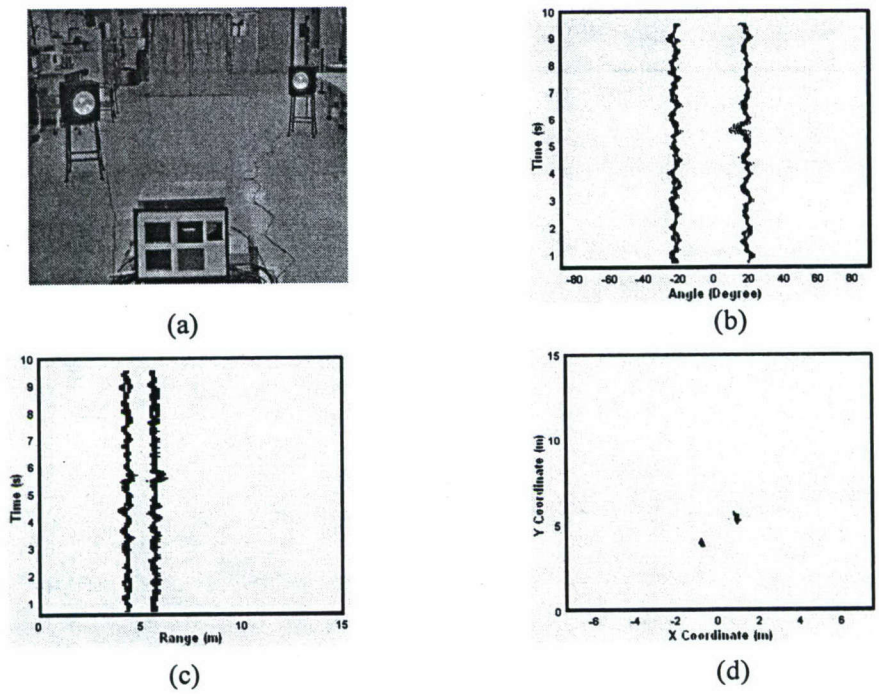

Figure 2. Loudspeakers measurements: (a) setup, (b) bearing track, (c) range track, (d) 2-D location map.

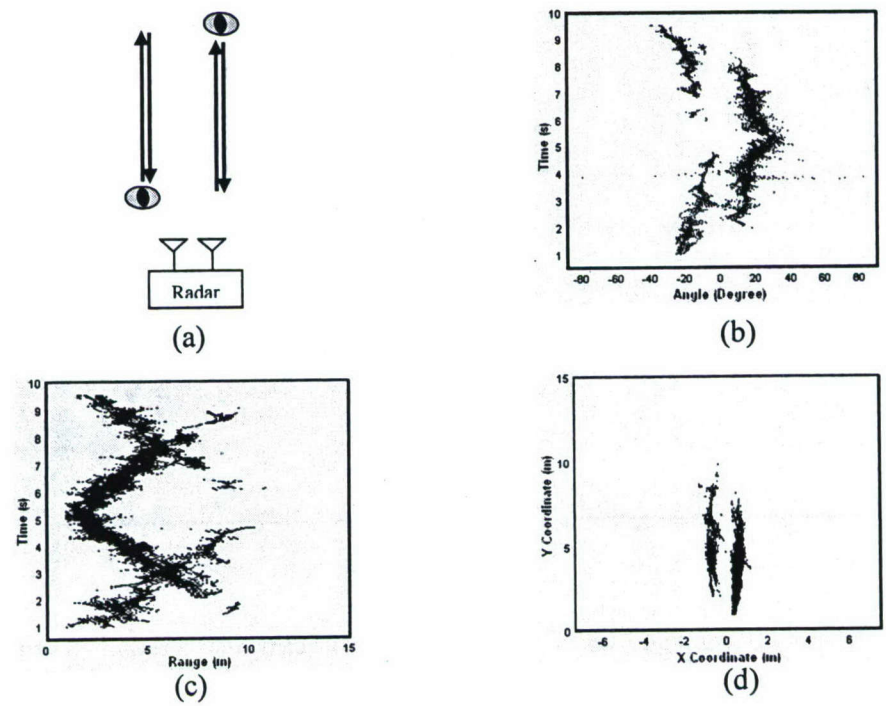

Figure 3. Humans walking measurements: (a) setup, (b) bearing track, (c) range track, (d) 2-D location map.

Human Tracking Using Doppler Processing and Spatial Beamforming

Shobha Sundar Ram, Yang Li, Adrian Lin and Hao Ling
Department of Electrical and Computer Engineering
University of Texas at Austin
1 University Station
Austin, TX 78712, USA
5124711910, shobhasram@mail.utexas.edu

Abstract— **We present a continuous-wave Doppler radar with a multi-element receiver array for tracking humans. Joint Doppler processing and spatial beamforming are used to resolve multiple movers in the Doppler and direction of arrival (DOA) space. The improvement in the performance of the multi-element array compared to a previously developed two-element system is evaluated through Monte Carlo simulation. In an array of limited size, the sidelobes of the strong targets prevent the detection of weaker targets. To overcome this limitation, the monopulse, CLEAN and RELAX algorithms are investigated in conjunction with software beamforming. The improvement in the performance of the radar towards the detection of multiple targets is evaluated by simulation. Measurements are conducted using a 4-element receiver for different targets in line-of-sight and through-wall scenarios.**

Index Terms—**beamforming, direction of arrival, Doppler, CLEAN, RELAX**

I. Introduction

Detection and tracking of human targets through walls by radar has important applications in law enforcement, urban area operations and search-and-rescue missions. Developments that have been reported include wideband radar using impulsive [1-3], stepped frequency [4] or FMCW [5] waveforms to obtain high spatial resolution. Alternately, continuous wave radars of low power have been implemented to suppress stationary clutter [6]. A low-complexity CW radar of two elements was reported by us in [7-9]. It uses the phase difference of the scattered signal at the two elements to determine the direction of arrival (DOA) of the target. In addition, Doppler discrimination facilitates the tracking of multiple movers. However when the Doppler separation among the multiple targets is poor, the DOA error is found to increase significantly.

In this paper, we investigate the performance gain achievable by a multi-element array versus the two-element system. We implement Doppler processing in conjunction with spatial beamforming in software to resolve multiple targets in the Doppler and DOA space. Monte Carlo simulations are carried out to assess the performance gain of a multi-element system. To further overcome the broad beamwidth and high sidelobes in a limited size array, three different DOA estimation algorithms are implemented. They are the amplitude-comparison monopulse technique [10], the CLEAN algorithm [11], and the RELAX algorithm [12]. The performance of the different algorithms is studied by simulation and experimentally verified by using a 4-element receiver array. Measurements are conducted under line-of-sight and through-wall scenarios for audio loudspeakers and human targets.

This work is supported by DARPA, the Office of Naval Research, Texas Higher Education Coordinating Board under the Texas Advanced Technology Program and the National Science Foundation Major Research Instrumentation Program.

II. Radar Theory and Simulation

A. Joint Doppler Processing and Spatial Beamforming

Fig.1 shows the basic radar architecture under consideration. A CW signal is radiated from a transmitter and each target introduces a Doppler shift on the scattered signal. The radar receiver consists of a multi-element antenna array, with each element connected to a separate receiver channel where the signal is amplified, downconverted and digitized before it is fed to a computer for further signal processing. To carry out the Doppler processing and spatial beamforming, the time domain signal from each receiver, $y_n(t)$, is first fast Fourier transformed to generate the Doppler information and then phase shifted and summed to generate the DOA information. This is described by

$$Y\left(f_d,\theta\right)=\sum_{n=1}^{N}\left\{\int y_n(t)e^{-j2\pi f_d t}dt\right\}e^{-j(n-1)\frac{2\pi d}{\lambda_c}\sin\theta} \quad (1)$$

In the above equation, N is the number of array elements, f_d is the Doppler frequency, d is the spacing between two adjacent elements, λ_c is the RF wavelength and θ is the steered beam angle from the array boresight. Note that the order in which the Doppler processing and spatial beamforming are applied could be reversed without any change in the results.

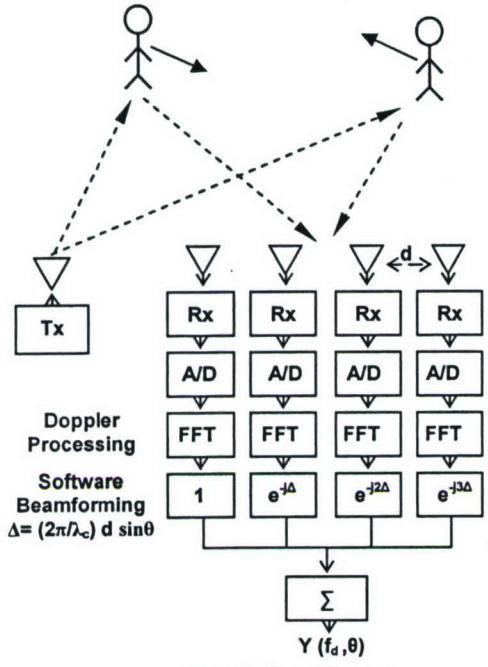

Fig 1. Radar architecture

B. Monte Carlo Simulation

Monte Carlo simulations are next performed to gauge the performance of the joint Doppler-beamforming algorithm towards the successful tracking of multiple targets. The following assumptions are made for the simulation. For each realization, a given number of targets are randomly placed inside a sectorial region of space bounded in range from 1 to 10m and DOA from -45° to +45°. Each target is randomly assigned a velocity of magnitude in the range of 0 to 2.5m/s and direction in the range of 0° to 360°. This yields Doppler values in the range of -40Hz to +40Hz for an RF wavelength of 12.5cm. We then assume that the ability of the radar to resolve a single target's returns is constrained in the DOA dimension by the beamwidth of the linear array, which for an antenna aperture of size D is $50°/(D/\lambda_c)$. In the Doppler dimension, the ambiguity is mainly caused by the microDoppler components from the arms and legs of the human movement [13]. A 40Hz Doppler spread is introduced to simulate the microDoppler spread for each target. With these two assumptions, each target is resolvable up to the rectangular ambiguity region in the DOA vs. Doppler space as shown in Fig. 2a. For multiple targets, the chance of overlap between the targets' ambiguity regions is increased. When the ambiguity regions of any two targets overlap by more than 50%, we consider that realization to be unresolvable by the radar. We perform this simulation for 500,000 realizations and tally the results. Fig. 2b shows the probability of successfully resolving multiple targets versus the number of targets. Each color represents a different assumed number of array elements, and therefore a different size antenna aperture. As expected, as the number of targets is increased, the probability of successfully resolving the targets drops. Using more array elements improves the performance, especially in the case of a large number of targets, since a narrower beamwidth improves the DOA resolution. This is done at the expense of increased system cost and complexity. We see that with 4 elements, there is a 78% probability of successfully resolving 4 targets.

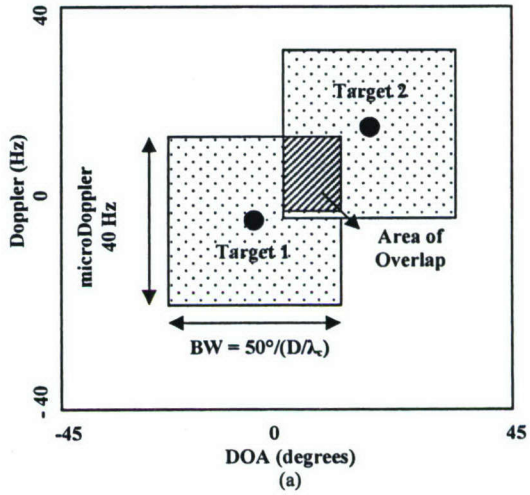

(a)

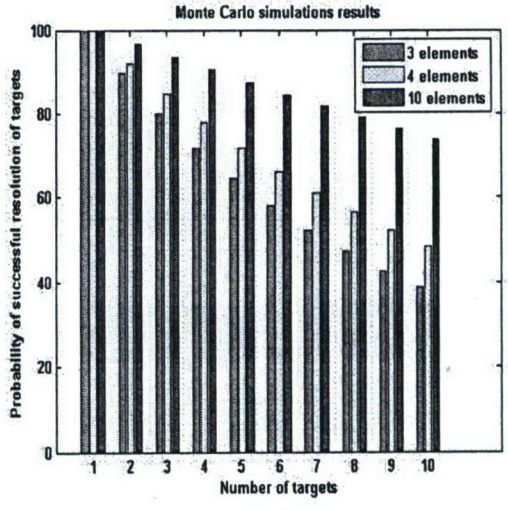

(b)

Figure 2: (a) Detection of targets in the Doppler versus DOA plot (b) Monte Carlo simulation results for probability of successfully resolving multiple targets with an antenna array

C. DOA Estimation

If multiple targets are not well resolved in the Doppler domain, their successful DOA determination becomes quite difficult using a small size array, especially when the target strengths are very different. This is understood from the following simulation performed in a two target scenario where the targets are of the same Doppler. Hence the detection of the two targets is entirely determined by spatial beamforming. The simulation is conducted for a four-element antenna array and the ratio of the strength of the two targets is set to 20dB. The angular position of the strong target is varied from -45°

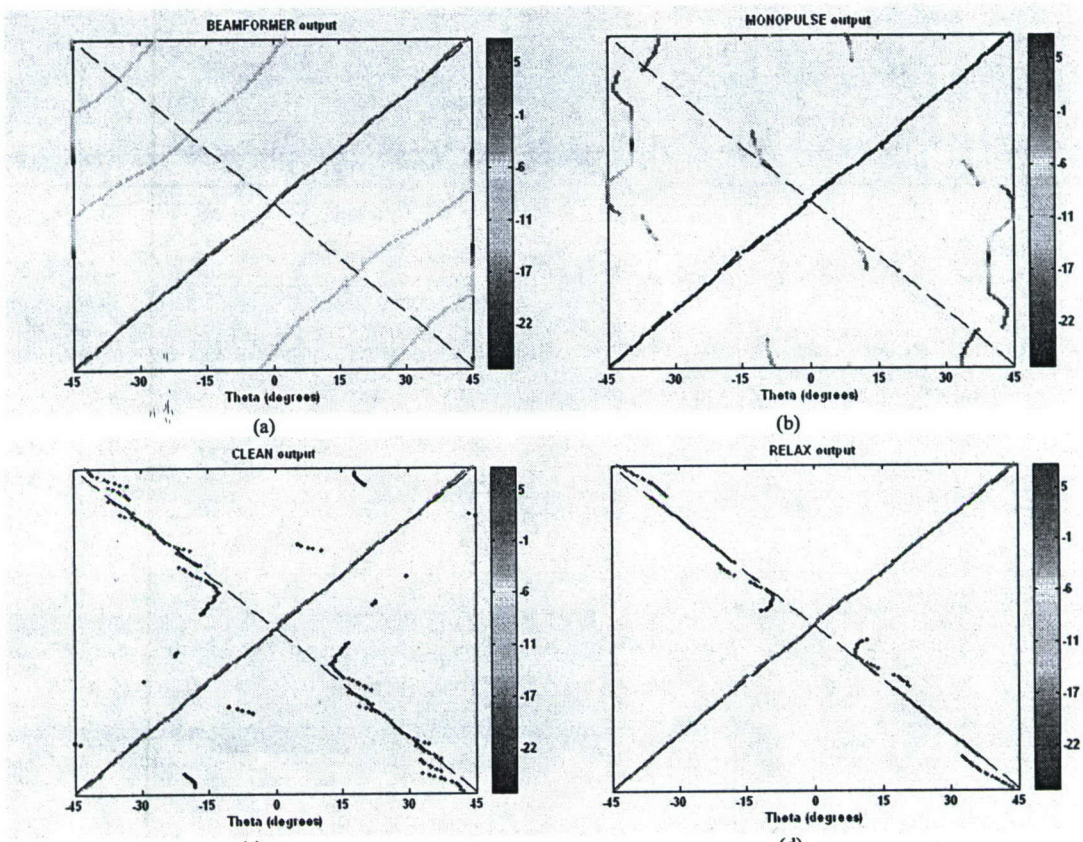

Fig.3. Simulation results when ratio of strength of targets is 20dB for (a) Spatial beamforming , (b) Monopulse, (c) CLEAN, and (d) RELAX techniques

to +45° while that of the weak target is varied from +45° to -45°as indicated by the dashed lines in Fig. 3a. For each pair of simulated angular positions of the targets, the main lobe and sidelobe patterns arising from the two targets are computed by spatial beamforming. The DOA of the targets are estimated to be at the peaks of the beamformer pattern and their strengths are represented by the colored intensity as indicated in Fig. 3a. It is observed that the DOA of the strong target is detected correctly at every possible DOA position of the targets. The weaker target however is not detected at all because it is buried beneath the sidelobes of the strong target. This result is unsatisfactory. In order to improve the tracking of weak targets in the presence of strong targets, we implement three different algorithms, namely, monopulse, CLEAN and RELAX, and evaluate their performance using the same simulation set up.

1) Monopulse: Monopulse processing is a standard technique to improve the angular resolution in target tracking. The amplitude comparison monopulse technique described in [10] is implemented here. In order to estimate the DOA of a single target, the strength of the scattered signal from the target is measured at two specific angular values or lobes using the beamforming equation (1). In order to try to handle multiple targets, the technique is modified by increasing the number of lobes to M ($Y_{1:M}$). Normalized difference values ($D_{1:M-1}$), of the signal strength are computed for each pair of adjacent lobes:

$$D_i = \frac{\left|Y_i\right| - \left|Y_{i+1}\right|}{\sum_{j=1}^{M}\left|Y_j\right|}, \quad i = 1,\ldots,M-1 \tag{2}$$

For each possible angular position of a target, a data set of difference values is computed theoretically and stored The measured data set is then compared with each of the multiple data sets obtained by theory. The DOA of the target is identified as that angular value which gives the closest fit between the measured and theoretical data sets. While it is possible to estimate the DOA of two targets of equal strength that are well resolved in the DOA space, the performance of the algorithm deteriorates for a higher dynamic range. This is seen when the technique is simulated in the two target scenario described earlier using M=5. The presence of the sidelobes prevents the detection of the weak targets as indicated in Fig. 3b

2) CLEAN: The CLEAN algorithm is a well-known technique to extract weaker features in the presence of strong features, given that the feature response function is known [11]. Here we apply the algorithm to extract the DOA of multiple targets. The DOA of the strongest target is first extracted by picking out the strongest response from the beamformer output:

$$|a_p|^2 = \max_{\theta_p} \left| \frac{1}{N} \sum_{n=1}^{N} y_n \, e^{-j(n-1)\frac{2\pi d}{\lambda_c}\sin\theta_p} \right|^2 \quad (3)$$

Once the DOA of the strongest target is found, its presence is removed from the original array signal:

$$y_{n,residual} = y_n - a_p e^{j(n-1)\frac{2\pi d}{\lambda_c}\sin\theta_p} \quad (4)$$

Since the strongest target is removed together with its sidelobe contribution, the weaker target becomes better revealed. The next strongest target and its DOA are then determined and removed from the residual signal. This procedure is continued in successive steps until the strength of the residual pattern converges or falls below the noise floor. This algorithm is simulated for the two target scenario described earlier and the results are presented in Fig. 3c. It is observed that the weak target is detected in the presence of a stronger target as long as their angular separation exceeds the beamwidth of the array. The algorithm clearly performs better than the ordinary beamforming and monopulse techniques towards detecting multiple targets. However there does appear to be false targets near the strong target due to the influence of the weaker target on the strong target.

3) RELAX: The RELAX algorithm is an enhanced version of CLEAN that relieves the error propagation tendencies in CLEAN [12]. It introduces a relaxation step that iteratively identifies target parameters (strength and DOA) until the energy of the residual pattern at each CLEAN step converges. Relaxation occurs in the CLEAN algorithm once the second target has been found. At that stage, the second target's contribution is extracted from the original signal. The goal is to more accurately extract the first and strongest target a second time, without the mutual interference effects of the second target. The re-extraction of the two targets repeats until convergence. Afterwards, the algorithm resumes in order to extract the next strongest target from the residual. The relaxation process is then initiated again to individually adjust the values of all known targets in the absence of the contribution of the others. While this inner relaxation loop makes the algorithm computationally more expensive than ordinary beamforming and CLEAN, it allows the accurate determination of the number of targets. The results obtained when this algorithm is implemented for the two target scenario described earlier are presented in Fig. 3d. It is observed that angular position and the strength of the two targets are detected with better precision. The number of erroneous detections or false targets is much smaller than the earlier cases. Additionally, successful detection is possible even when their angular separation is within the beamwidth of the antenna array. Thus RELAX enhances the performance of the CLEAN algorithm at the price of increased computation time.

III. Measurement Results

The radar prototype used to demonstrate the above concepts is shown in Fig. 4. It consists of a signal generator that transmits a 2.4GHz signal through a horn antenna. The receiver consists of a four-element microstrip array on an FR4 substrate of 1.6mm thickness. The inter-element spacing of the array is 0.56 λ_c. This allows the antenna array to scan from -45° to +45° without the occurrence of grating lobes. Each element is connected to an integrated quadrature receiver from which the signal is amplified, downconverted and fed to the A/D converter. The digitized output is fed to the computer for signal processing.

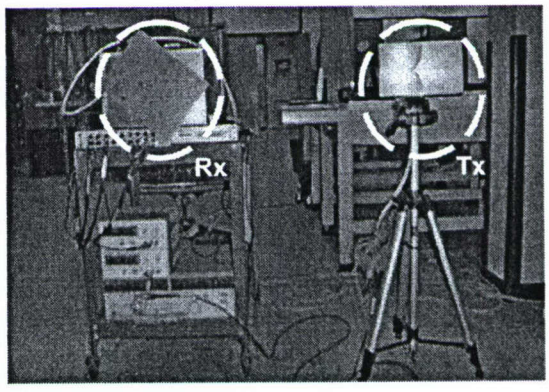

Fig. 4. RADAR set up

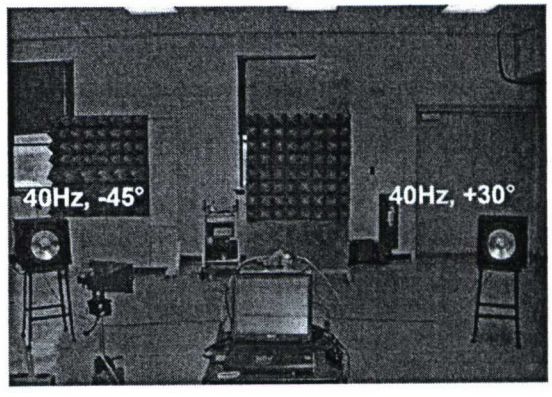

Fig. 5. Speaker test: speakers well resolved in DOA but identical Doppler

First we use audio loudspeakers as steady test targets. When a loudspeaker is driven by a single audio tone, the FM signal that is generated gives rise to a two-sided Doppler return. The two-element DDOA radar reported in [7-9] is not capable of resolving targets of identical Doppler. To demonstrate that the current radar is capable of resolving targets of identical Doppler along the DOA axis, the following measurement is made with two loudspeakers as shown in Fig. 5. Two loudspeakers are driven at the same frequency (40Hz) but are located at different DOA (30° and -45°). From the results presented in Fig. 6a, it can be seen that two targets of identical Doppler are resolved along the DOA axis using spatial beamforming. However,

the high sidelobes appear as false targets. When the CLEAN algorithm is tried on the same measurement, it becomes apparent from Fig. 6b that the algorithm is able to correctly identify the DOA of the two targets despite the presence of high sidelobes. To display the CLEAN results, which are a set of discrete DOA estimates, a point spread response with high resolution and low sidelobes is convolved with the discrete estimates. The RELAX result, which is not shown here, further improves the CLEAN result slightly.

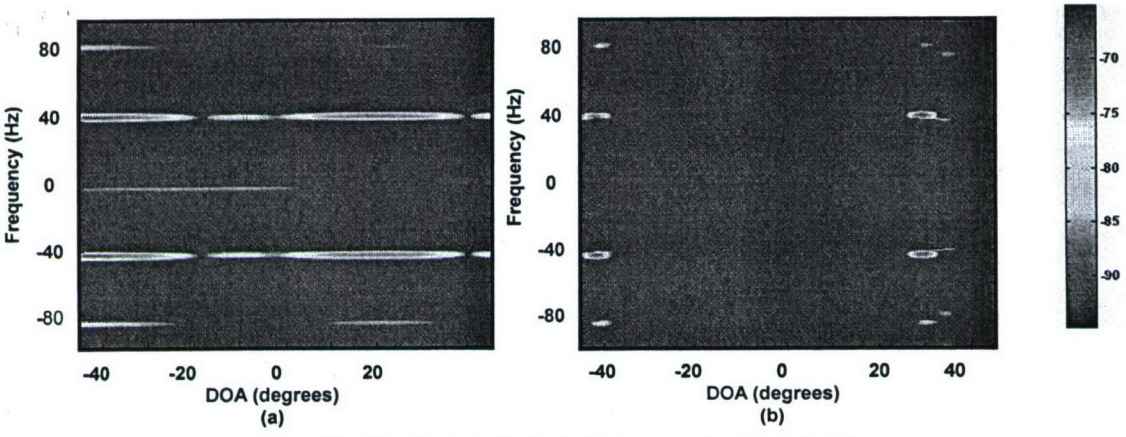

Fig. 6. Speaker test with: (a) Spatial beamforming and (b) CLEAN

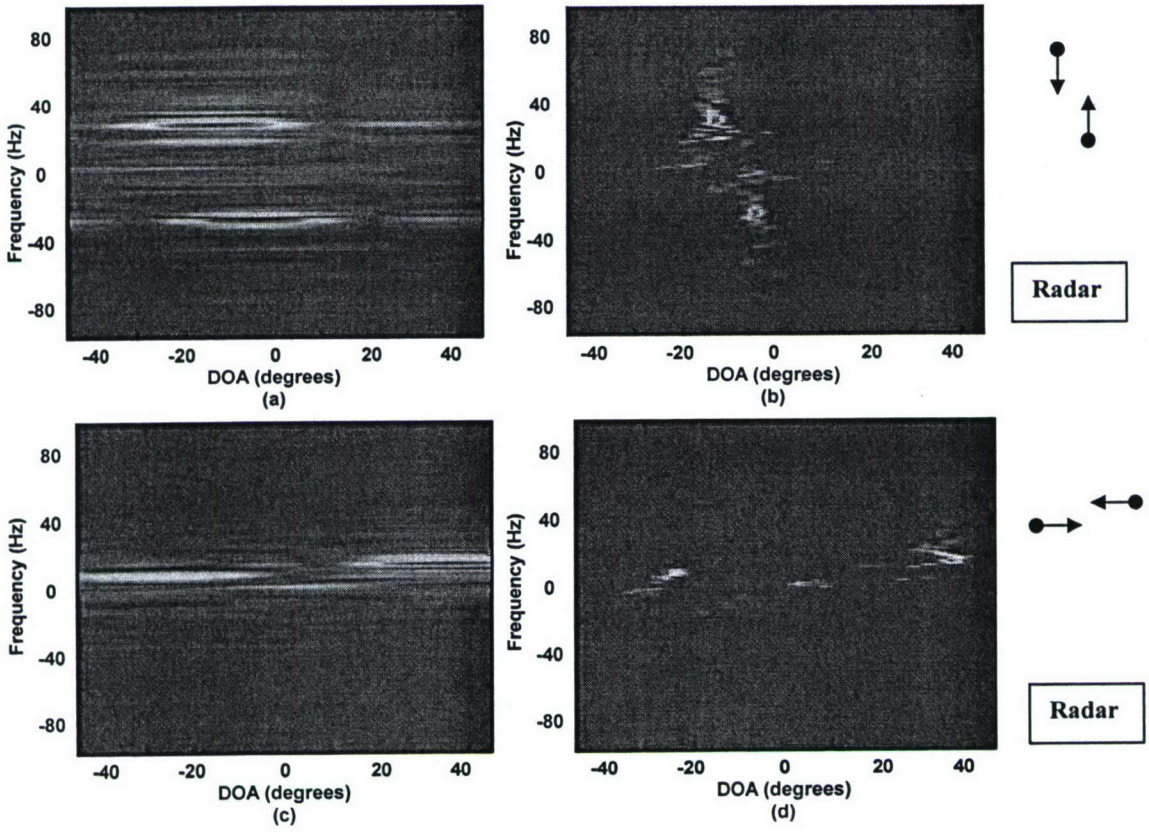

Fig. 7. Measurement results for human targets under line-of-sight.
Top figures illustrate two targets with high Doppler separation and low DOA separation: (a) Spatial beamforming. (b) CLEAN.
Bottom figures illustrate two targets with low Doppler separation and high DOA separation: (c) Spatial beamforming. (d) CLEAN.

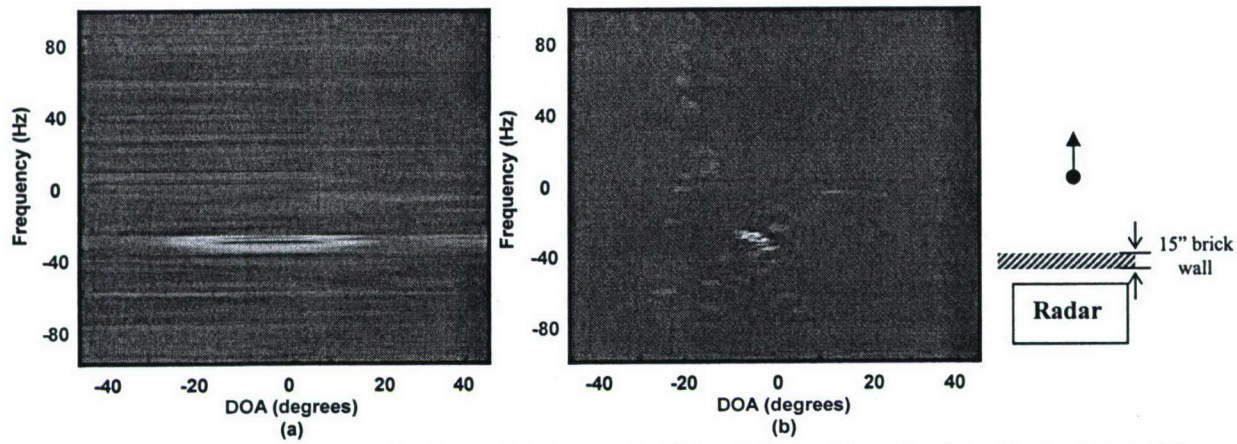

Fig 8: Measurement results for a human subject for through a 15" exterior brick wall . (a) Spatial beamforming. (b) CLEAN

Measurements are next conducted on two human subjects under an indoor line-of-sight environment. Human walking returns are characterized by microDoppler features, causing spreading along the Doppler dimension. Two cases are studied. In the first case, the first subject walks away from the radar (negative Doppler) while the second subject approaches the radar (positive Doppler) along two paths that lie very close to each other. Thus the Doppler separation between the two targets is high while the DOA separation is low as is apparent from the Doppler-DOA plot in Figs. 7a and 7b. In the second case, while one target approaches the radar from the right (positive Doppler), the second target approaches from the left (positive Doppler). Thus the Doppler separation is low while the DOA separation is high. This is seen in the Doppler-DOA plot in Fig. 7c and 7d. The two targets are clearly resolved in both scenarios. Again, the CLEAN algorithm (Figs. 7b and 7d) leads to improved DOA estimation and lower sidelobes as compared to the standard beamforming (Figs. 7a and 7c).

Measurements of human target are conducted for a through-wall paradigm on an exterior brick wall of 15" thickness. The results for a single human case are shown in Fig. 8. As we can see from the result, the target is successfully tracked in the through-wall scenario. The wall, however, introduces a significant attenuation on the signal and leads to a lower signal-to-noise ratio. Other types of walls are being investigated to assess additional wall phenomenology.

IV. Conclusion

Using the principles of Doppler processing and spatial beamforming, the performance of a radar for tracking multiple humans can be improved by using additional receiver elements. The resolution of the target along the DOA axis is limited by the beamwidth of the antenna array and the sidelobes give the appearance of false targets To overcome these limitations, three algorithms including monopulse, CLEAN and RELAX are investigated for use in conjunction with software beamforming. It was found that the CLEAN algorithm performed satisfactorily for multiple targets without excessive computational cost. These concepts are demonstrated by conducting measurements on different targets in line-of-sight and through wall scenarios.

References

[1] G.Franceschetti, J.Tatoian, D.Giri and G.Gibbs, "Timed arrays and their application to impulse SAR for "through-the-wall" imaging," *IEEE Antennas Propagat. Soc. Int. Symp. Digest*, vol. 3, pp.3067-3070, June 2004.

[2] A.R.Hunt, "Image formation through walls using a distributed radar sensor network," *SPIE Proc., Sensors, and Command, Control, Communications and Intelligence (C3I) Technologies*, vol. 5778, pp.169-174, May 2005.

[3] S.Nag, M.A.Barnes, T.Payment and G.Holladay, "Ultrawideband through-wall radar for detecting the motion of people in real time," *SPIE Proc. Radar Sensor Technology and Data Visualization*, vol. 4744, pp.48-57, July 2002.

[4] F.Ahmad, G.J.Frazer, S.A.Kassam and M.G.Amin, "Design and implementation of near field wideband synthetic aperture beamformer," *IEEE Transactions Aerospace and Electronic Systems*, vol. 40, pp.206-220, January 2004.

[5] D.G.Falconer, K.N.Steadman and D.G.Watters, "Through-the-wall differential radar," *SPIE Proc. Command, Control, Communications, and Intelligence Systems for Law Enforcement*, vol. 2938, pp.147-151, February 1997.

[6] D.D.Ferris Jr.and N.C.Currie, "Microwave and millimeter-wave systems for wall penetration," *SPIE Proc. Targets and Backgrounds: Characterization and Representation IV*, vol. 3375, pp.269-279, July 1998.

[7] A.Lin and H.Ling, "Human tracking using a two-element antenna array," *SPIE Proc. Radar Sensor Technology and Data Visualization*, vol. 5788, pp.57-64, May 2005.

[8] A.Lin and H.Ling, "Through-wall measurements of a Doppler and direction-of-arrival (DDOA) radar for tracking indoor movers," *IEEE Antennas Propagat. Soc. Int. Symp. Digest*, vol. 3B, pp.322-325, July 2005.

[9] A. Lin and H. Ling, "A Doppler and direction-of-arrival (DDOA) radar for multiple-mover sensing based on a two-element array," to appear in *IEEE Trans. Aerospace Electronic Syst.*, July 2007.

[10] S.M.Sherman, *Monopulse Principles and Techniques*, Dedham MA, 1984.

[11] J.Tsao and B.D.Steinberg, "Reduction of sidelobe and speckle artifacts in microwave engineering: the CLEAN technique," *IEEE Trans. Antennas Propagation*, vol. 36, pp 543-556, April 1988.

[12] J. Li and P.Stoica, "Efficient mixed-spectrum estimation with applications to target feature extraction," *IEEE Trans. Signal Processing*, vol. 44, pp 281-295, February 1996.

[13] J.L.Geisheimer, E.F.Greneker and W.S.Marshall, "High-resolution Doppler model of the human gait," *SPIE Proc. Radar Sensor Technology and Data Visualization*, vol. 4744, pp. 8-18, July 2002.

Tracking a Moving Target with Multiple Doppler Sensors Using an Artificial Neural Network

Youngwook Kim*, and Hao Ling
Department of Electrical and Computer Engineering
The University of Texas, Austin, TX 78712, USA
Email: ykim5@ece.utexas.edu

1. Introduction

Tracking of human movements using radar in a high-clutter environment or even through walls is a problem of current interest. Example applications include law enforcement, disaster search-and-rescue and urban military operations. One approach to human tracking is to use wideband waveforms [1-4]. Such system is capable of high range localization, but the cost of the hardware tends to be high. Doppler-based sensors, on the other hand, offer an inexpensive way to detect moving targets in the presence of stationary clutter. However, target location information is not possible, unless frequency or spatial diversity is incorporated [5,6]. In this work, we investigate the use of a collection of spatially diverse Doppler sensors to derive the location information of a moving target.

This problem has been investigated previously by Armstrong and Holeman in the context of tracking a baseball in 3-D using a number of speed guns [7]. In that work, a local search method was employed for the maximum-likelihood estimation of target parameters (position and velocity) from the measured Doppler shifts. However, the results can be very dependent on the initial guess so that the parameter estimation may not be robust. In this paper, an artificial neural network is proposed to estimate the target parameters using Doppler information measured by a set of spatially distributed sensors. The neural network is trained to relate the nonlinear relationship between the observed Doppler information and the target parameters. For the training, point scatterer data generated by simulation are used. Some preliminary measurement data are collected using a toy car that runs a round track. Its trajectory and velocity are estimated by the neural network. The simulation and measurement results are reported.

2. Problem Formulation

For tacking a moving target, the use of Doppler information measured by distributed radar sensors is considered. A collection of Doppler sensors can observe the signal from a moving target at different positions. The Doppler frequency is expressed as:

$$f_{doppler} = -\frac{f}{c} \cdot \vec{v} \cdot (\vec{T}x - \vec{R}x) \qquad (1)$$

where f is the radar frequency, c is the velocity of light, $\vec{v}$ is the velocity of the target, Tx is a unit vector pointing from the transmitter to the target position and Rx is a unit vector pointing from the target position to the receiver. As can be seen from (1), the Doppler shift from a target observed at a sensor depends not only on its velocity, but also the locations of the transmitter and receiver. Therefore, if a number of sensors are deployed around a moving target, each sensor will experience a different Doppler frequency because of its relative position with respect to the target. The statement of the problem is to process the Doppler information from the sensors to estimate the target position and velocity.

3. Artificial Neural Network

An artificial neural network [8] is proposed to estimate the target parameters of a moving target using the Doppler information from multiple sensors. The receivers detect the Doppler frequency caused by the moving target. The inputs to the neural network are the Doppler frequencies measured at the different locations and the outputs are the position and velocity of the target. For the ANN structure, the multi-layer perceptron (MLP) is selected.

In the simulation, six radar sensors are placed with equal angular spacing around the perimeter of a circular region with a diameter of 18m. Each radar sensor is assumed to have its own transmitter. The sensor positions are shown in Fig. 1(a). After the sensor positions are given, the target is assumed to have a random position and velocity inside the region. For each unique position and velocity realization, the Doppler frequencies at the 6 sensors are simulated and the data set is used for the ANN training.

For the learning process of the ANN, 3000 training data sets are generated, in which 2700 are used as the training set, and the remaining 300 are used as the validation set. The size of a hidden layer is determined empirically and set to be 150 in this case. Using a gradient descent method, the ANN is trained and iterated 500 times. The resulting training error in position is 0.29 m and that in velocity is 0.048 m/s. The validation error in position is 0.32 m and that in velocity is 0.051 m/s. These results are quite acceptable provided that they can be duplicated in real-world data.

4. Measurements

For a validation of the proposed method, we consider a target being observed simultaneously by six Doppler sensors in a laboratory experiment. However, to save cost in the actual experiment, we restrict the target motion to be periodic in time, and use only one Doppler sensor. We then replicate the measured data from this one sensor to six sensor outputs by shifting the data in time. The target chosen is a remote controlled toy car being driven around a circle of radius 6 m. A cylindrical reflector is mounted on top of the car to enhance its radar cross section. The configuration and a photo of the measurement setup are shown in Fig. 1. The radar operates at 2.4 GHz and uses a low-cost, off-the-shelf integrated receiver board. The down-converted signals are digitized for Doppler processing. The toy car is set to run around in a circle with a constant speed of 4.2 m/s. The assumed size of the monitored region is 18 m by 18 m in this case. The spectrogram of the measured data is shown in Fig. 2(a). As expected, the observed data is nearly periodic in time. The Doppler frequency corresponding to the strongest return at each time bin is first selected. Because the toy car is not an ideal point scatterer, the resulting graph is not a smooth curve. The selected data are then processed with a low pass filter and a median filter with a time window of 0.5 sec to remove the noisy high frequency components. The resulting data are shown in Fig. 2(b).

To emulate the Doppler data at six different locations, the measured data from the sensor is time-delayed and replicated. This emulation of the data is possible because the trajectory of the toy car is assumed to be in a perfect circle. The replicated data are input to the trained ANN and the target parameters are estimated through the net as the output. The actual trajectory of the car and the estimated trajectory are shown in Fig. 3(a) and the actual velocity and the estimated velocity are presented in Fig. 3(b). In the figure, Vx and Vy are the velocities along the x axis and y axis, respectively. The resulting RMS error in position is found to be 1.12 m and that in velocity is 0.43 m/s. The ANN estimates in both position and velocity show rapid variations in time. A low pass filter and a median filter with a time window of 1 sec are used for smoothing the data. The

filtered estimated trajectory and velocity of the car are shown in Fig. 4. They agree fairly well with the actual parameters.

5. Conclusion

In this paper, an artificial neural network was proposed to estimate the target position and velocity using the Doppler information measured at multiple locations. A trained neural network predicted the target parameters with 0.32 m error in position and 0.051 m/s error in velocity. The proposed concept was verified by the measurement of a toy car and the results showed that the error in position is 1.12 m and that in velocity is 0.43 m/s. Human tracking data are currently being collected and will be reported.

Acknowledgments

This work was supported by DARPA, the Office of Naval Research and the National Science Foundation under the Major Research Instrumentation Program.

References

[1] S.Nag, M.A.Barnes, T.Payment and G.Holladay, "Ultrawideband through-wall radar for detecting the motion of people in real time," *SPIE Proc. Radar Sensor Technology and Data Visualization,* vol. 4744, pp.48-57, July 2002.

[2] A.R.Hunt, "A wideband imaging radar for through-the-wall surveillance," *SPIE Proc., Sensors, and Command, Control, Communications, and Intelligence (C3I) Technologies*, vol. 5403, pp. 590-596, Sep. 2004

[3] J.Z.Tatoian, G.Franceshetti, H.Lackner and G.G.Gibbs, "Through-the-wall impulse SAR experiments," *IEEE Antennas Propagat. Soc. Int. Symp. Digest,* paper no. S099p04u , July 2005

[4] Y. Yang and A.E.Fathy, "See-through-wall imaging using ultra wideband short-pulse radar system," *IEEE Antennas Propagat. Soc. Int. Symp. Digest,* vol. 3B, pp. 334-337, July 2005.

[5] A. Lin and H. Ling, "Two-dimensional human tracking using a three-element Doppler and direction-of-arrival radar," *IEEE Radar Conf.*, pp. 24-27, Apr. 2006.

[6] A. Lin and H. Ling, "Three-dimensional tracking of humans using a very low-complexity radar," *Elect. Lett.*, vol. 42, pp. 67-68, August 2006.

[7] B. Armstrong and B.S. Holeman, "Target tracking with a network of Doppler radars," *IEEE Trans. Aeros. Electronic Sys.*, vol. 34, pp. 33-48, Jan. 1998.

[8] C. Bishop, *Neural Networks for Pattern Recognition*, Oxford University Press, 1995.

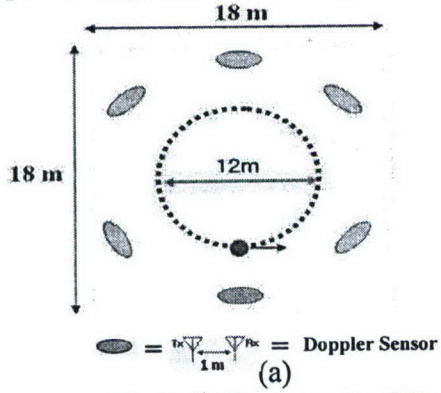

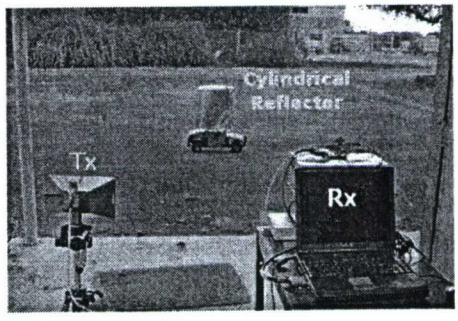

Fig. 1. (a) Deployment of Doppler sensors. (b) Measurement setup.

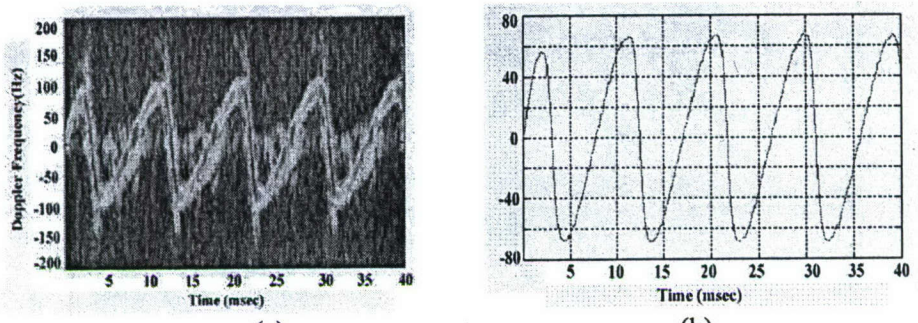

(a) (b)

Fig 2. (a) Spectrogram of measured toy car. (b) Filtered data.

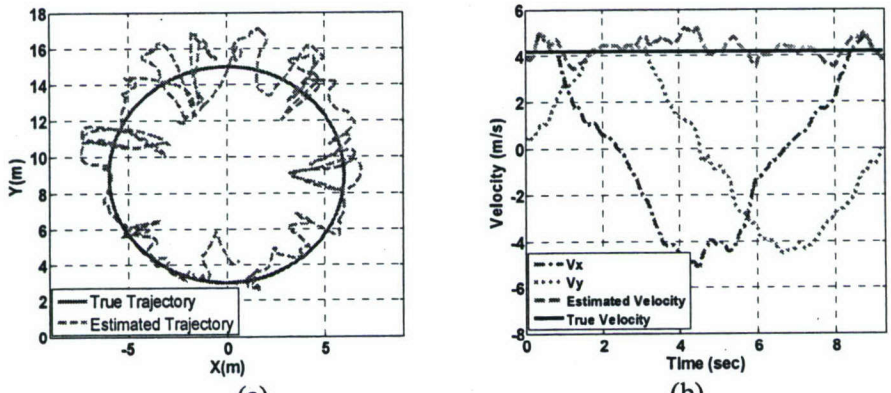

(a) (b)

Fig. 3 (a) Actual trajectory (blue) and estimated trajectory (Red) of the car.
(b) Actual velocity (black) and estimated velocity (green).

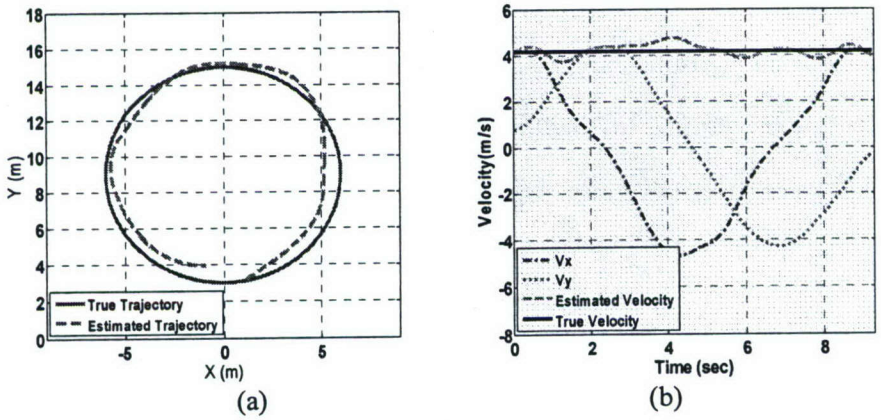

(a) (b)

Fig. 4. (a) Actual trajectory (blue) and filtered estimated trajectory (red) of the toy car.
(b) Actual velocity (black) and filtered estimated velocity (green).